UNIVERSITI TEKNOLOGI MARA

FABRICATION CHARACTERISATION AND DISSOLUTION PREDICTION OF ELECTROSPUN PVA/K-CARRAGEENAN ORAL DISPERSIBLE FILMS CONTAINING KELULUT HONEY OR ASCORBIC ACID

FETRIYA FATIHAH BINTI NASAR

MSc

August 2026

UNIVERSITI TEKNOLOGI MARA

FABRICATION CHARACTERISATION AND DISSOLUTION PREDICTION OF ELECTROSPUN PVA/K-CARRAGEENAN ORAL DISPERSIBLE FILMS CONTAINING KELULUT HONEY OR ASCORBIC ACID

FETRIYA FATIHAH BINTI NASAR

Thesis submitted in fulfilment
of the requirements for the degree of
Master of Science
(Chemical Engineering)

Faculty of Chemical Engineering

August 2026

CONFIRMATION BY PANEL OF EXAMINERS

I certify that a Panel of Examiners has met on 24 June 2026 to conduct the final examination of Fetriya Fatihah Binti Nasar on her Master of Science thesis entitled "Fabrication Characterisation And Dissolution Prediction Of Electrospun PVA/κ-Carrageenan Oral Dispersible Films Containing Kelulut Honey Or Ascorbic Acid" in accordance with Universiti Teknologi MARA Act 1976 (Akta 173). The Panel of Examiners recommends that the student be awarded the relevant degree. The Panel of Examiners was as follows:

Nur Hashimah Alias, PhD
Associate Professor
Faculty of Chemical Engineering
Universiti Teknologi MARA
(Chairman)

Fauziah Marpani, PhD
Associate Professor
Faculty of Chemical Engineering
Universiti Teknologi MARA
(Internal Examiner)

Syafiqah Saidin, PhD
Associate Professor
IJN-UTM Cardiovascular Engineering Centre
Universiti Teknologi Malaysia
(External Examiner)

PROF DR HJH ZURAEDA IBRAHIM
Dean
Institute of Postgraduate Studies
Universiti Teknologi MARA

Date: 19 August 2026

AUTHOR'S DECLARATION

I declare that the work in this thesis was carried out in accordance with the regulations of Universiti Teknologi MARA. It is original and is the results of my own work, unless otherwise indicated or acknowledged as referenced work. This thesis has not been submitted to any other academic institution or non-academic institution for any degree or qualification.

I, hereby, acknowledge that I have been supplied with the Academic Rules and Regulations for Postgraduate, Universiti Teknologi MARA, regulating the conduct of my study and research.

Name of Student	:	Fetriya Fatihah Binti Nasar
Student ID. No.	:	2024833376
Programme	:	Master of Science (Chemical Engineering) – EH750
Faculty	:	Chemical Engineering
Thesis Title	:	Fabrication Characterisation And Dissolution Prediction Of Electrospun PVA/κ-Carrageenan Oral Dispersible Films Containing Kelulut Honey Or Ascorbic Acid
Signature of Student	:	.
Date	:	August 2026

ABSTRACT

Oral Dispersible Film (ODF) is often consumed in a soluble format that dissolves or disintegrates rapidly in saliva, eliminating the need for chewing or swallowing as with conventional tablets. Recently, ODFs are getting a new recognition among people for their ease of administration, but the research is limited due to researchers focusing on conventional dosage forms (tablets, powders, and capsules). The research aims to investigate the synthesis and characterise the ODFs using polyvinyl alcohol (PVA), honey, and kappa-carrageenan, utilising electrospinning methods. The electrospinning method was utilised using a few parameters such as voltage, flow rate and distance of the needle tip from the collector plate. The ODFs were analysed for mechanical characteristics, surface morphology, and stability utilising scanning electron microscopy (SEM), Fourier transform infrared spectroscopy (FT-IR), and additional analytical techniques. The dissolving characteristics of ascorbic acid in the composite were forecasted using an artificial neural network (ANN). Electrospinning is selected for its success in generating nanofibrous films. This research highlights PVA/honey and PVA/ascorbic acid in promoting the pharmaceutical industry in drug delivery systems. The spinning solutions exhibited increases in viscosity and conductivity as the quantity of honey and AA was increased. The produced nanofibers were analysed using a scanning electron microscope (SEM). Films containing honey had average fibre diameters of 118 – 134 nm, which were smaller than the fibre diameters of AA-loaded films, which were between 495 and 643 nm. FT-IR measurements confirm the efficient incorporation of honey and AA into the polymeric matrix with no signs of chemical degradation, demonstrating great hydrogen-bonding interactions. All films had hydrophilic surfaces, and the honey-loaded films' water contact angles ranged from 50.6° to 65.5°, while AA decreased from 63.2° to 41.9°. The release of AA exhibited a quick concentration- dependent pattern and featured an initial burst followed by a plateau as evidenced by UV- Vis and FT-IR spectroscopies. Mechanical testing on ODF samples showed that the tensile strength decreased with increasing honey and AA concentrations. The Levenberg-Marquardt method, when modelling artificial neural networks (ANN) for predicting dissolution behaviour, showed a very high level of accuracy, with an almost perfect MSE and an R^2 value close to 1. The results indicate that the model accurately portrays the relationship between formulation variables and dissolution behaviour, and thus can predict the performance of dissolution with a high level of confidence. This research highlights PVA/honey and PVA/ascorbic acid in promoting the pharmaceutical industry in drug delivery systems. The results provide a foundation for the development of sustainable oral dissolving films with improved dissolution performance for pharmaceutical and nutraceutical applications. The ANN model also offers a reliable way to optimise the design of formulations, thus reducing the experimental workload, development time, and material consumption.

ACKNOWLEDGEMENT

I would like to express my gratitude and thank the Faculty of Chemical and Mechanical Engineering, UiTM Shah Alam, for the support throughout completing this research project. I wish to convey my heartfelt gratitude and give my warmest thanks to my supervisor, Professor Ir. Dr. Jamaluddin Mahmud, Prof. Madya Ir. Dr Noor Fitrah Abu Bakar and Dr Nur Asyikin Ahmad Nazri who made this work possible. Their guidance and advice have helped me throughout the stages of completing my Master's, writing my thesis, and completing it within the time frame. Their expertise in formulation development and analytical techniques greatly contributed to the successful fabrication and evaluation of the electrospun oral dissolving films.

Not to forget all the PIC lab members who willingly spent some of their time for me, asking questions regarding the lab. I would also want to thank my family for their continuous support throughout my final year, especially my mother, who always prays for me, my late father, who wishes for me to pursue my studies, and also my siblings, who always lend their ears to me. I would also like to thank all my friends (whether Master's or Degree) for their encouragement and knowledge sharing, especially in ANN modelling and data analysis and also for managing my mental health throughout completing my Master's journey. And not to forget my little sister Fetriya Fadila Nasar, who always hears my stories when I am confessing to her regarding this project.

TABLE OF CONTENTS

		Page
CONFIRMATION BY PANEL OF EXAMINERS		**ii**
AUTHOR'S DECLARATION		**iii**
ABSTRACT		**iv**
ACKNOWLEDGEMENT		**v**
TABLE OF CONTENTS		**vi**
LIST OF TABLES		**ix**
LIST OF FIGURES		**x**
LIST OF SYMBOLS		**xiii**
LIST OF ABBREVIATIONS		**xiv**
CHAPTER 1	**INTRODUCTION**	**1**
1.1	Research Background	1
1.2	Problem Statement	5
1.3	Research Objectives	6
1.4	Significance of the Study	6
1.5	Limitation of the Study	7
CHAPTER 2	**LITERATURE REVIEW**	**9**
2.1	Introduction	9
2.2	Oral Dispersible Films (ODFs)	9
2.3	Materials for Electrospun Polymeric Films	11
2.3.1	Polyvinyl Alcohol (PVA) & Polymers Used to Fabricate ODFs.	11
2.3.2	Kappa-Carrageenan (κ-Car)	16
2.3.3	*Kelulut* Honey	17
2.3.4	Ascorbic Acid (Vitamin C)	18
2.4	Fabrication Methods for Nanofibrous Films	20
2.4.1	Electrospinning: Principles and Parameters	20
2.4.2	Influence of Solution Viscosity and Conductivity on Electrospinning Performance	28
2.4.3	Alternative Film-Forming Techniques	30
2.5	Oral Dispersible Film (ODF) Dissolution Method	32

2.6 Artificial Neural Network (ANN) in Dissolution Predictions 34

CHAPTER 3 RESEARCH METHODOLOGY 39

3.1 Introduction 39
3.2 Materials 40
3.3 Methods 41
3.3.1 Preparation of the PVA/κ-Car/Kelulut Honey and PVA/κ-Car/AA Solutions 41
3.4 Conductivity and Viscosity Measurement 43
3.5 Electrospinning Procedure and Process Optimisation 43
3.6 Characterisation of Electrospun ODFs 44
3.6.1 Scanning Electron Microscopy (SEM) 44
3.6.2 Water Contact Angle (WCA) Measurement 45
3.6.3 Fourier Transform Infrared Spectroscopy (FT-IR) Analysis 45
3.6.4 Mechanical Testing: Tensile Strength 45
3.7 Dissolution of Electrospun PVA/κ-Car/Honey and PVA/κ-Car/AA ODFs 46
3.7.1 Formulation of Artificial Saliva 46
3.7.2 Batch Dissolution of Electrospun ODFs Using UV-Vis Spectroscopy 46
3.7.3 Instantaneous Dissolution of Electrospun ODFs Using FT-IR Spectroscopy 47
3.7.4 Instantaneous Dissolution of Electrospun PVA/κ-Car/AA ODF 48
3.8 Development of an ANN Model for Dissolution Prediction 48
3.8.1 Batch Dissolution Prediction of Honey from Electrospun PVA/κ-Car/Honey ODFs Using an ANN Model 49
3.8.2 Batch Dissolution Prediction of Ascorbic Acid (AA) from Electrospun PVA/κ-Car/AA ODFs Using an ANN Model 50
3.8.3 Instantaneous Dissolution Prediction of Ascorbic Acid (AA) from Electrospun PVA/κ-Car/AA ODFs Using an ANN Model 50

CHAPTER 4 RESULTS AND DISCUSSION 52

4.1 Introduction 52
4.2 Characterization of the PVA/κ-Car/Honey and PVA/κ-Car/AA ODFs 52
4.2.1 Viscosity and Conductivity of Spinning Solutions 52
4.3 Morphological Characterisation of Polymeric Films via SEM: Fibre Diameter Analysis 55

4.3.1 SEM Analysis of PVA/κ-Car ODFs Loaded with Honey 55
4.3.2 SEM Analysis of PVA/κ-Car ODFs Loaded with Ascorbic Acid (AA) 58
4.4 Water Contact Angle Analysis (WCA) 61
4.4.1 Water Contact Angle Analysis for Electrospun PVA/κ-Car/Honey ODFs 61
4.4.2 Water Contact Angle Analysis for Electrospun PVA/κ-Car/AA ODFs 63
4.5 Fourier Transform Infrared Spectroscopy (FT-IR) 64
4.5.1 FT-IR Analysis for Electrospun PVA/k-Car/Honey ODFs 64
4.5.2 FT-IR Analysis for Electrospun PVA/k-Car/AA ODFs 67
4.6 Mechanical Performances of Electrospun ODFs 69
4.6.1 For PVA/κ-Car/Honey Oral Dispersible Film 69
4.6.2 For PVA/κ-Car/AA Oral Dispersible Film 72
4.7 Dissolution of Electrospun PVA/κ-Car/Honey and PVA/κ-Car/AA ODFs 75
4.7.1 Batch Dissolution of Electrospun ODFs Using UV-Vis Spectroscopy 75
4.8 Instantaneous Dissolution of Electrospun PVA/κ-Car/AA ODFs Using FT-IR Spectroscopy 79
4.9 ANN Modelling and Prediction of Dissolution 82
4.9.1 Batch Dissolution Prediction of Honey from Electrospun PVA/κ-Car/Honey ODFs Using ANN 82
4.9.2 Batch Dissolution Prediction of Ascorbic Acid (AA) from Electrospun PVA/κ-Car/AA ODFs Using ANN 88
4.9.3 Instantaneous Dissolution Prediction of Ascorbic Acid (AA) from Electrospun PVA/κ-Car/AA ODFs Using ANN 95

CHAPTER 5 CONCLUSION 101

5.1 Conclusion 101
5.2 Recommendations 102
REFERENCES 104
APPENDICES 122
AUTHOR'S PROFILE 126

LIST OF TABLES

Tables	Title	Page
Table 2.1:	Electrospinning Materials Used in Past Studies	15
Table 2.2:	Electrospinning Process Parameters for ODFs Fabrication	26
Table 2.3:	List of Other Methods for Producing Thin Films	31
Table 2.4:	Past Studies of The Dissolution Test for Honey And AA	33
Table 2.5:	Predictions Using ANN	38
Table 3.1:	Mass of AA to Fabricate Electrospun ODFs	43
Table 3.2:	Parameter Used to Run the Electrospinning (Bakar et al., 2023; Bureau et al., 2019; Santos et al., 2019; Sapiee et al., 2023)	44
Table 4.1:	Viscosity and Conductivity Analysis for PVA/K-car/Honey ODF	53
Table 4.2:	Viscosity and Conductivity Analysis for PVA/K-car/AA ODF	55
Table 4.3:	Peak of the FTIR Spectra for ODFs with Honey Loaded	66
Table 4.4:	Peak of the FTIR Spectra for ODFs With AA Loaded	68
Table 4.5:	List of Parameters	83
Table 4.6:	Result of Neural Network Using *Trainlm*	84
Table 4.7:	List of Parameters	89
Table 4.8:	Result of Neural Network Using *Trainlm*	90
Table 4.9:	List of Parameters	95
Table 4.10:	Results of the Train Network	96

LIST OF FIGURES

Figures	Title	Page
Figure 2.1:	Honey Structure (Trigono Stingless Bee)	18
Figure 2.2:	Electrospinning Schematic Diagram	21
Figure 2.3:	Sol-Gel Method (G. Singh et al., 2023)	31
Figure 2.4:	The Spin Coating Method (Obregón & Rodríguez-González, 2022)	31
Figure 2.5:	Solvent Casting Method (Prete et al., 2023)	31
Figure 2.6:	Hot Melt Extrusion (Musazzi et al., 2018)	32
Figure 2.7:	Schematic Diagram of ANN Cited from Brooks & Tucker [40]	35
Figure 3.1:	Overview of Experimental Work and Methodology for Electrospun Nanofiber	40
Figure 3.2:	Solution Preparation of PVA/κ-car/Honey	41
Figure 3.3:	Solution Preparation of the ODF Solution PVA/κ-car/AA	42
Figure 3.4:	Schematic Diagram of Electrospinning	44
Figure 3.5:	Neural Network Diagram for 10 Hidden Layers	49
Figure 3.6:	Schematic Diagram of an ANN Model for Dissolution Prediction Using UV-Vis Spectroscopy	50
Figure 3.7:	Schematic Diagram of an ANN Model for Dissolution Prediction Using FT-IR Spectroscopy	51
Figure 4.1:	SEM Analysis for Electrospun ODF PVA/K-Car/Honey Of (a) 1 mL, (b) 1.5 mL, And (c) 2 mL	56

Figure 4.2: Distributions of Nanofiber Diameter for PVA/K-Car/Honey in Different Volumes: (a) 1 mL, (b) 1.5 mL, And (c) 2 mL 57

Figure 4.3: SEM Analysis for Electrospun ODF PVA/κ-car/AA of (a) 1 w/v%, (b) 3 w/v% , (c) 5 w/v%, (d) 7 w/v%, (e) 9 w/v%, and (f) 11 w/v% 59

Figure 4.4: Distributions of Electrospun Nanofibers Diameter for PVA/K-Car/AA in Different Concentration (a) 1 w/v%, (b) 3 w/v% , (c) 5 w/v%, (d) 7 w/v%, (e) 9 w/v%, and (f) 11 w/v% 60

Figure 4.5: Water Contact Angle of PVA/K-Car/Honey of Different Volume (a) 1mL (b) 1.5mL (c) 2mL 62

Figure 4.6: Water Contact Angle of PVA/K-Car/AA of Different Concentrations (a) 1 w/v% AA, (b) 3 w/v% AA, (c) 5 w/v% AA, (d) 7 w/v% AA, (e) 9 w/v% AA, and (f) 11 w/v% AA 63

Figure 4.7: PVA/K-car/Honey Detection Using FT-IR for Film (a) 1mL (b) 1.5mL (c) 2mL 66

Figure 4.8**:** PVA/K-Car/AA Detection Using FT-IR for Different Concentrations (a) 1 w/v% AA, (b) 3 w/v% AA, (c) 5 w/v% AA, (d) 7 w/v% AA, (e) 9 w/v% AA, and (f) 11 w/v% AA 68

Figure 4.9: Stress-Strain Curves of Honey-Loaded ODFs 70

Figure 4.10: Mechanical Properties of the Electrospun ODFs 71

Figure 4.11: Stress-Strain Curves Of AA-Loaded ODFs 73

Figure 4.12: Mechanical Properties of the Electrospun ODFs 74

Figure 4.13: Profile Release of Honey for Batch Dissolution Using Uv-vis, I) Lag Phase II) Burst Release III) Sustained Matrix Erosion and Diffusion IV) Plateau 77

Figure 4.14: Profile Release of AA for Batch Dissolution Using Uv-vis I) Lag Phase II) Burst Release III) Sustained Matrix Erosion and Diffusion IV) Plateau 79

Figure 4.15: Profile Release of AA for Instantaneous Dissolution Using FT-IR spectroscopy I) Lab Phase II) Burst Release III) Sustained Matrix Erosion and Diffusion IV) Plateau 81

Figure 4.16: Regression Plot of ANN; (a) ANN Training Model; (b) ANN Validation Model; (c) ANN Testing Model; (d) ANN All Data Model 85

Figure 4.17: Error Histogram Plot 86

Figure 4.18: Performance Plot: Mean Squared Error vs Epoch. 86

Figure 4.19: Comparison of the Volume of Honey, (a) ODFs with 1 mL; (b) ODFs with 1.5 mL; (c) ODFs with 2 mL 88

Figure 4.20: Regression Plot of ANN; (a) ANN Training Model; (b) ANN Validation Model; (c) ANN Testing Model; (d) ANN All Data Model 90

Figure 4.21: Error Histogram Plot 91

Figure 4.22: Performance Plot: Mean Squared Error vs Epoch. 92

Figure 4.23: Comparison of Concentration of AA, (a) ODFs with 1w/v% of AA; (b) ODFs with 3w/v% of AA; (c) ODFs with 5w/v% of AA; (d) ODFs with 7w/v% of AA; (e) ODFs with 9w/v% of AA; (f) ODFs with 11w/v% of AA 94

Figure 4.24: Regression Plot of ANN; (a) ANN Training Model; (b) ANN Validation Model; (c) ANN Testing Model; (d) ANN All Data Model 97

Figure 4.25: Error Histogram Plot 98

Figure 4.26: Performance Plot: Mean Squared Error vs Epoch. 98

Figure 4.27: Comparison of Concentration of AA, (a) ODFs with 1w/v% of AA; (b) ODFs with 3w/v% of AA; (c) ODFs with 5w/v% of AA; (d) ODFs with 7w/v% of AA; (e) ODFs with 9w/v% of AA; (f) ODFs with 11w/v% of AA 100

LIST OF SYMBOLS

Symbols	
C	Carbon
C	Celsius
°	Degree
hr	Hour
H	Hydrogen
κ	Kappa
k	Kilo
μ	Micro
m	Mili
n	Nano
O	Oxygen
V	Voltage

LIST OF ABBREVIATIONS

Abbreviations	
API	Active Pharmaceutical Ingredients
ANN	Artificial Neural Network
AA	Ascorbic Acid
CMC	Carboxy Methyl Cellulose
CAT	Catechin
C/P	Chitosan/Pullulan
DES	Deep Eutectic Solvent
DI	Deionised
FEX	Fexofenadine HCL
FDA	Food and Drug Administration
FT-IR	Fourier Transform Infrared Spectroscopy
FH	Fully Hydrolyzed
GEL	Gelatin
HCL	Hydrochloric Acid
OH	Hydroxyl Group
HPMC	Hydroxypropyl Methylcellulose
HPβCD	Hydroxypropyl-β-Cyclodextrin
HPγCD	Hydroxypropyl-γ-Cyclodextrin

κ-Car	Kappa-Carrageenan
LAA/HP-β-CD	L-Ascorbic Acid/HP-β-Cyclodextrin
Mh	Manuka Honey
MC	Methylcellulose
ODT	Oral Disintegrating Tablets
ODF	Oral Dispersible Film
PCurd	Phosphorylated Curdlan Gel
PAN	Polyacrylonitrile
PEG	Polyethene Glycol
PVA	Polyvinyl Alcohol
PVP	Polyvinylpyrrolidone
SEM	Scanning Electron Microscopy
SC	Sildenafil Citrate
Ag-NPs	Silver Nanoparticles
SA	Sodium Alginate
$NaHCO_3$	Sodium Bicarbonate
NaCl	Sodium Chloride
SSG	Sodium Starch Glycolate
UV-Vis	Ultraviolet Spectroscopy
UN SDG	United Nations Sustainable Development Goals
USP	United States Pharmacopoeia

WCA	Water Contact Angle
XG	Xantham Gum

CHAPTER 1
INTRODUCTION

1.1 Research Background

An oral dispersible film (ODF) is a solid dosage form designed to dissolve or disintegrate in the mouth without the need for water, chewing or swallowing, making it ideal for young children, older adults, and patients with swallowing difficulties (Celebioglu & Uyar, 2019; Garcia et al., 2018; Jacob et al., 2023; Topuz et al., 2021). The pharmaceutical industry has focused on the benefits of ODFs in dosage form flexibility, ease of use, rapid therapeutic effect, and improved patient compliance. Karki et al. (2016) point out that oral thin films are a promising alternative to conventional tablets and capsules that allow for the local or systemic delivery of drugs through mucosal absorption. This, combined with the ability to be designed as oral soluble films, strips, wafers, and orodispersible systems, further drives their use in patient-centred drug development. *Kelulut* honey was selected as a natural functional ingredient due to its rich phenolic compounds, flavonoids, antioxidant activity, antimicrobial properties, and local availability in Malaysia. This study selected *kelulut* honey, which has the dual properties of a natural functional ingredient and a taste-masking excipient. Ascorbic acid was used as the active pharmaceutical substance for the solubility assessment model. Compared with commercially studied honey such as Manuka and Tualang honey, *Kelulut* honey remains largely unexplored for electrospun oral dispersible film (ODF) applications. Besides contributing natural sweetness that may improve patient acceptability, its bioactive constituents may provide additional therapeutic value while maintaining the rapid dissolution characteristics required for ODF systems. In contrast, ascorbic acid was investigated as a separate formulation because it is a highly water-soluble model active compound with well-established UV-Visible absorbance characteristics. Its high aqueous solubility makes it suitable for evaluating rapid dissolution behaviour under simulated oral conditions. Therefore, *kelulut* honey and ascorbic acid were intentionally formulated separately to investigate their individual influence on electrospinnability, fibre morphology, hydrophilicity, mechanical

properties, dissolution behaviour, and ANN prediction without interference from each other.

Better methods of fabricating materials, such as nanofiber technology, have been researched to further enhance the performance of ODFs. Alongside progress in drug delivery systems, nanofiber engineering has surfaced as a potential technology in numerous medicinal and materials science applications. Shahid & Khan (2022) assert that electrospun nanofibers are extensively investigated for applications in membranes, tissue engineering, and wound-healing materials, owing to their elevated surface area and porosity. In the context of ODF manufacturing, nanofibrous structures improve dissolving rates (Cho et al., 2020) and disintegration efficacy. Moreover, Abou-Taleb et al. highlighted that ODFs constitute an innovative pharmacological platform with enhanced dosage flexibility and greater patient acceptance. The elevated surface-to-volume ratio of electrospun films facilitates rapid interaction with saliva, hence enhancing drug release velocity in comparison to traditional cast films.

Of the numerous techniques to produce nanofibres, electrospinning has been acknowledged as one of the most effective ways to create them in the form of extremely thin films. Electrospinning is a versatile and cost-effective technique employed to produce polymer-based nanofibrous thin films. The procedure entails the application of a high-voltage (Celebioglu & Uyar, 2021; Kanimozhi et al., 2020; Zhang et al., 2020) electric field to a polymer solution, resulting in the production of continuous fibres at micro- to nanoscale dimensions using electrohydrodynamic forces. Cheng et al. (2024) indicate that electrospinning allows for meticulous regulation of fibre shape, diameter, and porosity by optimising solution characteristics and processing conditions. In ODF applications, the resultant nanofibrous architecture facilitates fast disintegration and rapid dissolution due to the increase in surface area.

The effectiveness of an ODF is dependent on selecting the appropriate polymer materials to ensure the ODF can be produced and function correctly. Polyvinyl alcohol (PVA) is an example of a synthetic and hydrophilic polymer that is popular in the field of electrospinning because of its biocompatibility, good film-forming ability, and large number of hydroxyl (–OH) groups (Balasubramaniam et al., 2020; Teixeira et al., 2022a). PVA is an excellent candidate for use in oral dispersible films because it is non-toxic and hydrophilic, resulting in rapid dissolution in the saliva. However, single polymer systems can exhibit some limitations, such as low mechanical strength and

brittleness. For that reason, blending PVA with natural polymers such as kappa-carrageenan (κ-car), which is a sulfated polysaccharide (Zhou et al., 2021) from red seaweeds, can be beneficial for enhancing gel strength, film integrity, and rapid disintegration of blends. As a natural copolymer, κ-carrageenan can improve the viscosity and electrospinnability of solutions. It enhances the stability and mechanical integrity of fibres through intermolecular interactions with PVA and is a suitable raw material for preparing electrospun oral disintegrating films (ODF). The carrier shows excellent hydrophilic properties, which are very important for making stable but fast-disintegrating ODF matrices (Nasalapure et al., 2021). This study selected PVA/κ-carrageenan blends as the polymer carrier matrix. This matrix can support the formation of electrospun fibres, load either Kelulut honey or ascorbic acid individually, and maintain both the film's structural integrity and fast-dissolving properties.

Incorporating functional desired ingredients into the polymer matrix is also crucial in enhancing the properties of the film and its acceptability to people. Honey, a naturally supersaturated sugar solution predominantly consisting of fructose and glucose, is well-regarded for its antibacterial, antioxidant, taste-masking, and anti-inflammatory characteristics, as a food substances that contain nutrients. Honey has been used as a desired ingredient in fabricating films, such as Iran-Tabriz (Maleki et al., 2013), Thyme honey (Samadieh & Sadri, 2020), Manuka honey (Kassem et al., 2023; Mohd Azam & Amin, 2017; Santos et al., 2019; Schuhladen et al., 2021). According to Yupanqui Mieles et al. (2022), honey is widely utilised in biological applications owing to its beneficial properties. Furthermore, Das et al. (2020) revealed that honey may be integrated into nanofibrous matrices, imparting functional bioactive characteristics. In ODF formulations, honey serves as a natural sweetener (Poojar et al., 2017), plasticiser (Chin et al., 2024; Koosha et al., 2021), film modifier (Bobde & Tank, 2019), and stabilising ingredient in the polymer solution, enhancing film flexibility and mouthfeel.

Alongside honey, the desired ingredient is crucial for achieving the desired release kinetics of the ODF system. Ascorbic acid (AA), also referred to as vitamin C, is a water-soluble antioxidant vital for human health. Humans are incapable of synthesising ascorbic acid due to the lack of requisite biosynthetic enzymes, necessitating dietary consumption (Skrovankova et al., 2015). Ascorbic acid oxidation poses a challenge during storage, influenced by various factors including temperature, light, pH, and storage conditions, occurring in both aerobic and anaerobic environments

(Baptista et al., 2023). Its antioxidant characteristics and elevated water solubility render it an exemplary model medicine for dissolution and release investigations in ODF systems. Its susceptibility to environmental elements, including light and heat, necessitates inclusion into polymeric films, which offer protection and controlled release capabilities.

Since ODFs perform optimally with rapid release, a well-designed and systematic evaluation of the dissolution is necessary to assess the effectiveness of the formulation. Dissolution is a critical factor in evaluating ODF performance because it closely determines the rate of drug release and its subsequent bioavailability. Dissolutions are commonly analysed using UV-Visible spectroscopy to determine the release concentration in the dissolution medium. Batch dissolution testing has been investigated for the rapid and sensitive detection of electroactive substances. Advanced analytical methodologies, including instantaneous dissolution, can be performed to replicate direct saliva interaction for the rapid detection of desired ingredients. The formulation can also be optimised, the understanding of the process can be enhanced, and experimental dissolution testing can also be complemented with predictive modelling to improve formulation. To improve prediction properties, modelling using artificial neural networks (ANNs) can be used to relate formulation and electrospinning parameters to the film characteristics and dissolution behaviour based on the dissolution studies from past research using tablets (Galata et al., 2019, 2021; Nagy et al., 2019; Péterfi et al., 2023). The nonlinear data processing and formulation condition optimisation prediction capabilities of ANNs are used to improve efficiency, predict quality, and enhance the stability of the formulation.

With all of these considerations, the best approach to fabricate electrospun ODF is to combine conductive polymer blending with electrospinning technology alongside desired ingredients and ANN prediction. This study involves the fabrication of electrospun thin films from polymer blends of PVA and κ-car, with the addition of honey and ascorbic acid. The research was designed as two independent formulation systems rather than a combined formulation. The first system consisted of electrospun PVA/κ-carrageenan films containing Kelulut honey, whereas the second system consisted of electrospun PVA/κ-carrageenan films containing ascorbic acid. This design enabled the individual effects of each functional ingredient on solution properties, fibre formation, film characteristics, dissolution behaviour, and ANN prediction performance

to be systematically evaluated. The two substances were not tested in the same formulation to prevent interactions between them from obscuring the unique contribution of each component to fibre formation, membrane properties, and dissolution behaviour. Combining both ingredients within a single formulation was beyond the scope of this study and is proposed as future work. This study developed differentiated dissolution test protocols; *kelulut* honey-loaded samples use the batch dissolution method to evaluate their overall dissolution performance, while ascorbic acid-loaded samples use the instantaneous dissolution method, which aligns with ascorbic acid's high water solubility and requirement for rapid release in saliva.

1.2 Problem Statement

Oral dispersible films (ODFs) are expected to provide rapid dissolution, ease of administration, and improved patient compliance, particularly for paediatric, geriatric, and dysphagic patients. Electrospinning has emerged as a promising fabrication technique for ODFs because its highly porous nanofibrous structure offers a large surface-area-to-volume ratio that promotes rapid saliva penetration and dissolution. Despite these advantages, current research has predominantly focused on solvent-cast ODFs or electrospun systems incorporating conventional pharmaceutical ingredients and commercially available honey types, while studies involving locally sourced Kelulut honey remain scarce. Furthermore, limited information is available on the individual effects of Kelulut honey and ascorbic acid on the physicochemical properties, electrospinnability, fibre morphology, mechanical performance, and dissolution behaviour of electrospun PVA/κ-carrageenan ODFs.

This study developed two types of test oral dissolving film (ODF) formulations: one loaded with *kelulut* honey and the other loaded with ascorbic acid. The original aim of this work was to independently assess the effect of each added ingredient on the properties and efficacy of the formulations, and to use artificial neural network (ANN) modelling to optimise and predict the performance of the two formulation types. Since the two added ingredients have significantly different physicochemical properties and functional roles, this study does not conduct a direct comparison between them.

The lack of comprehensive understanding of these formulation systems restricts the optimisation and wider application of electrospun ODFs as rapid oral delivery platforms. In addition, formulation development continues to rely largely on

experimental trial-and-error approaches due to the limited use of predictive modelling for dissolution behaviour. Therefore, this study aims to fabricate electrospun PVA/κ-carrageenan oral dispersible films containing Kelulut honey or ascorbic acid as separate formulation systems, systematically evaluate their physicochemical characteristics and dissolution behaviour, and develop an Artificial Neural Network (ANN) model to predict dissolution performance within the investigated formulation range. The findings are expected to provide scientific knowledge for formulation optimisation and support the advancement of electrospun ODF technology for pharmaceutical and functional oral delivery applications.

1.3 Research Objectives

a) To synthesise, mechanically evaluate, and characterise the electrospun polyvinyl alcohol (PVA)/kappa carrageenan (κ-car) oral dispersible film (ODF) nanofibres blended with two different ingredients, honey and ascorbic acid.
b) To determine the dissolution behaviour of honey and ascorbic acid, the electrospun oral dispersible film (ODF) in simulated saliva using Uv-vis and FT-IR spectroscopy.
c) To predict the dissolution behaviour of honey and ascorbic acid in polyvinyl alcohol (PVA)/ κ-carrageenan ODF nanofibres using an artificial neural network (ANN).

1.4 Significance of the Study

This study advances the research and development of electrospun oral dispersible films (ODFs). Taking polyvinyl alcohol (PVA)/κ-carrageenan nanofibers loaded with Kelulut honey and ascorbic acid as its experimental subject, this study verifies that these materials possess optimal fibre morphology, mechanical properties, hydrophilicity, and fast-dissolving performance. This work not only provides scientific evidence supporting the use of local Kelulut honey as a natural functional component of ODFs, but also promotes the utilisation of local biological resources and creates prospects for high value-added products in the pharmaceutical and nutraceutical fields.

The original artificial neural network (ANN) model constructed in this study can effectively predict drug dissolution behaviour and serves as a reliable tool for formulation optimisation. This model can reduce experimental workload, research and development duration, and material usage, advancing pharmaceutical research and development to become more economical and sustainable.

The outcomes of this study may benefit society as they can support the research and development of patient-friendly pharmaceutical dosage forms, solve the medication challenges of three categories of special populations, and improve social welfare. From the national development level, the research pathway that uses local Kelulut honey aligns with three of the country's national-level development directions. Furthermore, this project supports the United Nations SDGs, particularly SDG3, SDG9, and SDG12, through the development of improved oral delivery systems, advancing electrospinning and predictive modelling for pharmaceutical applications and reducing material usage and experimental waste through ANN-assisted formulation optimisation.

1.5 Limitation of the Study

This study focuses on the development and evaluation of electrospun oral disintegrating films (ODFs) based on polyvinyl alcohol (PVA) and kappa-carrageenan (κ-car) as the polymer, and honey and ascorbic acid as functional/flavouring and desired ingredients, respectively. The study examines the impact of varying *kelulut* honey volume (1 mL, 1.5 mL and 2 mL) and ascorbic acid concentrations (ranging from 1 w/v% to 11 w/v%) on the mechanical strength, film morphology and dissolution properties of the film. The ODFs were produced by electrospinning, and the flow rate, voltage, and needle-to-collector distance were optimised. The films were assessed and characterised by morphology, mechanical properties, and the rate of dissolution. Dissolution studies were carried out by two different approaches of batch dissolution (10 mg of film in 30 mL of simulated saliva, assessed by UV–Vis, ranging from 200–800 nm wavelength) and instantaneous dissolution (4 mm film disc in 22 μL of saliva, assessed by FT-IR, ranging from 4000–400 cm^{-1} wavenumber) to mimic rapid dissolution in the mouth. Lastly, the dissolution profile of the films was predicted using artificial neural network (ANN) modelling, incorporating parameters of time, absorbance, UV-Vis wavelength, FT-IR wavenumber, and dissolution profile. This

study provides predictive modelling for formulation improvements and potential commercial developments.

This study was limited to laboratory-scale fabrication and in vitro evaluation of electrospun PVA/κ-carrageenan oral dispersible films. Kelulut honey and ascorbic acid were investigated as two separate formulation systems rather than as a combined formulation. The dissolution studies were performed under simulated saliva conditions, which may not fully represent the complexity of the human oral environment. Although UV–Visible spectroscopy and FT-IR provided reliable analytical measurements, both techniques possess inherent limitations, including spectral interference and simplified simulation of oral dissolution. Furthermore, the developed ANN model was trained and validated using the experimental data generated within the investigated formulation range. Consequently, the prediction capability of the model is reliable only within this experimental domain and should not be extrapolated to untested formulations without additional validation.

CHAPTER 2
LITERATURE REVIEW

2.1 Introduction

This chapter reviews the current state of knowledge related to electrospun oral dispersible films (ODFs), with emphasis on hydrophilic polymer systems, natural functional ingredients, dissolution behaviour, and predictive modelling using artificial neural networks (ANNs). The discussion begins with the fundamental principles and advantages of ODFs, followed by the selection of polyvinyl alcohol (PVA) and κ-carrageenan (κ-car) as the polymer matrix for electrospinning. The physicochemical properties and functional roles of Kelulut honey and ascorbic acid are then discussed in relation to their influence on electrospinnability, fibre formation, mechanical properties, and dissolution behaviour. Subsequently, the principles of electrospinning, factors affecting nanofibre formation, and dissolution evaluation techniques are reviewed. Finally, the application of ANN as a predictive tool for formulation optimisation and dissolution behaviour is presented to establish the scientific basis of this study.

2.2 Oral Dispersible Films (ODFs)

Oral dispersible films (ODFs) are thin polymeric dosage forms designed to rapidly disintegrate or dissolve upon contact with saliva without requiring water for administration. The rapid dissolution characteristic enables the active ingredient to become readily available in the oral cavity, making ODFs particularly suitable for paediatric and geriatric patients. Many studies have been conducted to fabricate ODFs (Abou - taleb et al., 2022; Qin et al., 2019; Abdelhameed et al., 2023; Olechno et al., 2022; Tedesco et al., 2016; Olechno et al., 2022; H. J. Shin et al., 2023). Compared with conventional tablets and capsules, ODFs provide improved patient compliance, ease of administration (Abou-taleb et al., 2022), dose flexibility, and faster onset of action due to their thin structure and large surface-area-to-volume ratio.

Besides serving as pharmaceutical dosage forms, ODFs have recently attracted considerable attention as carriers for nutraceuticals, functional ingredients, vitamins,

antioxidants, and natural bioactive compounds. The increasing demand for rapidly dissolving oral delivery systems has encouraged the development of electrospun nanofibrous ODFs, which provide significantly higher porosity and surface area than solvent-cast films. Consequently, electrospun ODFs generally exhibit faster water penetration, more rapid dissolution behaviour, and improved ingredient availability in the oral cavity (Sapiee et al., 2023). This study uses *kelulut* honey as the best natural functional ingredient due to its high level of phenolic compounds, flavonoids, vitamins, minerals, and enzymes, among other bioactive constituents. Compared to regular honey, *kelulut* honey has high moisture content, low pH, and other unique physicochemical properties, which may influence the viscosity, conductivity, the ease of electrospinning, the mechanical properties, the fibre morphology and the dissolution behaviour of electrospun ODFs (Agasi et al., 2021; Nordin et al., 2018). Being unique, Kelulut honey is an attractive natural ingredient for use in oral systems that rapidly dissolve, yet it still has some formulation challenges that require optimisation. As a water-soluble API that is an antioxidant with a broad range of uses in the pharmaceutical and nutraceutical industries, ascorbic acid was selected as the model API. Ascorbic acid was an effective delivery system essential to ensure its rapid dissolution and maintain its stability. Electrospun ODFs provide a suitable platform to investigate the formulation challenges and the dissolution of ascorbic acid, a highly water-soluble API.

Electrospinning was selected in this study because it is capable of producing ultrafine continuous nanofibres with exceptionally high surface-area-to-volume ratios, interconnected porous structures, and high porosity. These characteristics facilitate rapid saliva penetration and faster dissolution than conventional solvent-cast films. In addition, electrospinning is performed under relatively mild processing conditions, making it suitable for incorporating temperature-sensitive functional ingredients such as honey and ascorbic acid. The resulting nanofibrous structure also enhances flexibility, uniform ingredient distribution, and rapid oral dissolution, making electrospinning one of the most promising fabrication techniques for ODF development.

Hydrophilic polymers are very important for the manufacture of ODFs because they are very quickly soluble in aqueous environments. Such polymers include pullulan (Qin et al., 2019), pectin, alginate, chitosan (Qin et al., 2019), gelatin (Tedesco et al., 2016), starch, carboxymethyl cellulose, hydroxypropyl cellulose, polyvinylpyrrolidone

(PVP) (Abdelhameed et al., 2023), polyethene glycol (PEG) (Yasin et al., 2023), and polyvinyl alcohol (PVA) (Sapiee et al., 2023; Kozakiewicz-Latała et al., 2024), HPMC (Olechno et al., 2022) are commonly utilised in the production of orally dispersible films (ODF) (Celebioglu & Uyar, 2019). Among these, PVA is attractive because of its excellent film-forming ability, strong mechanical properties and good biocompatibility. The efficiency of ODFs had improved with the addition of natural ingredients incorporated into polymer solutions, which enabled them to perform as a drug delivery system or supplements. Besides serving as supplements, ODF can be advantageous in situations necessitating the swift administration of high nutrient doses.

Recent improvements in the fabrication of ODFs have been very beneficial for the performance of the films. Among these, electrospinning has proven to be an effective method in the fabrication of ODFs, as it provides a better surface area and dissolution profile than traditional solvent casting methods. Electrospun ODFs dissolved quickly and released their active ingredients more rapidly. ODFs serve as a delivery medium for active ingredients, including ascorbic acid and honey, with a PVA-based nanofibrous matrix.

2.3 Materials for Electrospun Polymeric Films

2.3.1 Polyvinyl Alcohol (PVA) & Polymers Used to Fabricate ODFs.

Polyvinyl alcohol (PVA) exhibits a diverse array of practical applications, attributed to its hydrophilic and biocompatible characteristics (Tran et al., 2024). This is a vinyl polymer that is interconnected through carbon-carbon linkages (Chopra et al., 2022). The composition of PVA includes different quantities of secondary alcohol groups, which are influenced by the degree of hydrolysis. This variation subsequently affects the polymer's chemical properties, solubility, and crystallinity (KOTA et al., 2024). Polyvinyl alcohol (PVA) is classified as a water-soluble synthetic polymer (Stoica et al., 2023) and can be easily sprayed into fibres as a solution. It exhibits chemical resistance and suitable physical properties for film formation (Tran et al., 2024). PVA is extensively utilised in biomedical applications because of its remarkable biodegradability, biocompatibility, chemical resistance, and favourable fibre-forming characteristics (El-attar et al., 2022). PVA is selected due to its straightforward preparation, effective adhesive and emulsifying properties, film-forming capability,

favourable mechanical properties, excellent chemical resistance, and barrier properties against oxygen and odours (Stoica et al., 2023). With its high tensile strength and flexibility, resistance to oxygen, and capacity to preserve the scent of active components within the film, polyvinyl alcohol (PVA) is an efficient film-forming agent distinguishable from others. Acting as a plasticiser, the water will reduce the tensile strength of the film while increasing elongation and grip strength.

A study by Abou-taleb et al. (2022) investigated the ODFs that were produced using vardenafil as an API. The polymers used in this study are PVA, MC, SA, and PVP K30 to fabricate the ODFs in the mouth without a large amount of water to ingest the ODFs. This research aims to prepare the vardenafil ODF and three selected sweetening agents (sorbitol, acesulfame potassium and sucralose). The analyses used were FT-IR (range of 400 to 4000 cm^{-1}), an in-vitro study. Vardanefil peak is around 340, 2900, 1720, 1650 and 1600 cm^{-1}. The stretching of C=C appeared at 1680 and 1620 cm^{-1}. For dissolution testing (in-vitro), the release medium used was saliva fluid (pH 7 at a temperature of 37°C) in 500 mL, and the sample was withdrawn at specified intervals ranging from 5 to 60 minutes. The result shows the fully dissolved vardenafil ODFs when they reached a certain time or number of minutes. The method used to produce the ODFs in this research is hot-melt extrusion.

Based on a study conducted by Qin et al. (2019), the fabrication of the ODFs was made from pullulan and chitosan by dissolving them in 50% v/v. The polymer content for C/P blend solutions is 10% w/v and the weight ratios used were 0/100, 10/90, 20/80, 30/70, 40/60, 50/50 and 60/40. The ODFs are prepared using an electrospinning method where the flow rate was 0.5mL/h, the voltage was 15 kV, distance from the collector plate was 10 cm. One of the analyses used is FT-IR, where it was used to detect the desired ingredient in the ODFs in the range of 4000 and 4 cm^{-1} for O-H, N-H, C-H and C=O. Another study conducted by Islam et al. (2023) shows that hydroxypropyl methylcellulose (HPMC 2208) blended with loratadine is produced by using hot-melt extrusion, and in vitro analysis in simulated saliva (pH 6.8) and acid solution (pH 1.2), while the FT-IR is in the wavelength range 500-4000 cm^{-1}.

A study conducted by Abdelhameed et al. (2023) shows the ODFs that have been produced using the solvent casting method. In this method, the desired ingredient used was FEX, while the polymers used were carboxy methyl cellulose (CMC), sodium starch glycolate (SSG) and Tween 80 (0.05% w/v), mannitol (0.1% w/v and glycerol

(1.25% w/v). The ODFs were fabricated using the solvent casting method, where the solution was poured into a glass Petri dish. An in vitro study was analysed in the 900 mL phosphate buffer with a pH of 68, and the sample was taken at intervals of every 2 minutes in a 5 mL syringe. A study conducted by H. J. Shin et al. (2023) shows the ODFs that were fabricated using a film applicator. The desired ingredient uses 4g of vitamin C (ascorbic acid) as well as catechin (CAT) that was dissolved in distilled (DI) water with a molar ratio of vitamin C: CAT, 1:0, 1:0.2, 1:0.4, 1:0.6, 10.8, 1:1. The in vitro study was conducted in simulated saliva (pH 6.8) and other two fluid which was simulated gastric fuid and intestinal fluid (pH 1.2 and pH 6.8 respectively). A study conducted by Cheng et al. (2024), the polymer used pullulan (20 wt.%) and xanthan gum (1.5 wt.%) as a source of vitamin C with different weight percentages. The electrospinning method was used to fabricate the ODFs with a voltage of 20 kV, a flow rate of 1mL/hr, and a distance between the needle and collector plate of 15.5 cm. A study conducted by Olechno et al. (2022) shows that the ODFs were prepared by the solvent casting method from a solution made of Hypromellose (HPMC) (in a concentration of 12%), glycerol (50% w/w of the polymer) and purified water. SEM analysis showed that the ODFs were smooth and spherical in shape, while in the dissolution part, the films dissolved in less than 30 seconds, in compliance with drug regulations and maintained drug content and uniformity. Lee et al. (2017) conducted a study to fabricate an ODF. In this study, the polymer used was Hydroxypropyl methylcellulose (HPMC), and the ingredients were sildenafil citrate (SC), and the fabrication method used was solvent casting. Results obtained from this study showed that SEM images of their surfaces and cross sections were non-porous and homogeneous. Contact angle results showed the films have moderate hydrophilicity and are suitable for oral mucosal applications without irritation. The improved ODFs had a biphasic release profile with rapid release in the first 10 minutes (Phase I) due to hydration and disintegration of the films, followed by a sustained release (Phase II).

Tedesco et al. (2016) conducted a study to fabricate ODF using Gelatin (GEL) and HPMC, and the method used was the solvent casting method. The results obtained showed that the film exhibited heterogeneous surfaces with discontinuities. The contact angle decreases with the increase of HPMC, which indicates that HPMC improves the hydrophilicity of the films. All films dissolved within 60 seconds, and the tensile strength decreased as the HPMC increased, significantly increasing the elongation and

enhancing flexibility. A study conducted by Yasin et al. (2023) showed a few technique in fabricate hydrogel blended with honey, which were film casting, electrospinning and hydrogel formation. Polymers used were separated into two types, which were natural and synthetic polymers. Natural polymers consist of chitosan, alginate, hyaluronic acid, cellulose, starch, and gelatin, while synthetic polymers include polyvinyl alcohol (PVA), polyacrylamide, and polyethene glycol (PEG). Zhang et al. (2020) conducted a study to create a fast-dissolving drug delivery using PVA and deep eutectic solvent (DES) with honey. The techniques used were electrospinning to produce films. The average diameter for PVA-DES-honey nanofibers was lower (~466.8±113.4 nm) due to the increased solution conductivity with the addition of honey. The drug-loaded nanofibers showed rapid dissolution in water and artificial saliva, indicating a rapid drug release.

Sapiee et al. (2023) conducted a study to fabricate ODF using PVA, ascorbic acid and κ-carrageenan by electrospinning. The results obtained showed that the diameters of the fibres were between 190 nm and 490 nm. The 8% vitamin C sample had the minimum mean diameter of 196 nm; thus, the mean diameter decreased with increased vitamin C content. All samples were found to be hydrophilic (WCA<90°) and were found to quickly disintegrate in water (under 5 seconds). Table 2.1 shows summarize of electrospinning materials and formulations used in past studies. Various polymers, such as HPMC, pullulan, chitosan, PVP, and others, have been evaluated for the development of orally dispersible films (ODFs). Compared to the standard methods of film fabrication, the benefits of using an electrospinning technique include the formation of ultrafine, high surface area to volume ratio nanofibers. These features are advantageous to ODFs as they promote excellent dissolution and good incorporation of the active ingredients. Water solubility, biocompatibility, and ease of electrospinning make PVA a good candidate as a synthetic polymer in ODFs. However, pure PVA films can be too sensitive to moisture and lack good mechanical properties. Blending PVA with natural polymers such as κ-carrageenan can add structural and mechanical enhancements to the films. PVA-based ODFs that have been electrospun have yet to have as many natural functional ingredients incorporated into them as *kelulut* honey and ascorbic acid. There is a lack of research in the area of assessing the effects of *kelulut* honey and ascorbic acid on the morphology and structure of electrospun ODFs and their mechanical properties, as well as their wettability, dissolving behaviour, and predictive

models of the ODFs. This research aims to address this lack by manufacturing and characterising electrospun ODFs based on PVA/κ-carrageenan and incorporating different ingredients using *kelulut* honey and vitamin C as separated formulation.

Table 2.1:
Electrospinning Materials Used in Past Studies

Study	Polymer/Formulation	Fabrication method	Structures	Applications
Abou‐taleb et al., (2022)	PVA, MC, SA, PVP K30	Hot-melt extrusion	Film	ODF
Qin et al., (2019)	Pullulan/Chitosan	Electrospinning	Film	ODF
Islam et al., (2023)	Hydroxypropyl methylcellulose (HPMC)	Hot-melt extrusion	Film	ODF
Abdelhameed et al., (2023)	Polyvinyl Pyrrolidone K25 (PVP K25)	Solvent casting	Film	ODF
H. J. Shin et al., (2023)	Hyaluronic acid (HA)/catechin (CAT)	Cast by the film applicator	Film	ODF
Cheng et al., (2024)	Pullulan (PUL)/Xantham gum	Electrospinning	Film	ODF
Kozakiewicz-Latała et al., (2024)	PVA	Solvent casting	Hydrogel	Drug delivery
Olechno et al., (2022)	Hypromellose (HPMC)	Solvent casting	Film	ODF
Lee et al., (2017)	Hydroxypropyl methylcellulose (HPMC)	Solvent casting	Film	ODF
Tedesco et al., (2016)	GEL/HPMC	Solvent casting	Film	ODF
Yasin et al., (2023)	Chitosan, alginate, cellulose, PVA, polyethene glycol (PEG)	Film casting, Electrospinning, composite hydrogel formation	Hydrogel	Wound healing
Zhang et al. (2020)	PVA/DES	Electrospinning	Film	ODF
Sapiee et al., (2023)	PVA/κ-car	Electrospinning	Film	ODF

PVA is highly hydrophilic and readily soluble in water, yet it possesses excellent film-forming ability, fibre-forming capability, flexibility, and mechanical stability. These seemingly contrasting characteristics enable electrospun PVA nanofibres to remain mechanically stable during handling while rapidly dissolving upon contact with saliva. Therefore, PVA is widely regarded as one of the most suitable synthetic polymers for electrospun oral dispersible film applications.

2.3.2 Kappa-Carrageenan (κ-Car)

A special form of carrageenan, a hydrocolloid extracted from particular seaweeds, particularly those of the species *Kappaphycus alvarezii* and *Hypnea musciformis*, is called Kappa carrageenan. Its capacity to form robust, stiff gels in the presence of potassium ions makes it very advantageous in food and medicinal applications. It is used in the pharmaceutical industry for its gel-forming properties, biocompatibility, and ability to modify the structural properties of polymeric formulations. As an excipient in pharmaceutical formulations, it helps increase the stability and release characteristics of the desired ingredient. Kappa carrageenan is a desirable gel former for the preparation of release systems to enhance the therapeutic benefits of pharmaceuticals. For this reason, κ-car is highly valuable in a drug delivery system. In ODFs, κ-car acts as a controlled release of diffusion drug particles. This is especially beneficial when used with the highly water-soluble desired ingredient, ascorbic acid, which, when processed alone, is prone to rapid release. Thus, κ-car can hinder drug release by forming a matrix within the polymer and acting as a barrier (Zhou et al., 2021). Aside from drug delivery, κ-car has been proven to possess bioactive compounds with antibacterial and wound-healing properties. The gelling properties of the material provide a coating over wounds with the formation of a protective barrier without inhibiting the moisture environment, which supports healing. Kappa carrageenan can inhibit the bacteria themselves and help cells migrate, both critical for optimum wound healing. Besides, it is biocompatible, such that it does not elicit an unfavourable response when utilised on injured tissue (Popescu & Boscornea, 2007). Kappa carrageenan is a versatile polysaccharide and is found within the pharmaceutical and wound healing sectors. For this research, κ-car is incorporated into electrospun PVA-based ODFs to control dissolving behaviour and balance the stability of the formulation. With the combination of PVA, κ-car, honey and ascorbic acid this work

attempts to establish a polymeric matrix with the characteristics of rapid dissolution and controlled release.

2.3.3 *Kelulut* Honey

Kelulut honey, derived from stingless bees of the subfamily Meliponini (Apoidea), is well distributed in tropical countries, namely Malaysia. *Kelulut* honey was characterised by higher moisture content, acidic pH, and the presence of phenolic compounds and flavonoids, thus increasing its antioxidant, antibacterial, anti-inflammatory, and wound-healing properties (Ali et al., 2023; Kassem et al., 2023). In Malaysia, *kelulut* honey has been used traditionally as a natural remedy due to its antioxidant, antibacterial and wound-healing properties. It has served as a medicinal agent and has also been utilised to address burns, severe injuries, and periodontitis (Naskar et al., 2024). Kelulut honey contains many bioactive compounds, including phenolic acids, flavonoids, vitamins, enzymes, amino acids, as well as organic acids, which contribute to its antioxidant, antibacterial and anti-inflammatory effects and wound healing properties. Moreover, its relatively high moisture and acidic properties distinguish it from many other types of honey. The nature of honey also enhances the initial wetting of ODFs once in contact with saliva. This is important to enable the films to achieve rapid release, as the saliva is absorbed into the matrix of the films to accelerate dissolution. In electrospun nanofibrous fibres, honey may also contribute to adding viscosity and conductivity, which may influence the fibre diameter and pore size as well as the overall morphology of the fibres. Unique physicochemical properties of Kelulut honey, such as high moisture content and naturally occurring sugars, may influence the viscosity and conductivity of the electrospinning solution. These characteristics affect fibre production, diameter and dissolution properties that make Kelulut honey an attractive functional agent for electrospun oral dispersible films. Considering the extensive uses of honey in healing and oral care, very little attention has been given to the use of honey in electrospinning ODFs. Current honey studies consider the medical uses of honey, especially in the management of oral ulcers, burns and infections, instead of looking at honey as a functional excipient in drug delivery systems (Shirzaiy et al., 2022; Siddeeq & Al-Douri, 2008). The properties of *kelulut* honey have been established over the years, and although much has already been published on its antibacterial and wound-healing attributes, few studies have explored

its use in electrospun oral dispersible films. The data about the effect of *kelulut* honey on electrospinning properties, nanofiber morphology, mechanical properties, and dissolving characteristics is still limited, which indicates that further studies are needed.

In this study, *kelulut* honey is used not only as a natural sweetener but also as a multifunctional ingredient that modifies the mechanical properties, fibre morphology and dissolution behaviour of electrospun PVA-based ODFs. Incorporating *kelulut* honey (Figure 2.1) into films is a unique method to improve the sweetness and dissolution of the films, which supports the objective of this research to synthesise and characterise novel formulations of PVA-based ODFs and to evaluate their dissolution profiles in simulated saliva.

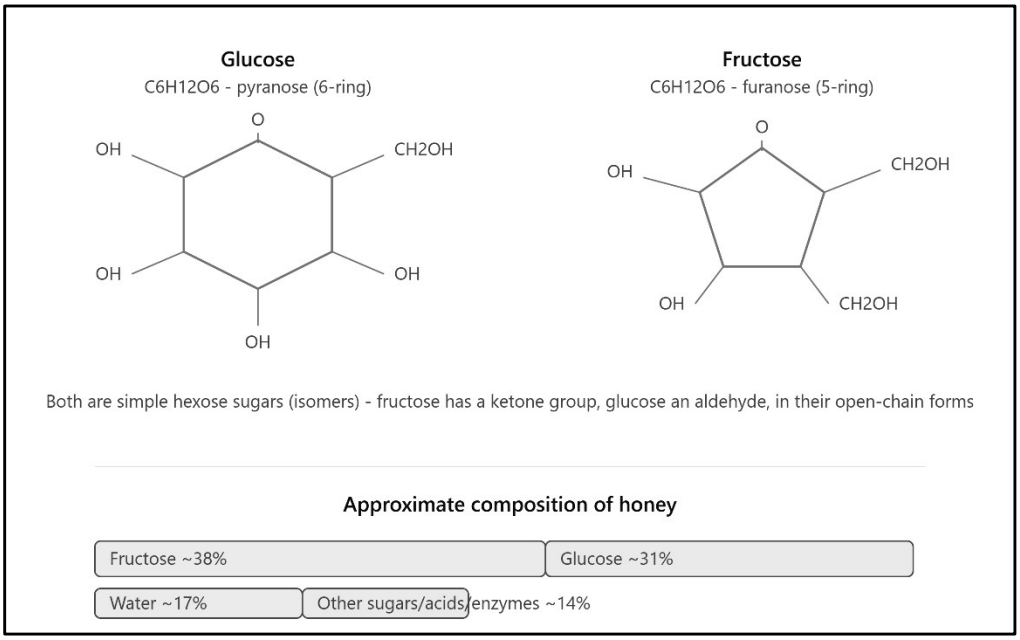


Figure 2.1: Honey Structure (Trigono Stingless Bee)

2.3.4 Ascorbic Acid (Vitamin C)

Ascorbic acid (AA), commonly referred to as vitamin C, is a six-carbon actone that structurally resembles glucose. The instability of AA restricts traditional pharmaceutical manufacturing processes, particularly those involving higher temperatures and extended processing times. For example, the hot-melt extrusion may promote the thermal degradation of sensitive compounds such as ascorbic acid, even though it is a relatively efficient method for producing uniform films. Consequently, alternative processing techniques that minimise heat and oxidative damage are required

to preserve the chemical structure and therapeutic properties of vitamin C. In this regard, electrospinning has the advantage of typically being conducted at room temperature. The rapid formulation of nanofibrous structures and the possible enhancement of stability for ascorbic acid within the polymer matrix are likely to improve encapsulation efficiency. Whenever AA is mixed in hydrophilic polymers, such as PVA, its distribution becomes uniform, which aids in the release kinetics of the formulation. In ODFs, AA is notable because it becomes dissolvable in saliva and provides action very rapidly, which can cause a range of dissolving profiles. Hydrogen bonding is the primary interaction between PVA and ascorbic acid, which alters the mechanical properties and dissolution of the film. Data-driven approaches like ANN have begun to model dissolution processes based on experimental data.

Ascorbic acid was utilised in this work to model an active pharmaceutical component to study dissolving behaviour in electrospun PVA-based ODFs. ODFs' sensitivity to both formulation and processing conditions, along with their swift dissolution, provides an extensive dataset for ANN-based prediction. This supports almost directly the aim of analysing dissolution behaviour through empirical methods and predicting drug release through ANN. AA is a vital nutrient for human health, predominantly sourced from fruits and vegetables. The food, beverage and pharmaceutical industries constitute a significant market for this vitamin, exceeding 50% (Blaga & Malutan, 2012). A deficiency in vitamin C has been associated with various health conditions such as infection, obesity, cardiovascular disease, cancer, diabetes, ocular disease, neurodegenerative disorders, mental health issues, dermatological conditions, and reproductive system diseases (Tuna et al., 2023). This vitamin is water-soluble and is essential for the immune system, as it enhances the production of white blood cells, particularly lymphocytes. Several studies indicate a potential association between high vitamin C intake and improved outcomes in cancer cases. Further investigation is required to comprehensively elucidate this relationship. Vitamin C is essential for numerous physiological functions, and a balanced diet is the most effective means of obtaining adequate amounts.

2.4 Fabrication Methods for Nanofibrous Films

Many methods have been used to form or make the nanofibers. Below are the types of methods used for fabricating the nanofibers.

2.4.1 Electrospinning: Principles and Parameters

William Gilbert initially presented the concept of electrospinning in an earlier study. Gilbert observed the formation of conical water droplets in the presence of an electrical field (Xue et al., 2019). In most common electrospinning setups, a polymer solution is supplied into a syringe with an attached metal needle (spinneret) and a high voltage is applied between the needle and a collector, which is grounded. Electrospinning is a multifaceted method employed to transform solutions, suspensions, or melts into elongated fibres with diameters in the nanometre or micrometre range (Cleeton et al., 2019). The electrospinning process is particularly effective for generating compound-encapsulated nanofibers. It provides several benefits, such as its direct and uncomplicated procedure, economic efficiency, and lack of heating necessities (Gao et al., 2021). Electrospinning occurs when the electrostatic force overcomes the surface tension present in the polymer solution. In such a case, a charged jet is ejected from the needle tip, shaped like a Taylor cone. The jet can travel towards the collector, and it is subjected to stretching and thinning due to the solvent evaporating rapidly, and is electrostatically repelled by the collector, where a surface is prepared to receive the ejected nanofibers (Qin et al., 2019).

The fibres are deposited and accumulated on the collected plate, which results in a nanofibrous mat. Among the benefits of using electrospinning in the production of ODFs is the potential for creating saliva-dispersible nanofibers. With the small diameter of electrospun fibres, the resulting film will dissolve and release the desired ingredient more rapidly. This characteristic is particularly advantageous for creating ODFs, which act as fast oral delivery systems (Sapiee et al., 2023). The quality of electrospun fibres and their morphology are impacted by processing parameters including voltage, solution flow rate, tip-to-collector distance and solution parameters (viscosity, conductivity). Thinner fibres are produced at higher voltages because they encourage jet instabilities, which lead to the formation of beads. In addition, the flow rate determines the volume of polymer solution introduced to the needle tip.

The polymer jet, as well as the rate of evaporation of the solvent, is influenced by the distance between the tip and the collector plate. Figure 2.2 shows the schematic diagram for the electrospinning technique. Continuous fibres can only be produced when the solution viscosity is adequate, as too low a viscosity will lead to the formation of beads, while too high a viscosity will make it difficult to propel the jet. The use of electrospinning technology for the creation of the rapidly dissolving ODFs has been documented in some literature. Studies conducted by Qin et al. (2019) show the electrospinning of ODFs at a voltage of 15 kV, a flow rate of 0.5 mL/h, and a collector plate distance of 10 cm. The author produced nanofibrous films with rapid disintegration times. Because of this study, it can be concluded that the electropinning parameters must be changed to obtain the desired films.

In contrast to traditional casting and film-forming techniques, such as solvent casting, electrospinning techniques offer a better way to fabricate the ODFs. Moreover, it has emerged as a preferred method owing to its beneficial attributes, including the capacity to improve the surface-to-volume ratio, leading to the effective dissolution of the ODF and favourable outcomes (Sapiee et al., 2023). It is also effective for the wound healing application, as increasing the surface area of the thin film increases the release.

Electrospinning may produce an independent matrix of these nanofibers, which provides sufficient strength for the rapid release of the main ingredients. The integration of this composite material is engineered to rapidly release vitamin C over time, ensuring a constant therapeutic administration (Calzado-Delgado et al., 2023).

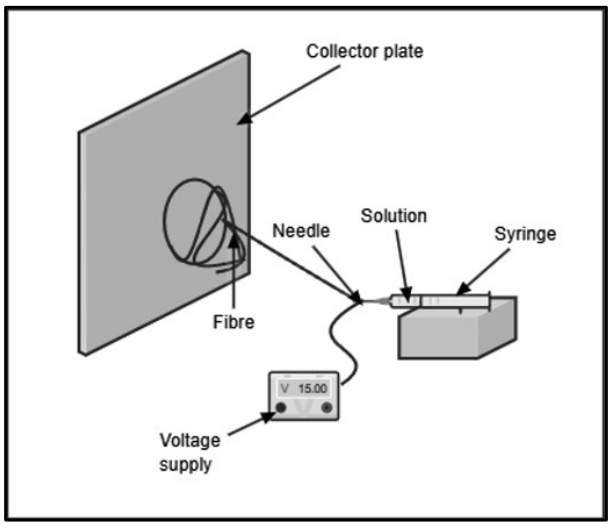


Figure 2.2: Electrospinning Schematic Diagram

The production of ODFs by electrospinning has been relatively underexplored. Rohani Shirvan et al. (2022) studied the fabrication of an electrospun mucoadhesive buccal film (PVA/chitosan) employing electrospinning techniques and solvent casting. The study utilised 3% w/v of chitosan, 2% v/v and 8% w/v of PVA solution with a ratio of 80:20. The parameters include a needle-to-collector plate distance of 12 cm, a voltage applied of 15 kV and a flow rate of 0.2 mL/hr. The result showed that electrospun ODFs had a better hydrophilicity value, which was supported by the higher water contact angle result compared to solvent casting, and also, it was brittle as it could not be handled without cracking when mechanical testing was conducted on it. The result also showed a fast release of the desired product when doing the in-vitro study because of the large surface area of electrospun ODF compared to the film from casting. Bakar et al. (2023) fabricated ODFs using PVA/κ-car. The formulation consisted of 10, 11, 12 and 13 w/v% concentration of PVA and κ-car utilised in a ratio of 70:30. Parameters used include a 5 mL syringe, flow rate was set at 0.3mL/hr, the needle-to-collector plate was 15 cm with an applied high voltage of 12 kV with a 23-G needle size. The result shows that the contact angle measurement decreases with increasing PVA FH (MW:145000g/mol) concentration in the nanofibers blend.

Another study conducted by Qin et al. (2019) fabricated the ODF for drug delivery prepared from chitosan/pullulan electrospinning nanofibers. The ODF was blended with various ratios (0:100, 10/90, 20/80, 30:70, 40:60, 50:50, and 60:40) in 10% (w/v) solution concentrations. Parameters used in electrospinning include a needle with a 0.8 mm internal diameter, 15 kV voltage, a flow rate of 0.5 mL/hr, and a tip-to-collector distance of 10 cm. Blend ratios of 0:100 and 10:90 form a spherical-like structure compared to a smooth fibre, while 30:70 produces the smallest diameter of nanofibers (51 nm). Two different ratios of 0:100 and 30:70 nanofiber films were dissolved in drops of water within 60 seconds. A study conducted by Khan et al. (2023) shows the preparation of L-ascorbic acid/HP-β-Cyclodextrin (LAA/HP-β-CD) inclusion complex-incorporated electrospun nanofibers. The electrospinning parameters were a 1 mL syringe and needle (21G), the flow rate was set to 0.5 mL/hr, the applied voltage was 15 kV, and the tip-to-collector distance was 15 cm with a 200% w/v concentration solution (LAA/HP-β-CD). The average fibre diameter was ~399 nm.

Ma et al. (2023) conducted a study regarding the fabrication of Polyacrylonitrile (PAN) using electrospinning. The solution was prepared at different concentrations of

6, 8, 10, 12, 14 and 16 wt%. Parameters of electrospinning are syringe (10 mL), needle (22G), voltage (10 kV – 22 kV), tip-to-collector (12 cm to 22 cm) and flow rate (0.1 mL/hr to 0.5 mL/hr). The uniform and smooth fibre was at a concentration of 12 wt% with a spinning voltage of 14 kV, a flow rate of 0.4 mL/hr, and a tip-to-collector distance of 20 cm. A study conducted by Kanimozhi et al. (2020) shows the fabrication of PVA/honey nanofibrous. The concentration of PVA was 8 wt%, while 50% of honey was diluted to prepare 1 – 4 mL. The electrospinning parameters employed were solution flowrate was 0.06 – 0.001 mL/min, distance between collector and syringe of 5 to 20 cm, applied voltage of 10 – 16 kV and needle size 22G. Flow rate 0.06 mL/min leads to spherical-shaped particles, and 0.001 mL/min leads to a smooth fibre formation. It also stated that as the honey increases, the size of the fibres formed increases because at a higher concentration of honey (4 mL), a thicker and smoother fibre is produced. Releasing honey for fibre at 4 mL was high compared to others.

Liu et al. (2023) studied the fabrication of PVA-aloe gel (ANFMs) by dissolving 6%, 9% and 12% w/v PVA. Parameters used in electrospinning to fabricate the film were a voltage of 8 – 10 kV, with a needle-to-collector plate distance of 10 cm. Results obtained from this film show that 9% ANFMs were uniform and similar to 9% PVA nanofibers, whose diameters both range in 1-2 μm, and also sustained the highest tensile stress while maintaining excellent elasticity. El-attar et al. (2022) conducted a study on the fabrication of electrospun synthesis and antibacterial and wound healing activities, where 10g of PVA was used with snail mucus and AgNPs-SM (3% each) and the electrospinning was performed using an 18G needle, an applied voltage of 25 kV and a flow rate of 1 mL/hr. The nanofibrous fibres had a homogenous structure with a fine diameter of about 100 – 170 nm. The release profile shows a sharp release during the first 6 hours, with a sustained release that lasted until 78 hours.

Sukum et al. (2023) conducted a study of poly (vinyl alcohol)/chitosan and PEG 400 plus Mangifera indica leaf extract electrospun nanofibers. By mixing PVA (4.5% w/v) and chitosan (0.05% w/v) in distilled water, and also poly (ethylene glycol) 400 in a ratio of 9:1:0.5. A 22G needle was used with 20 kV voltage and also a needle tip and collector plate distance of 15 – 20 cm. The SEM image shows smooth fibres with fewer beads formed. Suflet et al. (2022) conducted a study on phosphorylated curdlan gel/polyvinyl alcohol electrospun nanofibres loaded with clove oil. The PCurd/PVA solution with 6% w/w and 10% w/v, respectively undergo electrospinning process. The

parameters used were 22.7 kV voltage, flowrate of the solution was 10μL/min, distance needle tip to the collector plate of 14 cm and a 5 mL syringe and 25G needle. The average diameter of nanofibres decreases from 235 nm to 115 nm with an increasing PCurd content. The presence of PCurd led to decreases in elongation at break from (16.08%) to 25PCurd/PVA (7.58%) and 50PCurd/PVA (2%). The release profiles show a faster release in the first 8 hours (52%), followed by a slow and continuous release for the subsequent 48 hours. A total of 85% of the CEO was released after 24 hours.

Shahid & Khan (2022) conducted a study of an electrospun nanofiber membrane from polyvinyl alcohol loaded with Glycyrrhiza glabra extract. The solution was made by mixing liquorice extract and 10% w/v of PVA in a ratio of 40%, 30%, 20%, 10% and 0% of PVA and 60%, 70%, 80%, 90% and 0% of liquorice extract. For the electrospinning setup, a 30 mL syringe, a 22G needle, and a high voltage supply (-20 kV to +50 kV) were applied. The average fibre diameter was 245.54 ± 55.19 nm at a magnification of 7.5K. Uddin et al. (2022) conducted a study on electrospun nanofibers using nigella/honey/garlic/olive oil co-loaded PVA (PNH, PGHO and PVA). For the electrospinning process, 5 needles of 20G were used. The flow rate was between 1.5 mL/hr and 2.5 mL/hr, the tip-to-collector-plate distance was 15 cm, and the applied voltage ranged between 20 and 24 kV. It was shown that PVA had an average diameter of 230 ± 20 nm, PNH had an average diameter of 150 ± 10 nm, and PGHO had an average diameter of 170 ± 10 nm, with mesh and tiny porous structures and also fibres demonstrated slight stickiness due to the addition of honey. A study conducted by Celebioglu et al. (2022) shows a fabrication of ODFs using resveratrol/cyclodextrin, resveratrol/HPβCD, (hydroxypropyl-β-cyclodextrin), resveratrol/HPγCD (hydroxypropyl-γ-cyclodextrin) and pullulan, where the concentrations for both of the materials were 180% w/v and 20% w/v, respectively. The fabrication of the ODFs was by the electrospinning technique, using a 23G, flowrate, high voltage and needle, to collector distance was applied as 0.5 mL/hr, a high voltage of 15 kV and a collector distance of 15 cm. Resveratrol/CD nanofibrous films were able to complete total dissolution and form clear solutions in less than 2 s, while there was still a remaining layer of undissolved sample in the vial after 15 s in the case of the resveratrol/pullulan nanofibrous film.

Cheng et al. (2024) conducted a study on the fabrication of ODFs by vitamin C-loaded electrospun nanofibers of a mixture of polysaccharides of pullulan/xanthan gum.

Pullulan (20 wt%) and XG (1.5 wt%) were dissolved in DI water in various ration (10:0, 9:1, 8:2, 7:3, 6:4, and 5:5 respectively). In addition, Vitamin C was added (5 wt%, 10 wt%, and 15 wt%) into P9X1 solution named P9X1V5, P9X1V10, and P9X1V15, respectively. The solution was added into a 10 mL syringe with a 22G needle. The voltage, flow rate and needle-to-collector-plate distance applied were 20 kV, 1mL/hr and 15.5 cm, respectively. The tensile strength and elastic modulus increase after adding 5 wt% VC, but with further increase in VC content, the values gradually decrease. The elongation at break also decreases from 20.30% to 12.11% as VC increases, indicating that the addition of VC weakened the flexibility of the nanofiber film. Nanofibrous films were fully dissolved in water within 3s. The continuous and bead-free nanofibers with average diameters ranging from 181.17 nm to 260.84 from SEM analysis.

Okur et al. (2021) conducted a study on polyvinyl alcohol nanofiber webs containing β–cyclodextrin/Vitamin C inclusion complex. In this study, the concentration of PVA (6% w/v), β–CD (17%, 25% and 33% w/w) with respect to PVA and Vitamin C were 3%, 4% and 5% (w/w) with respect to PVA. The parameters used consist of flow rate, which was 1 to 1.5 mL/hr (best 1 mL/hr), voltage applied, which was 15 to 27 kV (best 18 kV), and the distance from the needle tip to the collector plate was 10 cm to 19 cm (best 18 cm). Bead-free nanofiber was produced with a fibre diameter of fiber ranging from 265 to 387 nm.

A study conducted by Kassem et al. (2023) shows that electrospun nanofibers from manuka honey@PVP enclosing chitosan-titanate are highly effective for wound healing. A 15% w/v PVP solution was mixed with Manuka honey following volume per cent ratios of Manuka honey to PVP v/v%: 1:3 (25%), 1:4 (20%), and 3:17 (15%). Electrospinning produces the best results at a 1 mL/hr flow rate, 19 kV applied voltage and 18 cm collecting distance. The result shows that as the concentration of honey increases, the tensile strength increases while the water contact angle decreases, proving the hydrophilicity of the nanofibers. The average diameter of Mh@PVP nanofibers increased (37 to 368 nm) as the honey concentration was increased from 15 to 25%. Zhang et al. (2020) conducted a study on the fabrication of green poly(vinyl alcohol) nanofibers using a natural deep eutectic solvent for fast-dissolving drug delivery. An electrospinning solution of PVA (8% w/v), DES (5% w/v) and honey (5% w/v) is prepared for ODFs and filled into a 10 mL syringe with a needle. The flow rate, distance from the needle tip to the collector plate and voltage are 0.75 mL/hr, 13 cm and 23 kV.

The diameter distribution of the fibre is 466.8±113.4 nm. Which likely because of a change in the conductivity of the solution, as the conductivity of honey is closely related to its concentration. The nanofiber was instantly absorbed by the artificial saliva and then immediately dissolved or dispersed in the saliva. With this, it is suggested that the PVA has an excellent hydrophilicity, and the water solubility of PVA can lead to the ability to dissolve rapidly.

Table 2.2 outlines the electrospinning parameters used to create polymeric nanofibrous films for biomedical applications and oral film applications. Different polymers have been studied. These variations demonstrate that the electrospinning parameters are primarily dependent on formulation and need to be adjusted depending on the type of polymer, its molecular interactions, and the purpose of the fibres. The table provides a summary of the main processing parameters and serves as a reference for the selection of suitable electrospinning parameters for the current study of PVA/κ-car/honey and PVA/κ-car/ ascorbic acid oral dispersible films.

Table 2.2:
Electrospinning Process Parameters for ODFs Fabrication

Study	**Polymer/Formulation**	**Key Electrospinning Parameters**		
		Voltage (kV)	**Flowrate**	**Distance tip to collector plate (cm)**
Rohani Shirvan et al. (2022)	3 w/v% PVA and 2 w/v% Chitosan, (80:20)	15	0.2 mL/hr	12
Bakar et al. (2023)	PVA/κ-car (70:30), 10-13 w/v% solution	12	0.3 mL/hr	15
Qin et al. (2019)	Chitosan/Pullulan in ratios of 0:100, 10/90, 20/80, 30:70, 40:60, 50:50, and 60:40 in 10% (w/v)	15	0.5 mL/hr	10
Khan et al. (2023)	L-ascorbic acid/HP-β-Cyclodextrin (LAA/HP-β-CD) in 200 w/v%	15	0.5 mL/hr	15
Ma et al. (2023)	Polyacrylonitrile (PAN), 6 – 16 w/v%	10 – 22	0.1 – 0.5 mL/hr	12 - 22

Kanimozhi et al. (2020)	8 w/v% PVA and 1-4 mL honey	10-16	0.06 – 0.001 mL/min	-
Liu et al. (2023)	6-12 w/v% PVA and aloe gel (ANFMs)	8 – 10	-	10
El-attar et al. (2022)	3g PVA and AgNPs-SM (3%)	25	1 mL/hr	-
Sukum et al. (2023)	4.5 w/v% poly (vinyl alcohol) and 0.04 w/v% chitosan and PEG 400 plus Mangifera indica leaf extract	20	-	15 - 20
Suflet et al. (2022)	6 w/w% phosphorylated curdlan gel (PCurd) and 10 w/v% PVA	22.7	10 µL/min	14
Shahid & Khan (2022)	PVA and Glycyrrhiza glabra	-20 - 50	-	-
Uddin et al. (2022)	nigella/honey/garlic/olive oil/PVA	20 – 24	1.5 and 2.5 mL/hr	15
Celebioglu et al. (2022)	resveratrol/cyclodextrin, resveratrol/HPβCD, resveratrol/HPγCD and pullulan	15	0.5 mL/hr	15
Cheng et al. (2024)	20 wt% pullulan and 1.5 wt% xanthan gum	20	1 mL/hr	15.5
Okur et al. (2021)	PVA (6% w/v), β–CD (17%, 25% and 33% w/w) and Vitamin C (3%, 4% and 5% w/w))	18	1 mL/hr	18
Kassem et al. (2023)	15% w/v PVP and manuka honey, ratio Mh to PVP 1:3 (25%), 1:4 (20%), and 3:17 (15%).	19	1 mL/hr	18
Zhang et al. (2020)	PVA (8% w/v), DES (5% w/v) and honey (5% w/v)	23	0.75 mL/hr	13

*Abbreviations: Ag-NPs, Silver nanoparticles; ANFMs, aloe nanofibrous membranes; β–CD, beta-cyclodextrin; DES, deep eutectic solvent; HPβCD, hydroxypropyl-β-cyclodextrin; HPγCD, hydroxypropyl-γ-cyclodextrin; LAA/HP-β-CD, L-ascorbic acid/HP-β-Cyclodextrin; PAN, polyacrylonitrile; PCurd, phosphorylated curdlan gel; PEG, polyethylene glycol; PVA, polyvinyl alcohol; PVP, polyvinylpyrrolidone; AgNPs-SM, silver nanoparticles-salvia moorcroftiana extract; XG, xantham gum; κ-car, κ-carrageenan; wt%, weight percent; w/v%, weight/volume percent; w/w%, weight/weight percent; mL/hr, millimetres per hour; µL/min, microliters per minute; kV, kilovolt; cm, centimetre.

2.4.2 Influence of Solution Viscosity and Conductivity on Electrospinning Performance

The viscosity and conductivity of a polymer solution, as well as the spinnability of the resulting solution, are directly related to the amount of dissolved additives. Viscosity is driven mainly by chain interlocking in the polymer mesh; if an additive increases solute concentration, viscosity increases very little. In contrast, when the additive is ionic or polyelectrolytic type, conductivity can be influenced more than viscosity (Doshi & Reneker 1995). Electrospinning requires sufficient viscosity so that chain entanglement maintains surface tension; otherwise, a jet will break into droplets or beaded fibres instead of continuous strands. On the other hand, too high viscosity impairs jet ejection and could clog the spinneret (Bhardwaj & Kundu 2010). The optimal viscosity for bead-free fibre production varies from system to system, but has been noted in the range of 100–2000 mPa·s (Zahra et al., 2023). Independently, conductivity regulates the charge density of the jet and so aids in electrospinning rather than bringing about Taylor-cone formation; stable jet elongation during electrospinning is possible, for example, 140–980 μS/cm (Bakar et al., 2023). Since viscosity and conductivity result from fundamentally different physicochemical mechanisms, chain entanglement.

The viscosity and conductivity of the solution are critical characteristics that influence the electrospinning process, as they directly impact jet stability, fibre morphology, fibre diameter, bead formation, and the overall quality of nanofibers. Effective electrospinning requires a suitable balance between these two qualities to produce continuous, uniform fibres. A study by Ramakrishna et al. clarified the functional mechanism of viscosity: insufficient viscosity will trigger electrospraying and beaded defects due to inadequate molecular entanglement, while excessively high viscosity will block liquid ejection from the spinneret, increase jet resistance, and ultimately result in fibre diameters that exceed the standard limit.

Likewise, electrical conductivity is crucial in regulating the quantity of electrical charge transported by the polymer jet. The study by Reneker & Yarin elucidated its mechanism of action: elevated conductivity can optimise fibre formation, while excessively high conductivity will trigger jet splitting, whipping instability, non-uniform deposition, and beaded defects. In the electrospinning process, conductivity is

a core variable that regulates the charge carried by polymer jets and influences the Taylor cone and the state of electrospinning jets.

In the electrospinning process, viscosity and electrical conductivity do not act independently; their interaction is the core factor that determines the overall process effect. A study on solution characteristics conducted by Haider et al. (2018) shows that viscosity obstructs jet deformation through polymer chain entanglement, while conductivity exerts an electrostatic stretching force on the charged jet. The final morphology of the fibres is the product of a balance between these two forces, and optimising either parameter alone will lead to process instability and unqualified fibres.

In hydrophilic polymer systems represented by polyvinyl alcohol (PVA), adding natural additives can simultaneously regulate the system's viscosity and conductivity. The research of Zhang et al. (2020) shows that when honey is added to electrospun PVA/deep eutectic solvent nanofibers, the sugars, minerals, and ions naturally contained in honey can increase the solution's electrical conductivity, promote electrostatic stretching, reduce fibre diameter, and optimise dissolution performance. The high-porosity fibres can dissolve rapidly in water and artificial saliva, and electrical conductivity is the core parameter that regulates fibre morphology and dissolution behaviour.

Experiments on electrospun membrane materials conducted by Sapiee et al. (2023) show that when electrospun PVA/κ-carrageenan oral fast-dissolving films are taken as the research subject, and the added amount of ascorbic acid is set as the independent variable, an increase in this additive's concentration will alter the physicochemical properties of the spinning solution, reduce fibre diameter, and trigger rapid disintegration of the nanofiber membrane. This outcome arises because the water-soluble additive changes the spinning solution's electrical conductivity and viscosity, interferes with electrostatic stretching, and thereby regulates the relevant material properties.

Previous studies have consistently noted that viscosity and conductivity are the core parameters regulating electrospinning performance: Viscosity ensures molecular chain entanglement to sustain the continuous formation of fibres, while conductivity determines the electrostatic stretching force that triggers fibre thinning. The two parameters influence multiple key characteristics of fibres, and clarifying their correlation is critical to optimising electrospun oral dispersible films. This study

evaluates these two parameters and clarifies the effects of *kelulut* honey and ascorbic acid on the spinnability of PVA/κ-carrageenan solutions, as well as the morphology and dissolution properties of the resulting nanofibers.

2.4.3 Alternative Film-Forming Techniques

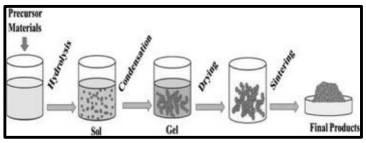
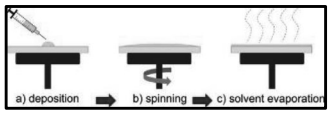
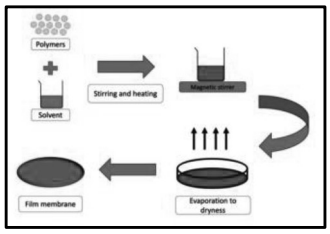
Solvent casting is a viable, advantageous, and undeniably favoured method, mostly because of its straightforward manufacturing procedure and minimal processing expenses. The solvent-casting film offers superior physical qualities, straightforward and economical manufacture, and exceptional thickness uniformity, among other advantages (Karki et al., 2016). This is an antiquated method employed to produce thin films. The resultant solution is mixed with the desired ingredients that have been solubilised in a suitable solvent. The solution is subsequently applied to a flat surface area at a specified wet film thickness and allowed to dry until a flexible film is created. The film can be positioned on a petri dish, depending on the equipment and size of production (Thabet & Breitkreutz, 2018). A vacuum is employed to expel trapped air. Upon drying and forming the solution into a film, it is subsequently sliced into the requisite dimensions (Priyanka et al., 2019). Solvent casting presents constraints. The thin polymer layer it forms may grow rigid and less flexible over time due to solvent evaporation. Moreover, the use of organic or harmful solvents may result in residues inside the end product. The primary drawback is its incompatibility with heat-sensitive materials (Kida et al., 2023).

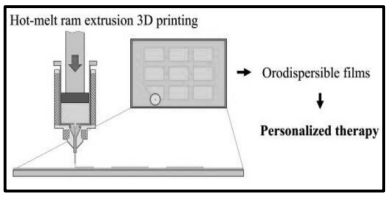
Based on the study conducted by Abou-taleb et al. (2022), the ODFs are fabricated by using the solvent casting method. This method is utilised to prepare the vardenafil ODFs with different blends of polyvinyl alcohol (PVP) solution (5% w/v), methylcellulose (MC) solution (2% w/v), sodium alginate solution (5% w/v) and polyvinylpyrrolidone.

K30 (PVP) solution (2% w/v). The stable vardenafil ODFs are produced. A study conducted by Abdelhameed et al. (2023) uses a solvent casting method where the FEX solution is poured into a petri dish, dried in the oven, and peeled from the petri dish before going into further analysis.

Table 2.3 below shows a comparative analysis of conventional fabrication methods that were employed to produce thin films in pharmaceutical and biomedical applications.

Table 2.3:
List of Other Methods for Producing Thin Films

Method	Procedure	Advantages	Disadvantages
Sol-gel	The precursor solution undergoes hydrolysis and is condensed into a gel, dried, and subjected to heat treatment to produce high-purity materials.  Figure 2.3: Sol-Gel Method (G. Singh et al., 2023)	Simple and cost-effective Can produce fibres and thin film Generates materials characterised by increased purity and uniformity	Necessitates meticulous regulation of parameters (e.g. pH, temperature) Time-consuming because it involves several stages. Restricted to specific material and application.
Spin Coating	A liquid precursor is applied to a substrate, distributed by spinning, and subsequently dried to provide a homogeneous thin film.  Figure 2.4: The Spin Coating Method (Obregón & Rodríguez-González, 2022)	generates consistent thin sheets with a regulated thickness Exceptional repeatability for extensive manufacturing Appropriate for a diverse array of materials (eg, Polymers, sol-gels)	Restricted to planar substrates Material wastage resulting from the spin-off. Necessitates exact regulation of rotational velocity and solution viscosity.
Solvent Casting Method	To make oral dispersible films using the solvent casting method, mix a material that forms the film with other ingredients in a liquid. Then, pour the mixture onto a flat surface and let the liquid evaporate, leaving a thin film behind.  Figure 2.5: Solvent Casting Method (Prete et al., 2023)	Straightforward and economical. Striking control of the film thickness. Suitable for any form of formulation.	Due to these solvents, the characteristics of the film can be altered in some way. More time is required for drying. They just do not have the leeway to expand their capacity to the fullest.
Hot Melt Extrusion	To create a film using the melt extrusion method, melt the mixture of materials, push the melted	Reduces the use of solvents, therefore reducing the risk of	High temperatures might lead to negative effects on the material

	mixture through a special shape, and then let it cool down to make the film.  Figure 2.6: Hot Melt Extrusion (Musazzi et al., 2018)	interaction with other materials. A continual process that can be suitable for mass production. Excellent mechanical characteristics.	used and would result in damage to specific parts. This threatens people's lives by requiring the use of specialised equipment. Limited to items that do not burn or undergo other changes in characteristics when exposed to high temperatures.

2.5 Oral Dispersible Film (ODF) Dissolution Method

The dissolution behaviour of ODFs is especially important because they are designed to rapidly break down and release the desired ingredient in the mouth. The dissolution profile of ODFs not only reflects the efficacy of the formulation but also impacts the overall performance of the product. Conventional tablets and capsules are designed to primarily dissolve in the stomach, but unlike those, ODFs are meant to dissolve in saliva in the mouth environment. As a result, ODF dissolution studies need to closely mimic the physiological conditions of the oral cavity. Indeed, parameters such as pH, temperature, and volume of dissolution medium influence the dissolution kinetics and should be adjusted in order to obtain relevant results. Dissolution is employed in stability trials to assist in determining shelf life, and because of its association with medication availability, it has been regarded as a significant laboratory tablet quality measurement (Maggio et al., 2008). The tablets were placed inside the beaker containing a revolving paddle, and the paddle was adjusted to a particular rpm (Mann et al., 2017). Then, the solution inside is taken as a sample at various times. In past studies, it is obvious that batch dissolution is a frequent method for measuring the release of the desired ingredient. Various equipment, like a paddle, was employed for this test. The differences in sample preparations, the mechanical functioning of the equipment, and the volume of liquid employed are critical factors in conducting a

dissolution test. Table 2.4 shows a variety of desired ingredients that had been used in the dissolution test, including volume and pH medium.

Table 2.4:
Past Studies of The Dissolution Test for Honey And AA

Active Ingredients	**Purpose**	**Absorbance by UV-Vis Spectroscopy (nm)**	**Volume (mL)**	**Temperature (°C)**	**References**
Honey	Skin	204	25	37	(Koosha et al., 2021)
Ascorbic acid	Antioxidant, boosts the immune system.	N/A	25	37	(Calzado-Delgado et al., 2023)
Ascorbic acid	Gastric release	521	50	37	(Kaimal & Singhal, 2023)
Honey	Scaffolds	241	5	37	(Maleki et al., 2013)
Honey	Scaffolds	200-800	10	37	(Kanimozhi et al., 2020)
Honey	Burn wound	340	100	37	(El-Kased et al., 2017)
Ascorbic acid	Antioxidants boost the immune system.	N/A	/	37	(Shin et al., 2023)
Ascorbic acid	Wound healing	290 - 265	20	37	(Ghahremani-nasab et al., 2023)

Artificial saliva is routinely used as the dissolving medium for ODFs with pH levels ranging between 6.8 and 7.5 at 37°C to replicate the human oral environment. Artificial saliva offers a consistent and stable setting compared to various formulations. While the absence of enzyme activity and variable salivary flow rates are drawbacks of using simulated saliva, it is still a useful medium for initial in vitro dissolution testing (Abdelhameed et al., 2023; Abou-taleb et al., 2022). Using simulated saliva is especially suitable for rapidly dissolving systems where saliva causes dissolution in seconds.

Dissolution behaviour in desired ingredient analysis is commonly analysed using Uv-Vis spectroscopy. Uv-Vis monitors the changes in concentration of the dissolved desired ingredient in the medium over time. It is even suggested for the analysis of water-soluble desired ingredients, such as honey and ascorbic acid (AA), due to its simplicity and applicability. The release of desired ingredients and dissolution profiles can be constructed using Uv-Vis analysis by measuring absorbances at certain wavelengths and by calculating the concentration using the calibration curve. Dissolution data can be obtained.

2.6 Artificial Neural Network (ANN) in Dissolution Predictions

Inspired by human brain functioning, Artificial Neural Networks (ANN) model the brain's neuronal network. An ANN consists of billions of interconnected neurons organised into three architectural layers: input, output and hidden. They learn the correlations of non-linear, complex input and output variables through iterative training. Thus, ANNs are useful in modelling non-linear systems, such as in pharmaceutical formulation and drug delivery studies (Mallick et al., 2024; P. Singh et al., 2019). It transmits the error from the output layer to the input layer, modifying the connections between neurons for satisfactory performance (Ebube et al., 1997). Figure 2.7 shows the schematic diagram of how the ANN works with input and output variables and the hidden layer. An artificial neural network is generally known for its learning capability, suitable generalisation properties, and defect tolerance (Mallick et al., 2024). During the past several decades, various artificial neural networks (ANNs) have been invented to resolve many pattern recognition, classification, grouping, regression, and optimisation problems. One of the significant advantages of artificial neural networks is their ability to handle nonlinear conditions using historical or partial data (P. Singh et al., 2019).

The Levenberg–Marquardt algorithm is used in the ANN to run the analysis. Among all the approaches used to optimise artificial neural networks (ANNs), the Levenberg-Marquardt (LM) algorithm is one of the most popular due to its high convergence and reasonably low error rate. This method is considered most efficient in medium-sized networks, and, compared to other gradient methods, it works well, attaining high convergence rates (Mammadli, 2017; Sarić & Xiao, 2011). Artificial neural networks tend to be trained exceptionally well by the LM algorithm, typically

outperforming conventional back propagation methods by making use of second-order derivative information to estimate the Hessian matrix, thus speeding convergence (Mammadli, 2017; Sarić & Xiao, 2011; Üstün et al., 2023). The primary goal of the LM method is to minimise the sum of squared errors of the projected outputs deviating from actual objectives by re-adjusting weights in the network. When the training dataset is limited and the model is highly complex, it is mainly used to converge faster and more stably than other training methods.

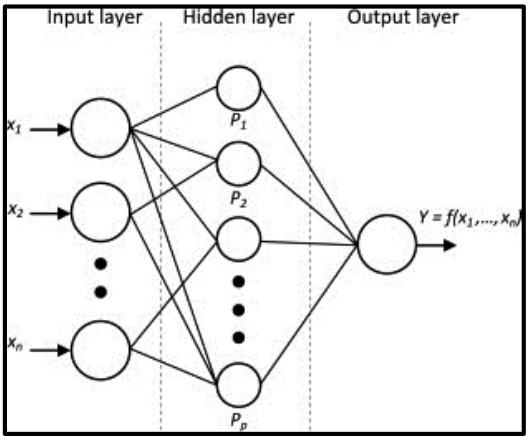


Figure 2.7: Schematic Diagram of ANN Cited from Brooks & Tucker [40]

Artificial Neural Networks can predict in vitro dissolution characteristics that employ multiple input data. A study conducted by Ebube et al. used ANN to assess the effect of numerous experimental variables on the ability of a neural network to predict in vitro dissolution rates dependent upon product formulation changes, where they used the theoretical composition of the drugs as input variables (Konstantinidis et al., 2015). Recent studies have expanded the scope of ANNs to include the optimisation of formulation parameters, similar to dissolution profiles, and the prediction of release profiles under different conditions. These studies show strong correlation coefficients for predicted and observed values, which speaks to the reliability of the ANN models.

However, most of the studies in ANN-based research have concentrated on conventional dosage forms such as tablets and capsules. There is a limited availability of research involving oral dispersible films, especially electrospun nanofibrous systems. In this work, the ANN modelling approach is used to estimate the dissolution behaviour of ascorbic acid in PVA-based electrospun ODFs. The output variables were the formulation and analysis parameters. By employing the Levenberg–Marquardt

algorithm to train the ANN, the model attempts to provide the best possible representation of the dissolution performance.

A study by Nagy et al. (2019) conducted an ANN prediction for the tablet profile release where the samples were divided into training, validation and testing randomly in a 70-15-15% ratio, respectively. Random partitioning of the training data into subgroups using the MATLAB Neural Network Toolbox's Nguyen-Widrow method for weight and bias initialisation attained a degree of fluctuation. This study indicates that ANN can successfully predict the in vitro dissolution curve. Another study conducted by Galata et al. (2019), this study used a training function, Levenberg-Marquardt and Bayesian regularisation, and the network consisted of 53 points. With each cycle of training conducted 100 times, the number of neurons was gradually raised from 1 to 10. 15%-15% of the training samples were chosen at random for cross-validation and evaluation per cycle.

Based on a study conducted by Sheth & Acharya (2024), data from this study are separated into three sections: training, validation, and test for the development of artificial neural networks and their verification of accuracy. Constructed using data from the training, testing, and validation sets, 70% for training, 15% for testing, and 15% for validation. The models used were MATLAB tools that allowed data sets for validation, testing, and training to be randomly chosen. This work found that, by means of formulation factor optimisation, the ANN model best reflected the technique of assessment of drug release similarity. 10 neurones in all made up the hidden layer. The network was trained using the Levenberg–Marquardt approach. MATLAB's "trainlm" utility uses this method for training feedforward neural networks. The drug release properties for different drug concentrations were projected using the simulated network. Another study by Üstün et al. (2023) used an MLP model to allow 5, 10, 15, or 20 neurons as well as 2, 3, or 4 hidden layers. Until the lowest training error rate is reached, the modelling process is repeatedly carried out during the training phase. Whereas logsig is recommended for the activation function of the final neuron in the hidden layer, tansig is chosen for the other layers. Based on a study conducted by Mészáros et al. (2024), the ANNs had an input layer, a hidden layer, and an output layer set in a feedforward configuration. The training mechanism was Bayesian regularisation back-propagation. Training and testing 100 neural networks helped one to ascertain the ideal number of neurons in the hidden layer. Fifteen per cent of the sample was utilised for

testing and eighty-five per cent for training. The hidden layer's neuron count ranges from 1 to 5. Based on the latter, the relative error was 5.6%, considering the midpoint of the applicable range. The ANN model is so appropriate for forecasting desired ingredient content. The observed and expected values are rather close to one another. The findings show that the ANN effectively forecasted the desired ingredient content on white tablets.

In a study conducted by Cuahuizo-Huitzil et al. (2023), with a learning rate of 0.4, the artificial neural network was trained using the Levenberg–Marquardt backpropagation (trainlm) approach. Training, validation, and test sets—about 70%, 15%, and 15% of the whole dataset, respectively. These were the three categories into which the experimental data were arranged. Whereas one neuron matching the size of the electrospun nanofiber was assigned in the output layer, four neurons representing four electrospinning factors (flow rate, voltage, viscosity, and conductivity) were used in the input layer. A study by Péterfi et al. (2023) used a Bayesian regularisation learning method; the hidden layer's neurons made use of a tangent sigmoid transfer function. Three groups comprised the training samples. Fifteen per cent of the data was used for cross-validation, seventy per cent for training the artificial neural network, and the last fifteen per cent for testing.

Based on all the past research that has been conducted, the gap that can be seen is the use of honey as a taste enhancement agent in ODFs and also ascorbic acid as the desired ingredient. The material used in this research is PVA and also K-car, and the way to synthesise the ODFs is by electrospinning. From the past research, it can be concluded that the use of PVA is very limited, and in this study, PVA was used to overcome this. Electrospinning also shows some limited usage in fabricating the ODFs, especially in the prediction of profile release using ANN. As can be seen in Table 2.5 below, the prediction of ANN mostly uses tablets as samples.

Table 2.5:
Predictions Using ANN

Study	Structures	Approach	Algotrithm
Nagy et al., 2019)	Extended @ Sustained	ANN	Bayesian-regularisation algorithm
Sheth & Acharya, 2024)	Modified Release	ANN	Levenberg–Marquardt approach
Galata et al., (2019)	ODT	ANN	Levenberg-Marquardt and Bayesian regularisation
Üstün et al., (2023)	ODF	ANN	Bayesian-Regularisation (trainbr), Quasi-Newton (trainlm) and Gradient-Descent (trainrp)
Mészáros et al., (2024)	ODT	NA	Bayesian regularisation back-propagation
Cuahuizo-Huitzil et al., (2023)	ODF	NA	Levenberg–Marquardt backpropagation (trainlm)
Galata et al., (2021)	Extended @ Sustained	ANN	Bayesian regularisation algorithm
Péterfi et al., (2023)	ODT	ANN	Bayesian regularisation learning method
Lourenço et al., 2025)	ODT	ANN	Levenberg-Marquardt training algorithm
Mandal et al., (2008)	ODT	ANN	NA

CHAPTER 3
RESEARCH METHODOLOGY

3.1 Introduction

This chapter shows materials used and methodology for sample preparations, characterisation of electrospun nanofibers for PVA/κ-car/*kelulut* honey and PVA/κ-car/Ascorbic Acid and dissolution of ascorbic acid from the ODF. Figure 3.1 shows the flow of the experimental work conducted throughout the study. It starts with the solution preparations, where the solution was prepared using PVA/Honey and PVA/K-car and mixed homogeneously. The viscosity and conductivity of the solutions were characterised before electrospinning, which produced the electrospun ODF. The electrospinning was conducted using parameters that have been set (flow rate, voltage, and distance from the syringe to the collector plate) to produce the fabricated thin film.

The electrospun ODF was characterised using SEM and water contact angle for physical evaluations, FTIR for chemical evaluations and a universal testing machine was used to analyse tensile strength for mechanical methods. Dissolution of ascorbic acid and honey from the electrospun ODF was conducted under batch conditions using FTIR and UV-Vis. On top of that, the instantaneous dissolution was conducted for ascorbic acid only using FTIR. The obtained dissolution data were used for the prediction approach using ANN, whereby dissolution behaviour was predicted and compared with the experimental values in assessing the release behaviour of the AA and honey in electrospun PVA/κ-car ODFs.

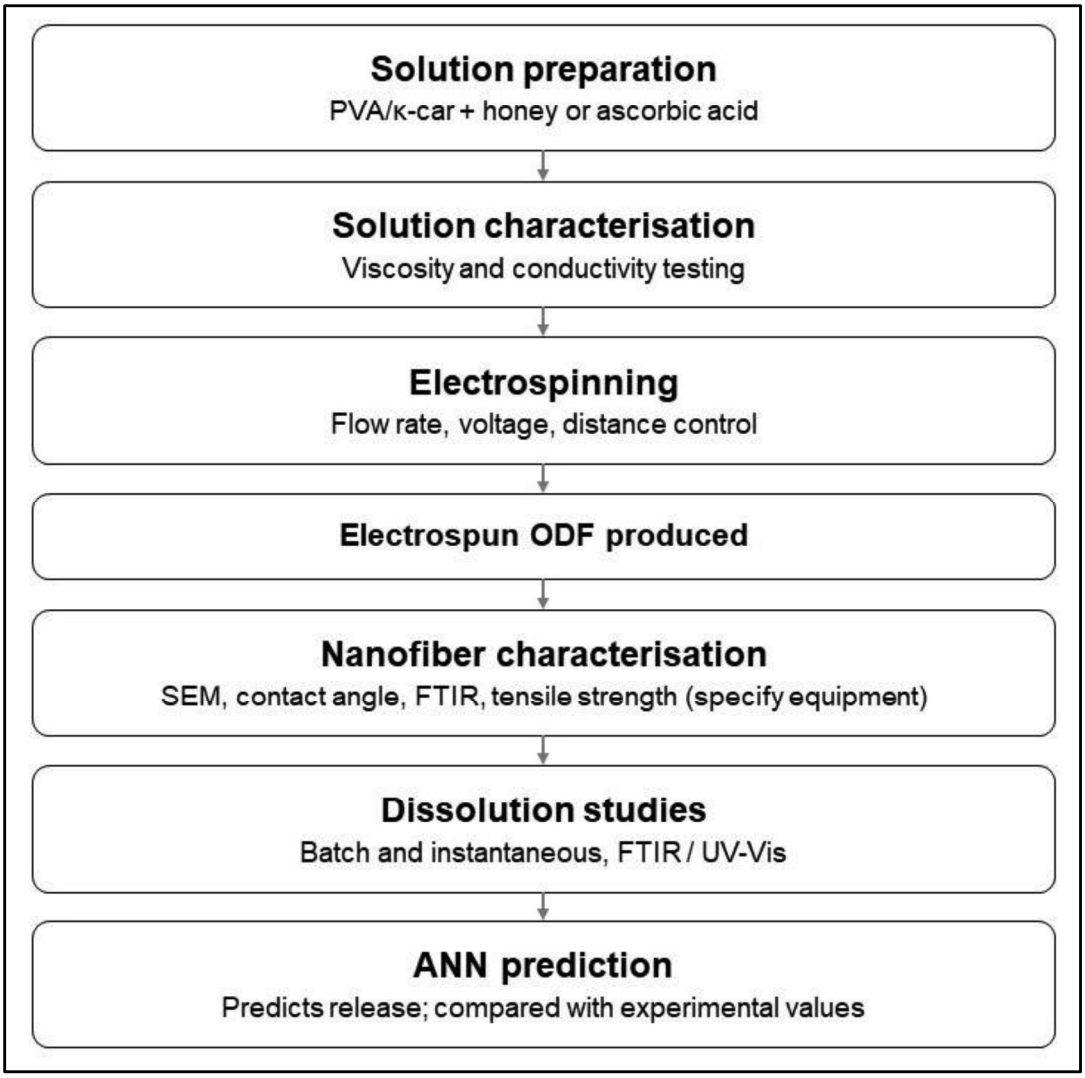


Figure 3.1: Overview of Experimental Work and Methodology for Electrospun Nanofiber

3.2 Materials

Materials that were used in this research are Polyvinyl alcohol (PVA, MW: 145,000 Da, Merck, Germany), Honey (Syamille Agro Farm, Malaysia), kappa-carrageenan (κ.car), l-Ascorbic acid (AA, R&M Chemical, Malaysia), and also deionized water (DI water), Sodium bicarbonate ($NaHCO_3$, Merck, Germany), sodium chloride (NaCl, Chemiz, Malaysia), Potassium chloride (KCl, Merck, Germany) and hydrochloric acid (HCL, 37%, MW: 36.64 g/mol, Chemiz, Malaysia).

3.3 Methods

This section shows the formulation of PVA/κ-car/honey and PVA/κ-car/AA for preparing the electrospun ODF thin film that consists of honey and AA for dissolution profiling.

3.3.1 Preparation of the PVA/κ-Car/Kelulut Honey and PVA/κ-Car/AA Solutions

i) PVA/κ-Car/kelulut honey solution preparation

Figure 3.2 shows that the preparation of PVA/ κ-car/honey solution was prepared by dissolving PVA (10 w/v%) in 20 mL of deionised water at an elevated temperature (around 90°C). On the other hand, Kappa-carrageenan (κ-car) was dissolved in 100 mL of DI water with rapid, continuous stirring in a water bath at 80°C. The K-carrageenan (κ-Car) solution was sonicated for 3 minutes at 60 Hz to remove air bubbles before heating in the water bath at 80°C for another 1 hour. The PVA and K-carrageenan solutions were mixed in a 90:10 ratio, with 18 mL and 2 mL, respectively, and heated to fully dissolve both materials while avoiding excessive heating. The mixing ratio and concentration of PVA were based on a study conducted by Teixeira et al. (2022b) and Arianto et al. (2021), while the concentration of PVA and κ-Car was referred to the optimisation value determined by Bakar et al. (2023). The solution was stirred and let cool to room temperature before adding honey (1 mL, 1.5 mL and 2 mL), and it was stirred until uniformly blended.

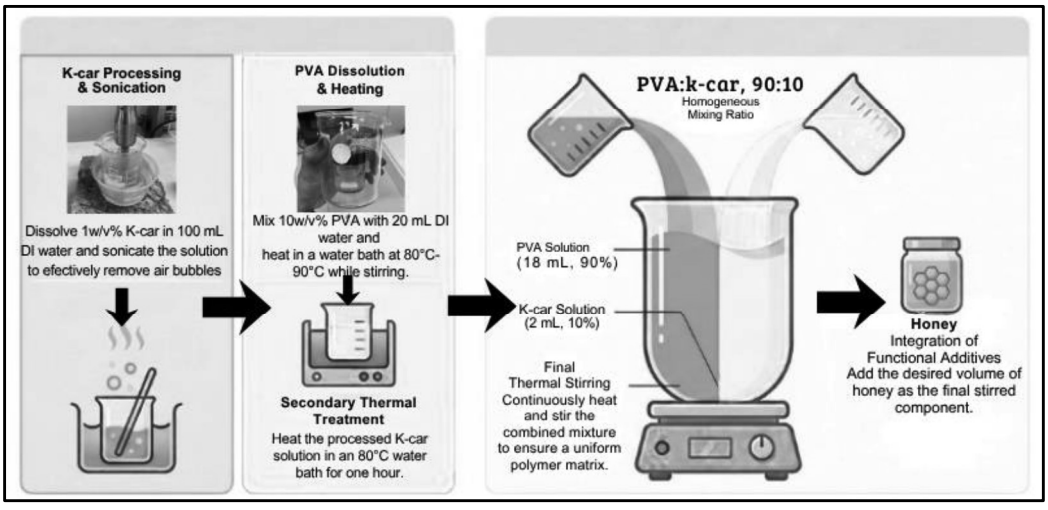


Figure 3.2: Solution Preparation of PVA/κ-car/Honey

ii) PVA/κ-Car/AA solution preparation

The mixing ratio and concentration of PVA were based on a study conducted by Teixeira et al. (2022b), while the concentration of PVA and κ-Car was referred to the optimisation value determined by Bakar et al. (2023). For the PVA and ascorbic acid formulation, PVA (12 w/v%) were dissolved in 20 mL deionised (DI) water and heated to around 90°C with constant stirring. Meanwhile, κ-car was dissolved in 100 mL of DI water with rapid, continuous stirring. The κ-car solution was sonicated for 1 to 3 minutes at 60 Hz to remove air bubbles before being heated for another hour. The PVA and κ-car solution was mixed in the ratio of 90:10 into a total volume of 20 mL and heated again with continuous stirring. The solution was cooled to room temperature before adding the ascorbic acid (0.2g, 0.6g, 1g, 1.4g, 1.8g and 2.2g), and it was stirred until uniformly blended. Figure 3.3 and Table 3.1 show the process flow for solution preparation of the PVA/κ-car/AA.

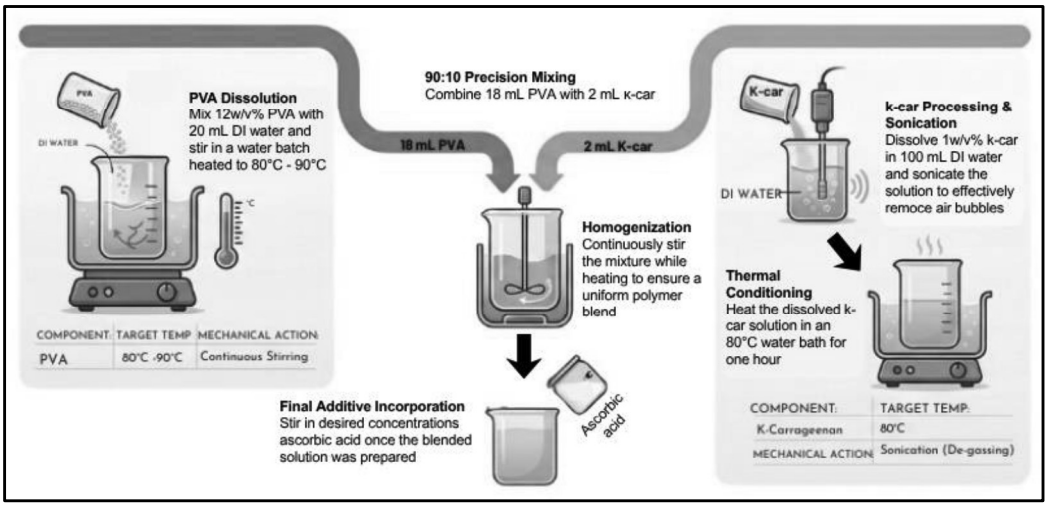


Figure 3.3: Solution Preparation of the ODF Solution PVA/κ-car/AA

Table 3.1:
Mass of AA to Fabricate Electrospun ODFs

Weight per volume of Ascorbic Acid, w/v%	Mass of Ascorbic Acid, g
1	0.2
3	0.6
5	1
7	1.4
9	1.8
11	2.2

3.4 Conductivity and Viscosity Measurement

Viscosity and conductivity measurements were performed on the polymer solution prepared as in Section 3.3. A volume of 30 mL of the polymer solution was analysed using a Vibro Viscometer (SV-10/SV-100) and a Hach SensION 7 Conductivity-TDS meter, respectively.

3.5 Electrospinning Procedure and Process Optimisation

Electrospinning setup and parameters are shown in Figure 3.4 and Table 3.2, respectively. The prepared solution was fed into a 5 mL syringe and placed on top of the syringe pump with a 15-16 kV voltage applied. The flow rate was set at 0.54 mL/hr – 0.6 mL/hr, and electrospinning was initiated (Bakar et al., 2023; Bureau et al., 2019; Santos et al., 2019; Sapiee et al., 2023). The needle tip is 15-16 cm away from the collector plate, which was wrapped with aluminium foil. The electrospinning process was conducted for up to 4-8 hours. The excess electrospun solution that accumulated at the needle tip during spinning was discarded hourly to prevent an uneven fibre jet. The power supply was monitored to prevent sparks. The environment was maintained at room temperature throughout the process. The solution properties of the viscosity and conductivity were analysed using a viscosity and conductivity meter.

Table 3.2:
Parameter Used to Run the Electrospinning (Bakar et al., 2023; Bureau et al., 2019; Santos et al., 2019; Sapiee et al., 2023)

Electrospinning parameter	
Voltage	16 kV
Flowrate	0.4-0.6 mL/hr
Time taken	4-8 hours
Distance	16 cm
Volume	5 mL

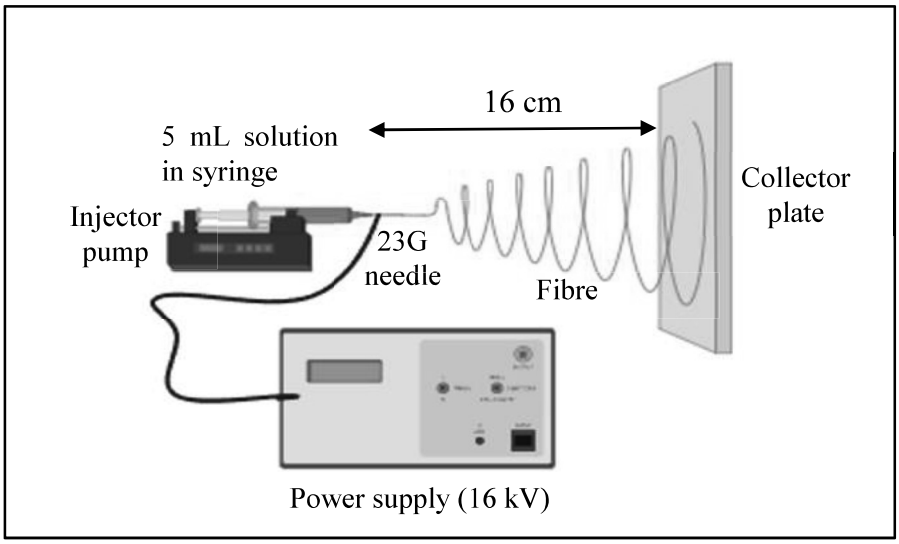


Figure 3.4: Schematic Diagram of Electrospinning

3.6 Characterisation of Electrospun ODFs

The physical and chemical characterisation of electrospun ODF was conducted using SEM, water contact angle, FT-IR, and tensile strength. This analysis was important to observe the surface morphology and the diameter.

3.6.1 Scanning Electron Microscopy (SEM)

The surfaces and internal structures or morphology of the films were analysed using a scanning electron microscope (Hitachi SU3500, Hitachi High-Tech Corporation, Tokyo, Japan) at 15 kV. A sample of thin film was cut to a size of 1x1 cm

and previously stored in an airtight container to prevent film damage. The samples were carbon coated using a Jeol JFC-1600 Auto Fine Coating Machine for enhanced conductivity. The analysis was conducted by projecting a laser beam onto a small spot on the sample surface. The magnifications for this analysis were 100, 250, 1000, 10 000, 20 000, and 50 000 times. For quantitative analysis of fibre diameter, ImageJ software (Version 13.0.6) was used, where the diameter of 100 random fibres was selected from the acquired images.

3.6.2 Water Contact Angle (WCA) Measurement

The nanofiber films were evaluated by water contact angle analysis. The films were measured using a goniometer (AST/VSA-3000s) with a charge-coupled device (CCD). A 4 µL droplet of distilled water was gently placed on the surface of each film (1 x 1 cm). The droplet was dispensed slowly and consistently to minimise impact on the droplet profile. After a few seconds of exposure, the water drop video was recorded by a CCD camera and a few images were selected from the video and conveyed to the computer for static water contact angle measurement. Three different random positions of each film were tested, and the mean values were calculated.

3.6.3 Fourier Transform Infrared Spectroscopy (FT-IR) Analysis

The functional group of the samples were evaluated at ambient temperature utilising Fourier transform infrared spectroscopy (FT-IR); Spectrum One, Perkin Elmer, USA. Spectral analysis was conducted within the region of 4000-450 cm^{-1} at room temperature with a resolution of 4 cm^{-1} and accumulation of 32 scans for each sample using attenuated total reflectance mode with a diamond crystal.

3.6.4 Mechanical Testing: Tensile Strength

The elongation and tensile strength of the biopolymer film were measured by a universal testing machine. The test was conducted according to ASTM D882 (Tooraj,2020). The film and PVA/Honey and PVA/K-car samples from electrospun nanofibers were cut into 15 mm x 70 mm and placed between the two pneumatic grips before the testing. The analysis was performed at a speed of 5 mm/min. The initial gap between the grips was determined.

3.7 Dissolution of Electrospun PVA/κ-Car/Honey and PVA/κ-Car/AA ODFs

Dissolution analysis was conducted to evaluate the release behaviour of the PVA/κ-car/honey and PVA/κ-car/AA electrospun ODFs. The analysis was segregated into batch and instantaneous dissolution. Batch dissolution analysis was performed in a controlled medium to obtain the release of the desired ingredients using UV-Vis spectroscopy across a wavelength range of 400 – 200 nm. In contrast, an instantaneous dissolution analysis was designed to mimic the mouth conditions and limit the amount of artificial saliva and the time taken for the desired ingredient to release from the electrospun ODFs using FT-IR spectroscopy across a wavenumber range in the 4000 – 400 cm^{-1} region.

3.7.1 Formulation of Artificial Saliva

4200 mg/mL$NaHCO_3$, 500 mg/mL NaCl and 200 mg/mL KCl were mixed in deionised (DI) water until the solution was homogeneous. The pH probe was used to check the pH value of the solution. The pH of the solution was adjusted to 7.3 by adding HCL drop by drop.

3.7.2 Batch Dissolution of Electrospun ODFs Using UV-Vis Spectroscopy

3.7.2.1 Calibration curve for honey

10 mL of honey was prepared freshly and dissolved in 100 mL of DI water. The solution was diluted for the other six concentrations of honey (i.e., 0.2, 0.4, 0.6, 0.8, 1.0 and 1.2 v/v%) to plot a calibration curve. The absorbance of the solution was measured using UV-Vis spectroscopy across a wavelength range of 800 – 200 nm. A calibration was plotted based on the obtained peak (refer to Appendix 1)

3.7.2.2 Calibration curve for ascorbic acid (AA)

A freshly prepared standard solution of ascorbic acid at a concentration of 0.1 mg/mL was initially prepared. Calibration curves were constructed using various concentrations of AA (i.e., 0.008, 0.009, 0.01, 0.02, 0.03, 0.04, and 0.05 mg/mL),

prepared through appropriate dilution methods. The absorbance of the solutions was measured by using UV-vis spectroscopy across a wavelength range of 400 – 200 nm. A calibration curve was plotted based on the obtained peaks. A calibration was plotted based on the obtained peaks (refer to Appendix 2)

3.7.2.3 Batch dissolution of electrospun PVA/κ-Car/honey ODF

10 mg of electrospun nanofiber from each sample (1 mL, 1.5 mL and 2 mL) was dissolved in 30 mL of artificial saliva, heated at 37°C in a water bath shaker at 50 rpm. Every 5 mL of the solution was taken at a time interval of 20 seconds for 3 minutes. The absorbance of honey for all samples was measured using UV-Vis spectroscopy at a wavelength range between 800 and 200 nm and fingerprint region of honey is between 280 – 285 nm (Geană et al., 2024; Mitra et al., 2023).

3.7.2.4 Batch dissolution of electrospun PVA/κ-Car/AA ODF

A 10 mg of electrospun nanofiber from each sample (1w/v%, 3w/v%, 5w/v%, 7w/v%, 9w/v% and 11w/v%) was dissolved in 30 mL of artificial saliva, heated at 37°C in a water bath shaker at 50 rpm. Every 5 mL of the solution was taken at a time interval of 20 seconds for 3 minutes. The absorbance of AA for all samples was measured using UV-Vis spectroscopy at a wavelength range between 400 and 200 nm.

3.7.3 Instantaneous Dissolution of Electrospun ODFs Using FT-IR Spectroscopy

i) Calibration curve for ascorbic acid (AA)

1 w/v% of AA was prepared and dissolved in 100 mL of water (standard solution). The solution was diluted for the other five concentrations. (3 w/v%, 5 w/v%, 7 w/v%, 9 w/v% and 11 w/v% of AA). The absorbance of the solutions was measured by using FT-IR spectroscopy across a wavenumber range in the 4000 – 400 cm^{-1} region. A calibration curve was plotted based on the obtained peaks (refer to Appendix 3).

3.7.4 Instantaneous Dissolution of Electrospun PVA/κ-Car/AA ODF

1 w/v% electrospun ODF were punched into 4 mm diameter pieces. It was placed on the slide of the FT-IR platform, and 22µL of artificial saliva was added to the film using a micropipette, allowing it to gradually dissolve over time. Readings were taken at 10-second intervals. The absorbance of AA for all samples was measured using FT-IR spectroscopy in the wavenumber range of $4000 - 400\ cm^{-1}$. The step was repeated for 3w/v%, 5w/v%, 7w/v%, 9w/v% and 11w/v% electrospun ODFs.

3.8 Development of an ANN Model for Dissolution Prediction

Firstly, the input for the ANN prediction was declared based on the desirable value of dissolution that was obtained from the experiment, which was from FT-IR and UV-Vis. The output data were the dissolution releases. 5 – 15% of the dataset was divided into training, validation and test to evaluate the model's generalisation capability of the ODF samples. In this study, the full experimental dataset obtained from research on oral dissolving film (ODF) formulations was randomly divided into a training set, a validation set, and a test set at a ratio of 90%, 5%, and 5%, respectively. The training set supports the development of the artificial neural network (ANN) model, the validation set monitors the training process to avoid overfitting, and the test set evaluates the prediction performance of the final completed model. As the original dataset has a small scale, this division (90%/5%/5%) approach enhances the ANN's ability to learn from sample data and also enables the model's generalizability to be evaluated via an independent subset. This prediction was developed using the feed-forward back-propagation neural network structure. The optimal number of hidden neurons was determined as 10, which resulted in the lowest Mean Squared Error (MSE) and the highest correlation coefficient (R). The Levenberg-Marquardt (LM) algorithm was used to train the network. This was trained within the MATLAB version 2018b (MathWorks Inc., Natick, MA, USA) environment using the *trainlm* function. The LM algorithm was chosen because it was expected to have a fast convergence rate and a low prediction error, which was better for medium dataset sizes (Makram et al., 2024; Mallick et al., 2024). The modelling process was trained using the MATLAB Neural Fitting Tool (command *nftool*), after which the data was imported, the network was created, the data sets were divided, and the training started. The predicted dissolution

values that the ANN generated were compared to the experimental values to evaluate the accuracy of the model. Figure 3.5 below shows an overview of how the running was trained in this ANN and the hidden layer. The illustration shows an Artificial Neural Network (ANN) model designed to predict concentration in the dissolution analysis of electrospun oral dispersible films (ODFs). The input layer of this model has three parameters: time, absorbance, and wavelength or wavenumber derived from UV-Vis or FTIR analysis. The inputs are multiplied by weights and summed with biases before being processed in the hidden layer, which has 10 neurons that capture the nonlinear relationship between spectral data and concentration. The output layer comprises a single neuron that generates the expected concentration value, facilitating precise modelling of dissolution behaviour based on experimental data.

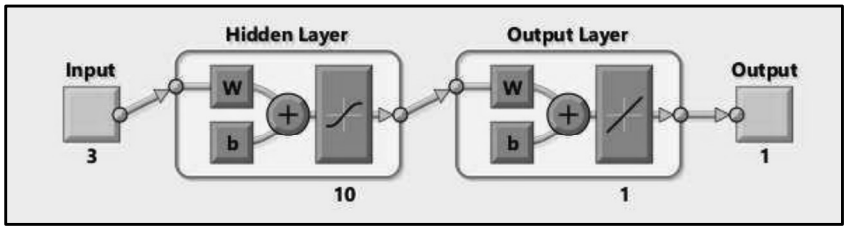


Figure 3.5: Neural Network Diagram for 10 Hidden Layers

3.8.1 Batch Dissolution Prediction of Honey from Electrospun PVA/κ-Car/Honey ODFs Using an ANN Model

Time, absorbance and wavelength were included as input, and the dissolution profile release (concentration, mg/mL) from the experiments was labelled as the output. The model was partitioned into training, validation and testing for 30 samples. The data was randomly divided into training, validation and testing sets, with 5% of the data reserved for testing and 5% for validation, with two samples assigned to each category, while 90% was allocated for training, utilising the remaining 26 samples. The feed-forward backpropagation network was trained using the Levenberg-Marquardt algorithm in MATLAB (command *nftool*). The MSE and the correlation coefficient between the predicted and experimental dissolutions were determined. Figure 3.6 shows the schematic diagram of the ANN model.

3.8.2 Batch Dissolution Prediction of Ascorbic Acid (AA) from Electrospun PVA/κ-Car/AA ODFs Using an ANN Model

Time, absorbance and wavelength were included as input, and the dissolution profile release (concentration, mg/mL) from the experiments was labelled as the output. The model was partitioned into training, validation and testing for 42 samples. The data was randomly divided into training, validation and testing sets, with 5% of the data reserved for testing and validation, with two samples assigned to each category, while 90% was allocated for training, utilising the remaining 40 samples. The feed-forward backpropagation network was trained using the Levenberg-Marquardt algorithm in MATLAB (command *nftool*). The MSE and the correlation coefficient between the predicted and experimental dissolutions were determined. Figure 3.6 shows the schematic diagram of the ANN model.

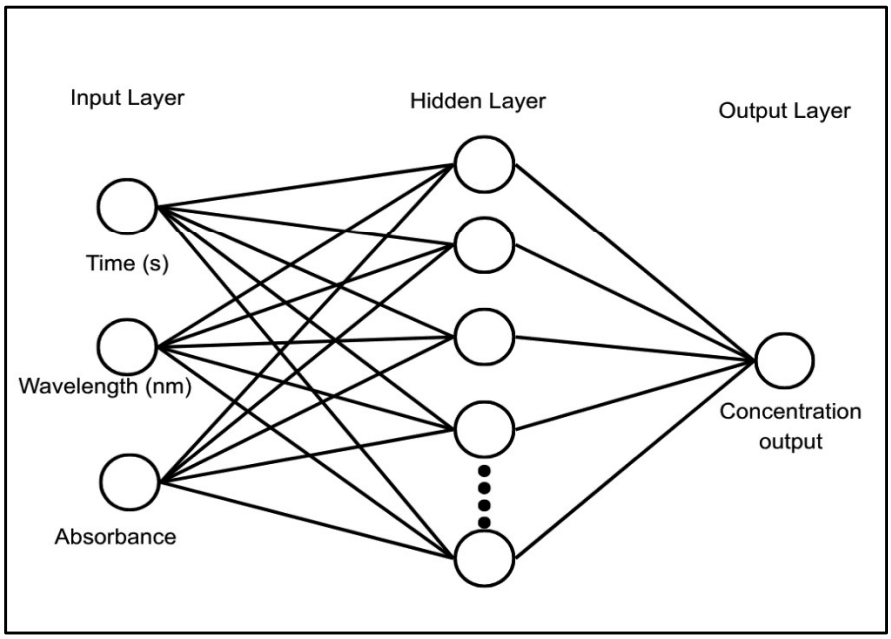


Figure 3.6: Schematic Diagram of an ANN Model for Dissolution Prediction Using UV-Vis Spectroscopy

3.8.3 Instantaneous Dissolution Prediction of Ascorbic Acid (AA) from Electrospun PVA/κ-Car/AA ODFs Using an ANN Model

Time, absorbance and wavenumber were included as input, and the dissolution profile release (concentration, mg/mL) from the experiments was labelled as the output. The model was partitioned into training, validation and testing for 48 samples. During

training, 5% of the data is reserved for testing and validation, with two samples assigned to each category, while 90% is allocated for testing, utilising the remaining 44 samples. The resulting structure was a feed-forward backpropagation neural network with 10 hidden neurons. Training was performed using the Levenberg-Marquardt (*trainlm*) algorithm, and the model was evaluated using MSE and regression analysis of predicted and experimental dissolution data. The ANN structure for the FT-IR-based model (schematic diagram is displayed in Figure 3.7)

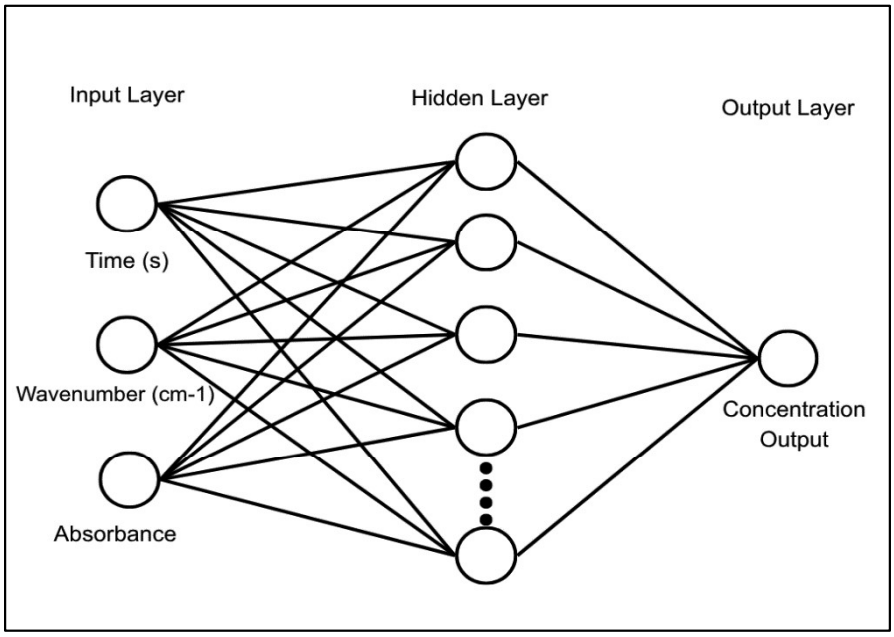


Figure 3.7: Schematic Diagram of an ANN Model for Dissolution Prediction Using FT-IR Spectroscopy

CHAPTER 4
RESULTS AND DISCUSSION

4.1 Introduction

This chapter is divided into seven sections. The first section discusses the results obtained in the fabrication of PVA/κ-car/honey and PVA/κ-car/Ascorbic acid. The preparation of the solution and the process of electrospinning to fabricate the desired film, which is an oral dispersible film. In the first section, the characterisation of the film, such as viscosity, conductivity, scanning electron microscopy (SEM), water contact angle, Fourier Transform Infrared (FT-IR), and tensile strength. In the second section, dissolution profile or dissolution rate of honey and ascorbic acid are discussed, concerning the different volumes of honey and concentrations of ascorbic acid that have been analysed by UV-Vis spectroscopy. The result is then analysed using Uv-vis. The last section is the discussion part for ANN evaluation in batch dissolution using UV-Vis and instantaneous dissolution using FT-IR.

4.2 Characterization of the PVA/κ-Car/Honey and PVA/κ-Car/AA ODFs

4.2.1 Viscosity and Conductivity of Spinning Solutions

To regulate the physical qualities and drug release characteristics of the final films, the honey and ascorbic acid content and polymer composition can be modified. These modifications will also affect the viscosity and conductivity of ODF formulations. Table 4.1 shows viscosity and conductivity for honey-loaded ODFs. When the honey volume increased from 1.0 to 2.0 mL, the viscosity of the ODFs spinning solution increased from 199 mPa · s to 208 mPa · s. This indicates that the solution's resistance to flow increased, which is important for the electrospinning process and the fibres produced. In electrospinning, the viscosity plays a role in determining the ability of the solution to produce continuous fibres and not droplets or beads. Optimal viscosity allows for adequate polymer chain entanglement and jet formation, and adequate conductivity allows for the electrostatic stretching of the jet, which results in the formation of fine and even fibres. If there is insufficient viscosity, then beading will occur. If there is excess viscosity, jet formation will be hindered. The

same applies to conductivity, where beading and poor jet formation occur with inadequate conductivity and overly destabilised jets occur with excess conductivity. The lowest volume of honey was 1.0 mL, producing a solution that had a viscosity of 199 mPa.s and conductivity (670 µS/cm), which was considered a small value and produced small bead fibres. An increase in honey volume to 1.5 mL increased the viscosity to 205 mPa.s (793 µS/cm**),** indicating that the solution produced a continuous fibre whilst minimising bead effects. An increase of honey volume to 2.0 mL results in a viscosity of about 208 mPa.s (804 µS/cm**).** The results show that the volume of honey in the solution impacts viscosity and conductivity differently. The viscosity had a slight increase in the sample range (199–208 mPa·s) while the increase in conductivity was greater (670–804 µS/cm), which can be attributed to honey sugar-based bulk viscosity and its ionic/mineral contents influencing the solution conductivity (Doshi & Reneker, 1995). Both viscosity and conductivity remained in the established ranges for ideal conditions of bead-free electrospinning (100–2000 mPa·s; 140–980 µS/cm) (Bakar et al., 2023; Zahra et al., 2023). The optimal working volume in this study was determined to be 1.5 mL, as this volume was the first to produce aligned, continuous fibres and also reduced bead formation. At this volume, the solution's viscosity (205 mPa·s) and conductivity (793 µS/cm) were within the ideal conditions for the electrospinning process to occur.

Table 4.1:
Viscosity and Conductivity Analysis for PVA/K-car/Honey ODF

Honey volume (mL)	**Viscosity, mPa.S**	**Conductivity µS/cm**
1	199±2.08	670±4.04
1.5	205±4.04	793±8.3
2	208±2.08	804±8.9

The polymer solution viscosity affects the release of AA from the electrospun films. The changes in viscosity and conductivity of AA-loaded ODF solutions affect the size of electrospun fibres in the ODF fabrication. Tabulated data in Table 4.2 show that the viscosity of the solution remains moderately constant, though with some variation within 740 to 902 mPa.s, for an increasing AA concentration from 1% to 11% (w/v). Conversely, the solution conductivity increased approximately from 706 to 1369 µS/cm. Unlike polymer concentration, increasing the amount of ascorbic acid did not correspond to an increase in viscosity. Since ascorbic acid is a low molecular weight solute and not a chain- forming polymer, the relationship is not the same. Higher AA concentration increased the total amount of dissolved solids and AA molecules bonded with the hydroxyl groups of PVA via hydrogen bonds. AA partially disrupted polymer-polymer interactions and reduced chain entanglements. Therefore, opposing forces of the hydrogen bonds and chain entanglements brought about moderate changes in viscosity, as opposed to an increase. On the other hand, ascorbic acid (AA) increased conductivity, as dissolved AA added ions to the solution, which improved the conductivity. Resulting from the increased conductivity, electrostatic stretching of the spinning jet improved the process of electrospinning. This led to the production of finely electrospun fibres at higher AA concentrations. During electrospinning, solutions with viscosity that is below the critical or essential value (>100 mPa.s) tend to form beads as well as irregular fibres, while high viscosity (ranging between 100 mPa.s and 2000 mPa.s) levels mean that a bead-free and smooth fibre is produced (Zahra et al., 2023). An increase in AA leads to a greater conductivity and should lead to a decrease in fibre diameter (Abdul Rahman et al., 2010; Nurhadi et al., 2019), which could result in collecting nanofibrous mats that have a greater homogeneity and reduced fibre diameter. Recent studies of electrospun vitamin C (AA) ODFs suggest that smaller fibre diameters are advantageous for ODFs because they increase the surface area and more effectively promote drug release (Sapiee et al., 2023).

Table 4.2:
Viscosity and Conductivity Analysis for PVA/K-car/AA ODF

Concentration (w/v % of AA)	Viscosity, mPa.S	Conductivity µS/cm
1	740±1.53	706±1.53
3	878±2.08	940±2.08
5	856±1.53	1032±2.0
7	847±2.08	1221±2.0
9	902±2.0	1324±2.08
11	866±2.1	1369±2.0

4.3 Morphological Characterisation of Polymeric Films via SEM: Fibre Diameter Analysis

Scanning electron microscopy (SEM) was used to observe the surface structure of the electrospun honey oral dispersible film (ODF). This technique enabled detailed visualisation of fibre distribution, surface texture, and uniformity, which are essential for the film's performance and patient usability. Measurements of film thickness and surface roughness were taken at several points to evaluate consistency. SEM analysis was performed at various magnifications (Figure 4.1) with a 15 kV accelerating voltage. The micrographs revealed surface features and fibre arrangement.

4.3.1 SEM Analysis of PVA/κ-Car ODFs Loaded with Honey

Fabrication of PVA/κ-Car with honey loaded was characterised using SEM (Hitachi SEM SU3500), micrographs of PVA/κ-Car/honey with different volume nanofiber membranes are presented in Figure 4.1. In all three, the nature of the nanofiber was preserved. The preserved nanofiber structure is anticipated to encapsulate the medicine and facilitate the delivery of desired compounds that enhance the healing process (Roopesh et al., 2023). The ODFs were obtained at collector distances from 15 to 16 cm, with voltage applied at 16 kV and flow rate from 0.4 mL/hr to 0.6 mL/hr as stated in Table 3.2.

The distribution of fibre diameters in electrospun oral dispersible films (ODFs) containing different volumes of honey was illustrated using histograms (Figure 4.2) with measurements categorised from 100 to 300 nm.

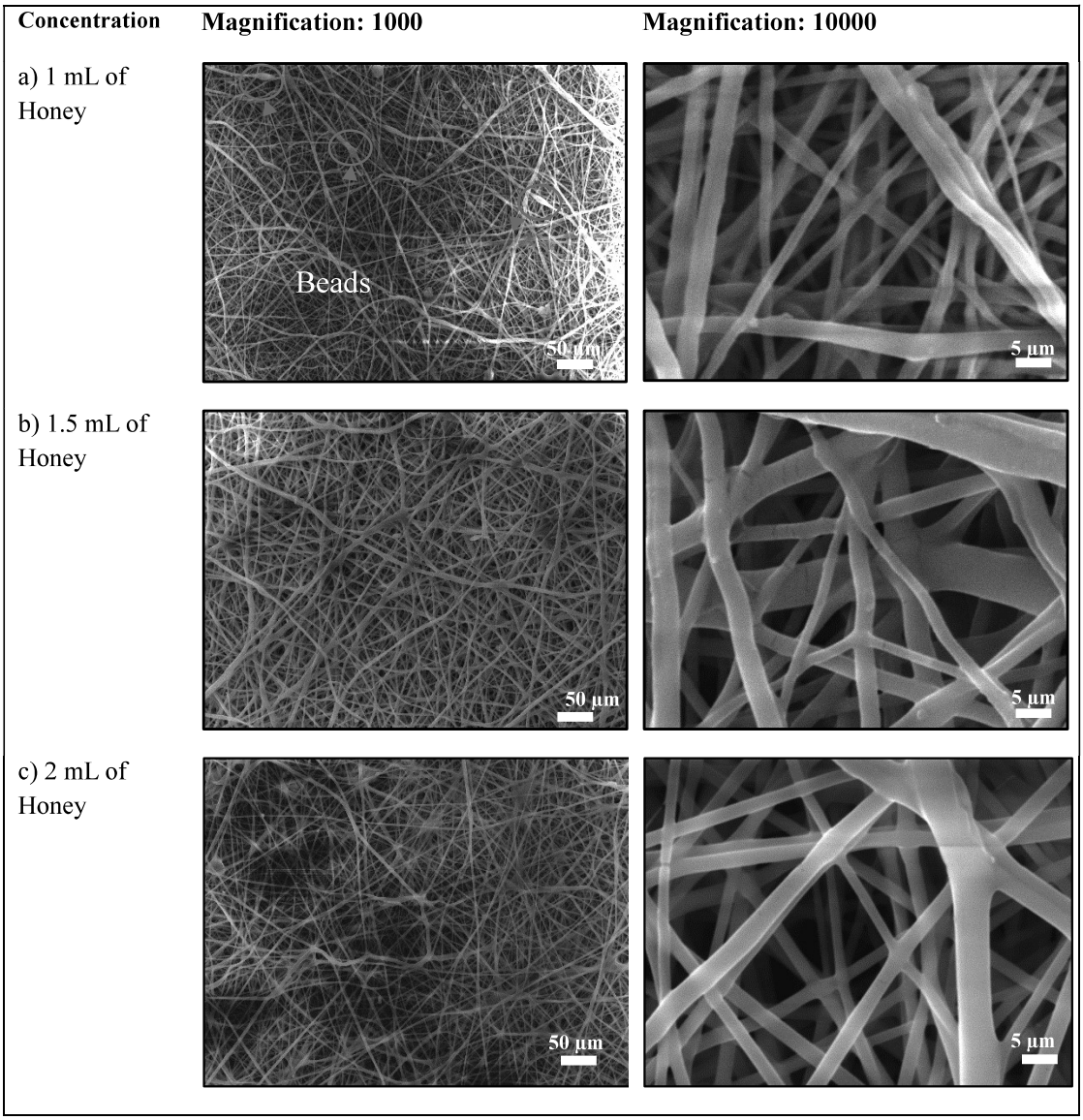


Figure 4.1: SEM Analysis for Electrospun ODF PVA/K-Car/Honey Of (a) 1 mL, (b) 1.5 mL, And (c) 2 mL

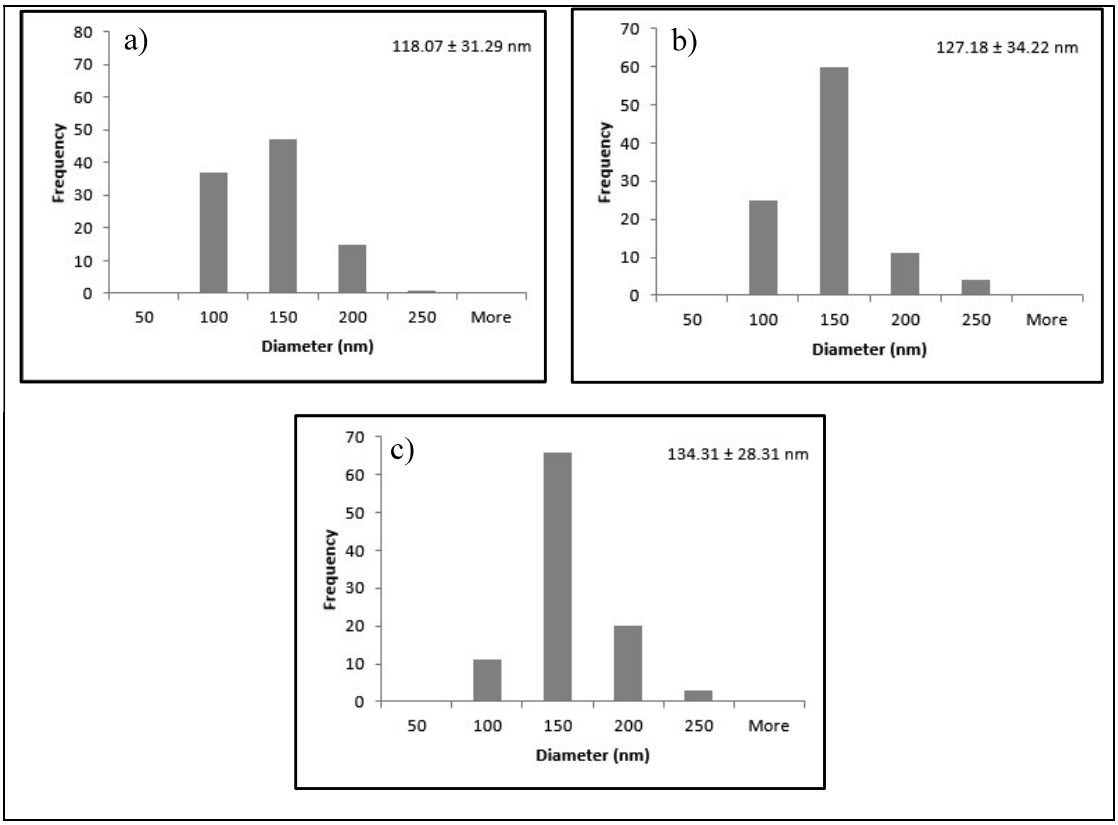


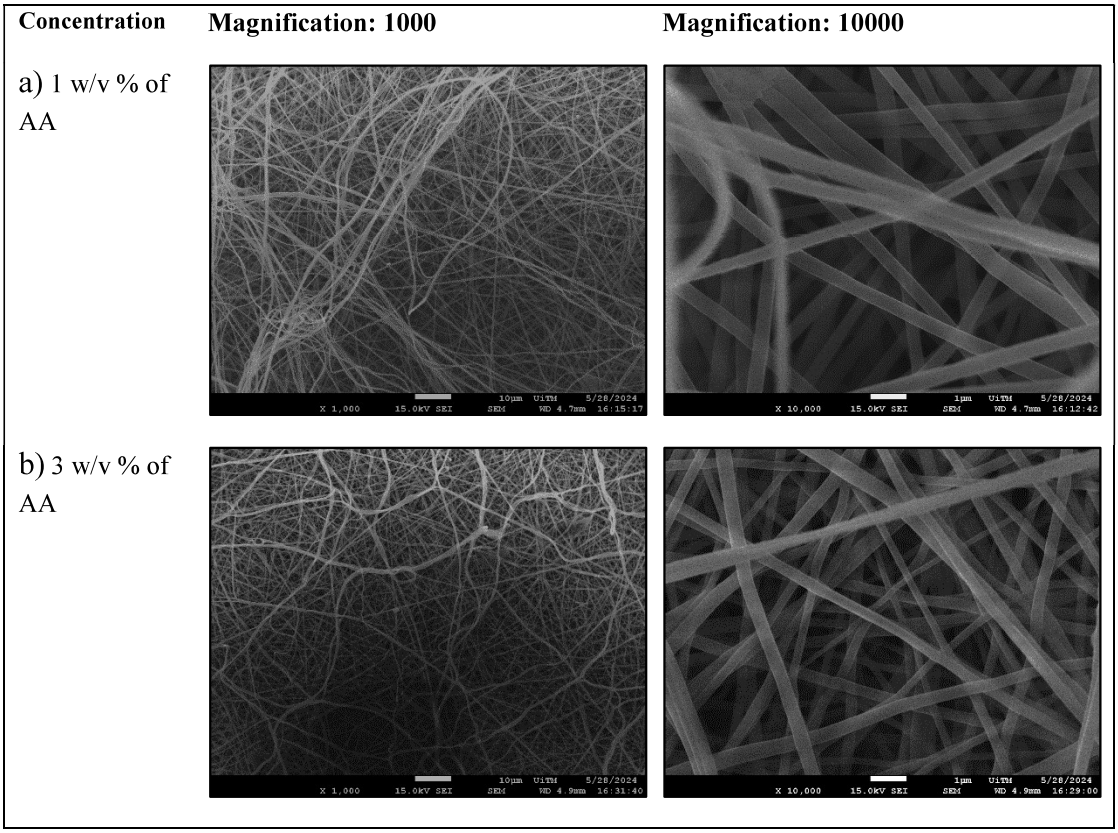
Figure 4.2: Distributions of Nanofiber Diameter for PVA/K-Car/Honey in Different Volumes: (a) 1 mL, (b) 1.5 mL, And (c) 2 mL

The SEM images in Figure 4.1 and Figure 4.2 show how solution viscosity affects the morphology and fibre diameter of electrospun PVA/κ-car/honey ODFs. The formulation with the lowest viscosity (Figure 4.1a) exhibited bead formation, implying some electrospinning instability, which was probably due to decreased viscosity and less entanglement of the polymer chains. As the solution viscosity increased (Figure 4.1b), the fibres became more homogenous. At the highest viscosity (Figure 4.1c), smooth and uniform nanofibers were obtained. This is because the greater viscosity of the solution caused by the sugars in honey increases the entanglement of the polymer chains and the stability of the jet during electrospinning (Deshawar et al., 2020; Yu et al., 2006). The mean fibre diameter was determined using an average of 100 fibres. Consistent with the increase in solution viscosity, the average fibre diameter increased from 118±31.29 nm to 127.18±34.22 nm and finally to 134.31±28.31 nm, as seen in Figure 4.2. Two prior studies have confirmed that the increased diameter of electrospun nanofibers stems from a rise in spinning solution viscosity, which enhances polymer chain entanglement and restricts jet stretching under an electric field (De Vrieze et al., 2009; Yu et al., 2006). This study finds that increasing the solution viscosity for

electrospinning can reduce bead formation, enhance spinning stability, and produce smooth, uniform nanofibers, with only a small increase in fibre diameter. The fibre diameters of all tested formulations are below 200 nm, and their high specific surface area meets the fast-dissolution requirements of oral fast-dissolving films. The highest-viscosity formulation, which contains 2 mL of honey, delivers the best overall performance.

4.3.2 SEM Analysis of PVA/κ-Car ODFs Loaded with Ascorbic Acid (AA)

Figure 4.3 shows SEM analysis of the fabrication of PVA/κ-Car loaded with AA, which was characterised using the electrospinning parameters listed in Table 3.2. The electrospun ODFs were obtained at collector distances from 15 to 16 cm, with voltage applied at 16 kV and a flow rate from 0.4 ml/hr to 0.6 ml/hr. The distribution of fibre diameters in electrospun oral dispersible films (ODFs) containing different concentrations of ascorbic acid (AA) was determined using histograms (Figure 4.4).



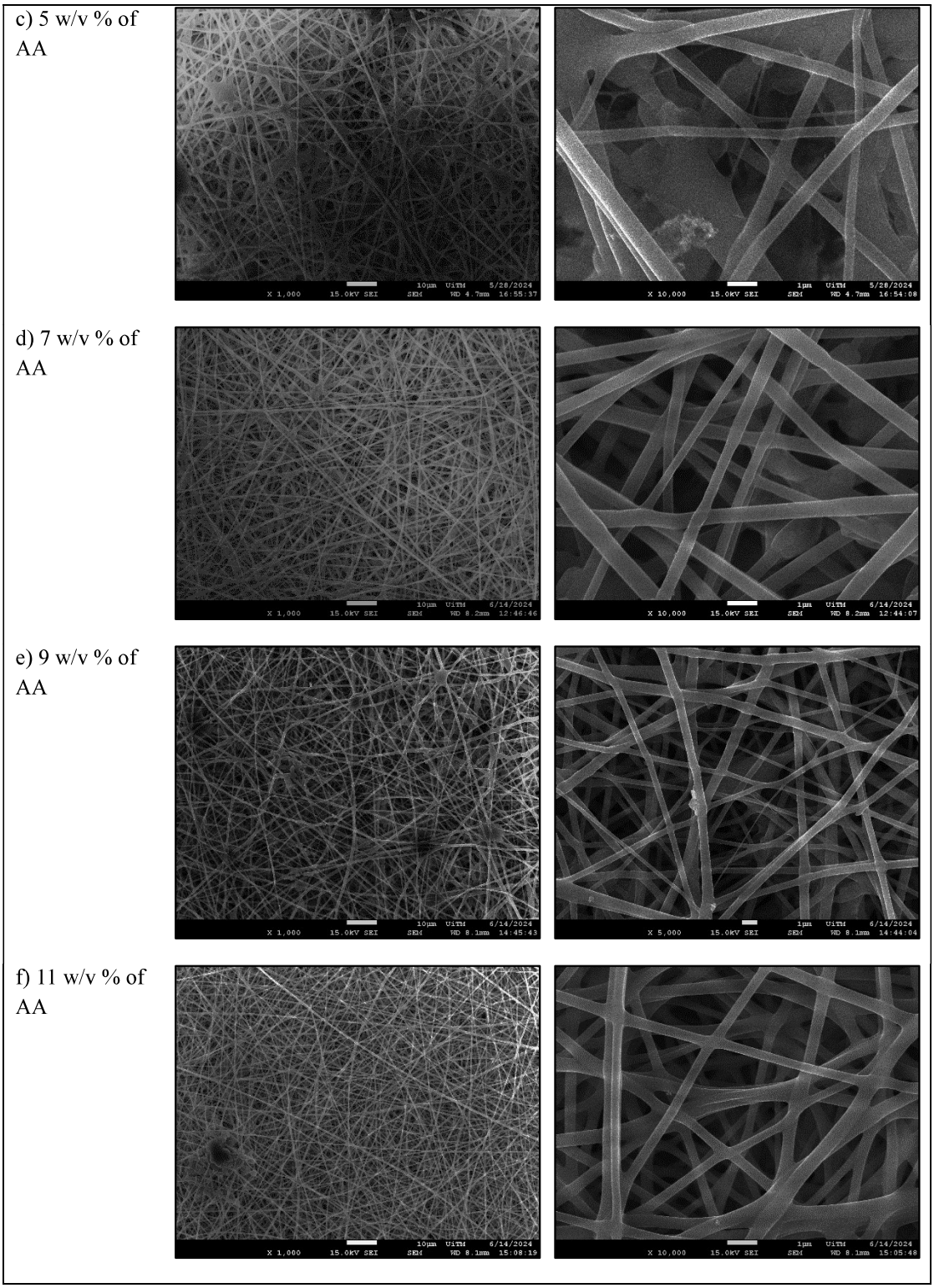


Figure 4.3: SEM Analysis for Electrospun ODF PVA/κ-car/AA of (a) 1 w/v%, (b) 3 w/v% , (c) 5 w/v%, (d) 7 w/v%, (e) 9 w/v%, and (f) 11 w/v%

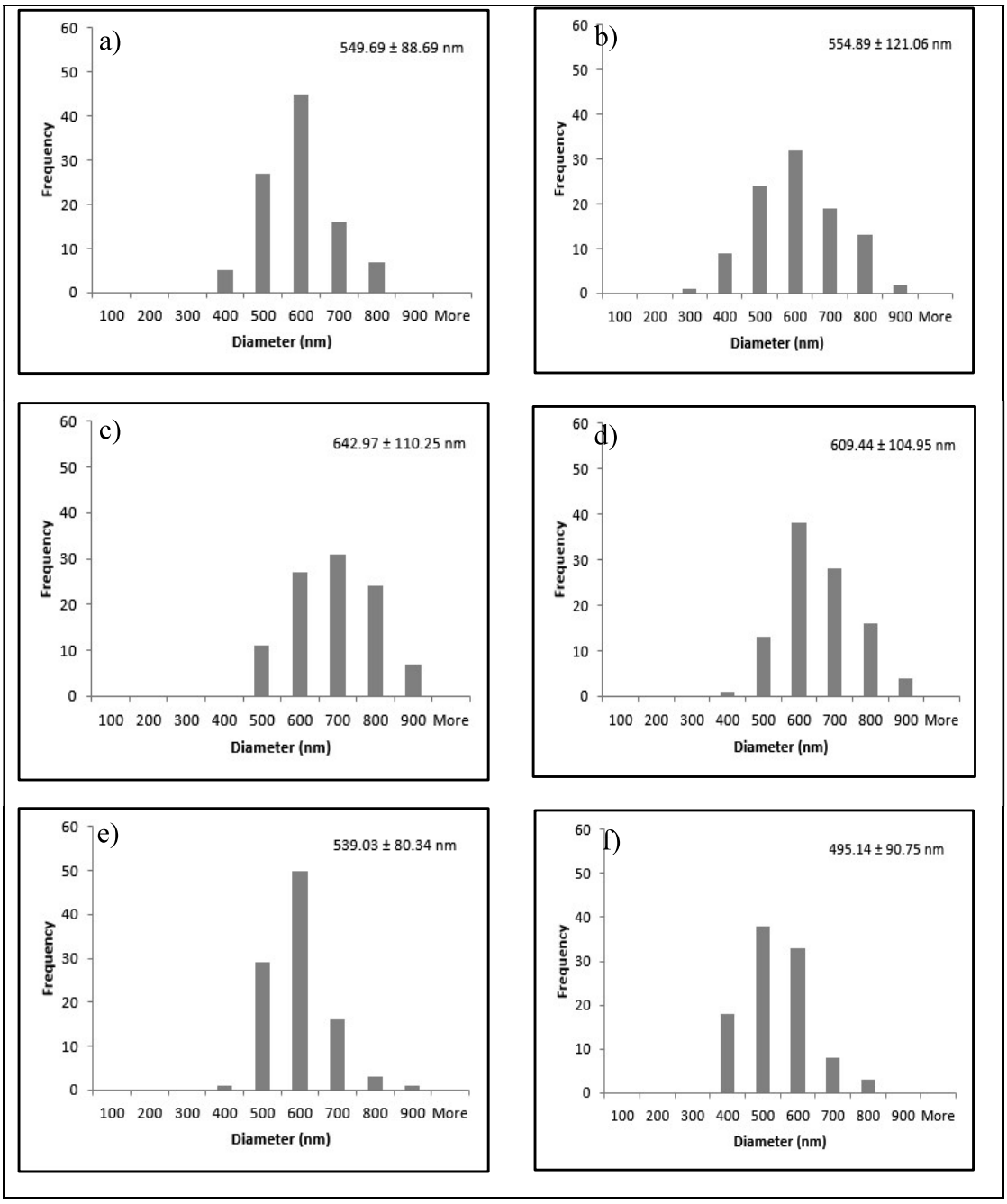


Figure 4.4: Distributions of Electrospun Nanofibers Diameter for PVA/K-Car/AA in Different Concentration (a) 1 w/v%, (b) 3 w/v% , (c) 5 w/v%, (d) 7 w/v%, (e) 9 w/v%, and (f) 11 w/v%

Scanning electron microscopy (SEM) investigation confirmed the formation of smooth, bead-free nanofibers across all formulations Figure 4.3. The fibre diameter was markedly affected by the AA concentration; however, not in a pattern that was linear. Increasing the concentration of AA can result in a refined surface texture, as indicated by Cheng et al. (2024), where the average diameter of the nanofiber increased with the increase in vitamin C content. Conversely, increasing viscosity inhibits the

formation of a beaded structure (Nuraje et al., 2013). The thickest fibres (642.97 ± 110.25 nm) were produced at a 5% AA formulation with a viscosity of 856 ± 1.53 mPa.s and conductivity of 1032 ± 2.0 µS/cm. The 9% AA solution had the highest viscosity (902 ± 2.0 mPa.s); however, its higher conductivity (1324 ± 2.08 µS/cm) probably increased charge density on the polymer jet, leading to more stretching and thinner fibres (539.03 ± 80.34 nm). Likewise, the thinnest (495.14 ± 90.75 nm) resulted at 11% formulation with a viscosity of 866 ± 2.1 mPa.s and the highest conductivity (1369 ± 2.0 µS/cm). Shahbazi et al. (2016) proposed that incorporating κ-carrageenan into PVA can enhance the intermolecular forces between polymer chains, improve fibre uniformity and reduce defects. All experimental formulations in this study produced smooth, defect-free nanofibers, which align with this conclusion.

Characterisation results from this study show that the ideal nanofiber morphology of PVA/κ-car ODFs is smooth, continuous, and bead-free. This morphology supports a reliable electrospinning process and enables the formation of a homogeneous network that promotes rapid dissolution. Among all tested formulations, the 11% AA formulation is the optimal option: its ideal viscosity and higher electrical conductivity allow for the production of the finest and most uniform fibres.

4.4 Water Contact Angle Analysis (WCA)

Section 4.4.1 and Section 4.4.2 discuss the water contact angle for ODFs with honey and ascorbic acid. The water contact angle is used to determine the water resistance of the films. In assessing membrane behaviour in humid conditions, its hydrophobicity must be evaluated from the contact angle measurement. The hydrophobicity of the membrane from the solid/liquid/vapour boundary is thus measured. If this contact angle is less than 90°C, the membrane is hydrophilic. If the contact angle is greater than 90°C, the membrane is hydrophobic (Sthefany et al., 2025)

4.4.1 Water Contact Angle Analysis for Electrospun PVA/κ-Car/Honey ODFs

Figure 4.5 shows the water contact angle characteristics of the PVA/κ-car/honey samples, which were measured at approximately 50.6°, 61.8° and 65.5° for samples with honey volumes of 1.0ml, 1.5ml and 2.0ml, respectively. This study tested the water contact angle (WCA) of polymer films with different volumes of honey. All samples

had a WCA below 90°, confirming that the films have hydrophilic surfaces. WCA rose as the amount of added honey increased, which indicates that high concentrations of honey reduce the accessibility of hydrophilic groups on the film surface. The results obtained regarding samples 1.5 mL and 2.0 mL are in accordance with the 60° – 69° range values, which are associated with pure and edible κ-car films (Mavelil-sam et al., 2023). Bakar et al. (2023) stated that the quantitative definition of hydrophilic surfaces is characterised by a contact angle of $\theta < 65.0°$. This confirms that the addition of honey merely validates the surface characteristics similar to those of the other carrageenan biopolymer films designed for food and biomedical applications. With increased volume concentrations of honey, a slight increase in water contact angle (WCA) was recorded, indicating a decrease in surface hydrophilicity with a lesser volume of honey. This experiment found that all PVA/κ-car/honey composite preparations are hydrophilic, and the experimental group with 1.0 mL of honey added had the strongest surface hydrophilicity.

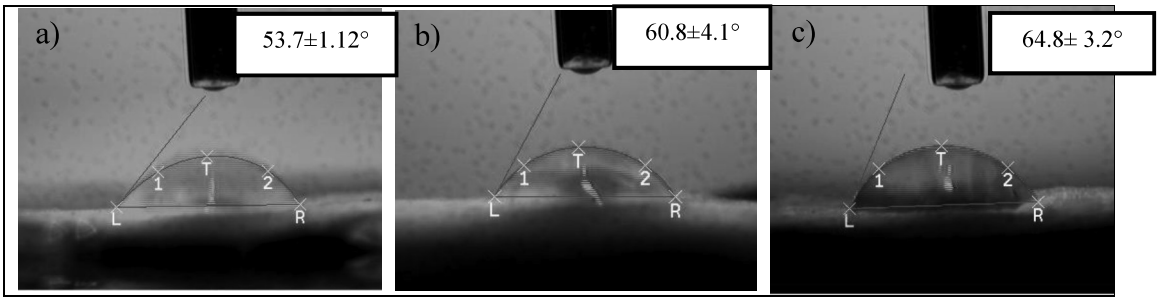


Figure 4.5: Water Contact Angle of PVA/K-Car/Honey of Different Volume (a) 1mL (b) 1.5mL (c) 2mL

PVA/κ-car/honey with 1mL of honey exhibits the lowest contact angle values (50.6°), indicating the most hydrophilic among the samples. As the honey volume increases to 1.5mL and 2 mL, the contact angle increases to 60.8±4.1° and 64.8± 3.2°, respectively, suggesting reduced surface wettability. Published studies from Bakar et al. (2023) show that electrospun PVA/κ-carrageenan films have a water contact angle lower than 61.7° and possess inherent hydrophilicity. All honey-loaded oral dispersible films developed in this study have a contact angle of less than 90° and retain their hydrophilicity. Even though the surfaces were still hydrophilic, such a high WCA indicates a decrease in surface hydrophilicity. A study conducted by Zainuddin et al. (2025) showed that higher honey concentrations decreased the hydrophilicity of the surface, as the contact angle value increased. The experimental findings of this study

demonstrate that the inclusion of honey imparts additional bioactive properties to the ODF system. However, excessive addition of honey weakens the ODF system's surface wettability, an effect that arises from altered interactions between the polymer and honey. In this study, the contact angles of all tested PVA/κ-car/honey ODF formulations were all lower than 90°, which met the qualification standard for hydrophilic performance. The samples with 1 mL of honey had the strongest hydrophilicity (53.7±1.12°) while the high-concentration groups had moderate hydrophilicity, a characteristic that preserves the mechanical stability of the films while ensuring practical usability.

4.4.2 Water Contact Angle Analysis for Electrospun PVA/κ-Car/AA ODFs

Figure 4.6 show**s** water droplets on a thin film for contact angle measurements on PVA/κ-car/AA for different concentrations. Throughout the water contact angle (WCA) analysis, the series shows a decreasing angle as the AA concentration increases. Indicating that it is a progressive trend towards more hydrophilic.

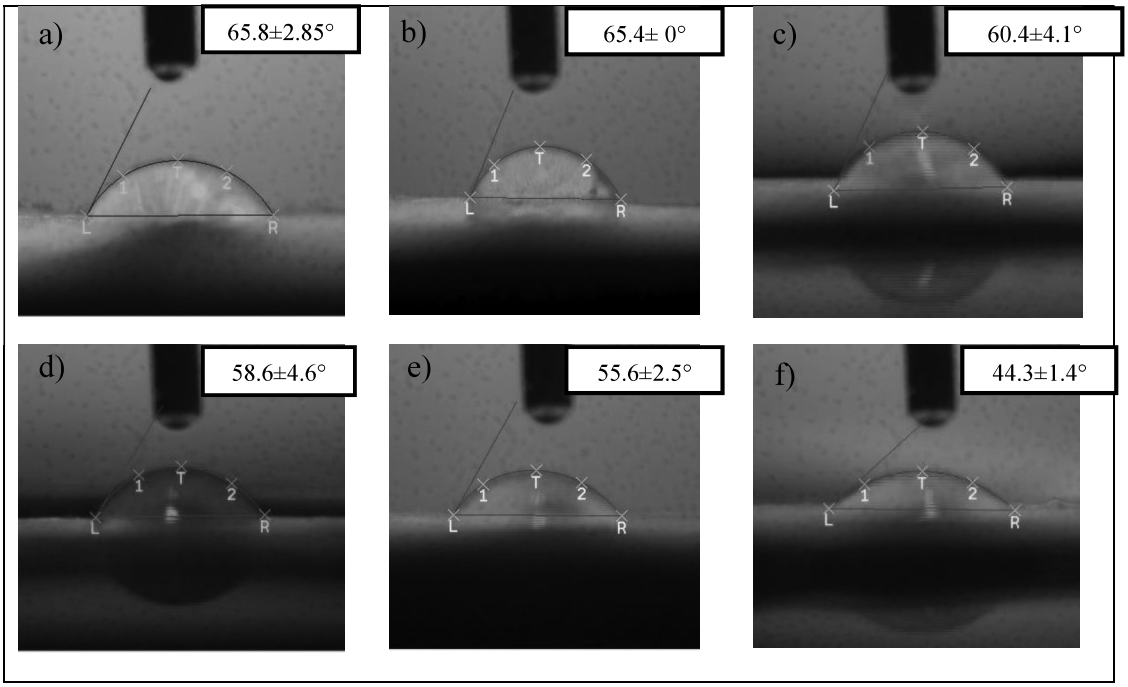


Figure 4.6: Water Contact Angle of PVA/K-Car/AA of Different Concentrations (a) 1 w/v% AA, (b) 3 w/v% AA, (c) 5 w/v% AA, (d) 7 w/v% AA, (e) 9 w/v% AA, and (f) 11 w/v% AA

From the 1 w/v% and 3 w/v% concentration of AA, the contact angles were around 65.8±2.85° and 65.4± 0°, which were moderately hydrophilic surfaces. As the concentration of AA increased (5 w/v% and 7 w/v%), the contact angle showed a lower value, which was 60.4±4.1° and 58.6±4.6°, respectively. This shows that the surface around the AA was wider in a lower contact angle with the droplet and that it was also hydrophilic at AA with concentrations of 9 w/v% and 11 w/v%, the contact angle showing around 55.6±2.5° and 44.3±1.4°, respectively, demonstrating clear hydrophilicity as concentration increases, the angle decreases. Similar findings were reported by Sapiee et al. (2023), where as the concentration of AA increases, the WCA decreases, with 8% of AA exhibiting the lowest WCA, which is 38.5°. In this study, ascorbic acid (AA) was added to electrospun oral dispersible films (ODFs). Compared with the PVA/κ-car film of Bakar et al. (2023), AA was found to reduce the films' water contact angle, an effect that grew more significant at higher AA concentrations. AA has strong hydrophilicity due to its multiple hydroxyl groups, so high-concentration AA formulations have superior wettability, which facilitates the rapid hydration and dissolution of the oral films. The inclusion of ascorbic acid (AA) in polymer films tends to increase the hydrophilicity as a direct result of ascorbic acid's polar structure, which aligns with the explanation of the lower contact angle observed at higher AA concentrations. AA contains a large number of hydroxyl groups (-OH), and its strong polarity enables it to form hydrogen bonds with water molecules. As AA concentration increases, the number of polar functional groups on the film surface rises, the film's water affinity strengthens, and eventually water droplets spread easily on the surface; the water contact angle decreases, and the surface wettability is effectively improved (Gupta et al., 2025; Handley & Callanan, 2023; Khan et al., 2023).

4.5 Fourier Transform Infrared Spectroscopy (FT-IR)

4.5.1 FT-IR Analysis for Electrospun PVA/k-Car/Honey ODFs

Figure 4.7 shows an FTIR image for PVA/κ-car loaded honey in different volumes: 1ml, 1.5ml, and 2ml. Axis-x represents wavenumber (cm^{-1}) in the range from 4000 cm^{-1} down to 500 cm^{-1}, which corresponds to the vibrational frequency of chemical bonds, while the axis-y represents transmittance or absorbance producing the peaks associated with different stretching and bending variations. In general, the trend

was similar to past studies conducted by Chopra et al. (2022), Şalva et al. (2023) and Santos et al. (2019). It is interesting to observe the peak of honey for these ODFs, which act as active ingredients. A comprehensive overview and other past studies of ODF spectra are presented in Table 4.3.

The spectrum indicated various functional groups; thus, the identification of possible combinations and interactions with each other explained the figure as a formulation component. A broad band, resulting from O-H stretching vibrations, as in the 3200-3600 cm^{-1} region, is typical of polymers with hydroxyl groups such as PVA, as well as κ-carrageenan and honey. (Uddin et al., 2022; Şalva et al., 2023; Zhang et al., 2020). This band in films is observed to shift further due to the formation of additional hydrogen bonds with the hydroxyl groups in the polymer matrix and the sugars or phenolic molecules present in honey (Sabbagh et al., 2023). The region around 2800 – 3000 cm^{-1} (Sabbagh et al., 2023; Zhang et al., 2020; Kanimozhi et al., 2020; Şalva et al., 2023) is caused by C-H stretching and is associated with the polymer in PVA and the carbohydrate chain in κ-car, as well as the honey compounds. Approximately 1600 – 1750 cm^{-1}, the carbonyl group (C=O) and other functional groups, as well as the fingerprint region peak, appeared; for κ-car, it corresponds to the sulfate ester groups (S=O) as well as C-O-C, typically in the 1000 – 1250 cm^{-1} (Sabbagh et al., 2023). A peak around 1700 – 1740 cm^{-1} (Seleka et al., 2025) has been assigned to C=O stretching, which is likely for PVA and the κ-car compound. Honey peak appeared in the fingerprint region ~1000 – 1150 cm^{-1} (Chopra et al., 2022) and also at 1400 to 1450 cm^{-1} (Vuković et al., 2025), which corresponds to the carbohydrate group. A peak at ~840 – 920 cm^{-1} (Vuković et al., 2025) resembles the C-O-S functional group or sulfate ester group. Variations in water content, thickness of samples, or even how they were prepared may change the position of the O-H and carbohydrate molecules. Hence, consistent experimental condition are crucial for comparative analysis.

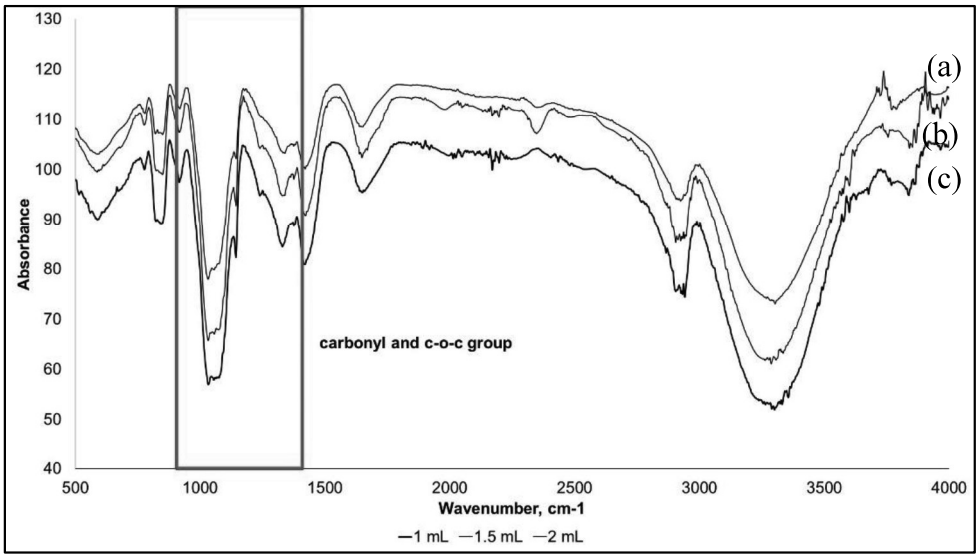


Figure 4.7: PVA/K-car/Honey Detection Using FT-IR for Film (a) 1mL (b) 1.5mL (c) 2mL

Table 4.3:
Peak of the FTIR Spectra for ODFs with Honey Loaded

Wavenumber (cm-1)	Functional groups	References
3360 - 3279	O-H	(Uddin et al., 2022), (Zhang et al., 2020), (Uddin et al., 2022), (Kanimozhi et al., 2020)
2922	CH_2 stretching	(Uddin et al., 2022)
1479 - 1280	CH_2 bending	(Uddin et al., 2022)
2930	C-H stretching	(Zhang et al., 2020)
2922		(Uddin et al., 2022)
2900		(Kanimozhi et al., 2020)
741 - 710		
1664 - 1337	C=O stretching	(Uddin et al., 2022)
1650		(Şalva et al., 2023)
1090 - 1054	C-O	(Zhang et al., 2020) & (Şalva et al., 2023)
1857		(Kanimozhi et al., 2020)

4.5.2 FT-IR Analysis for Electrospun PVA/k-Car/AA ODFs

The FTIR spectra of the samples are depicted in Figure 4.8. Axis-x represents wavenumber (cm^{-1}) in the range from 4000 cm^{-1} down to 600 cm^{-1}, which corresponds to the vibrational frequency of chemical bonds, while the axis-y represents transmittance or absorbance producing the peaks associated with different stretching and bending variations. In general, the trend was similar to past studies conducted by Bratu et al. (2009), Cortés-Estrada et al. (2020), Devianti et al. (2023), and Munir et al. (2024). A comprehensive overview and other past studies of ODF spectra are presented in Table 4.4. The interpretation of the spectra is aligned with past research ; Chaudhry & Rangra (2023) conducted where the band at 3100 – 3600 $cm^{-1,}$ which represented O-H stretching vibration of water, PVA and κ-car. For film samples, this peak tends to broaden or shift slightly to the right, signifying the presence of hydrogen binding interactions between the hydroxyls of PVA and κ-car. The peak in the range of ~2900 – 3000 cm^{-1} (Adel Rashiq et al., 2025; Calzado-Delgado et al., 2023; Cheng et al., 2024; Cortés-Estrada et al., 2020) indicated the C-H stretching typically for polymer (PVA). This range suggests there are no changes to the polymer structure – PVA and κ-car- during the incorporation of AA. The region around 1600 to 1700 cm^{-1} corresponds to the overlapping of carbonyl (C=O) stretching of the five-membered lactone ring of AA, which is similar to past studies conducted by Okur et al. (2021) and Munir et al. (2024), and carbon-carbon double bond (C=C) stretching vibrations. A study conducted by Sabbagh et al. (2023) has analysed the formation of hydrogels that consist of PVA and κ-car. The FTIR analysis was provided with a broad band at ~3400 cm-1 (O-H stretching) and a peak around ~2940 cm-1 (C-H stretching. This study does not include ascorbic acid, but it provides the baseline FTIR patterns of the PVA/κ-car films.

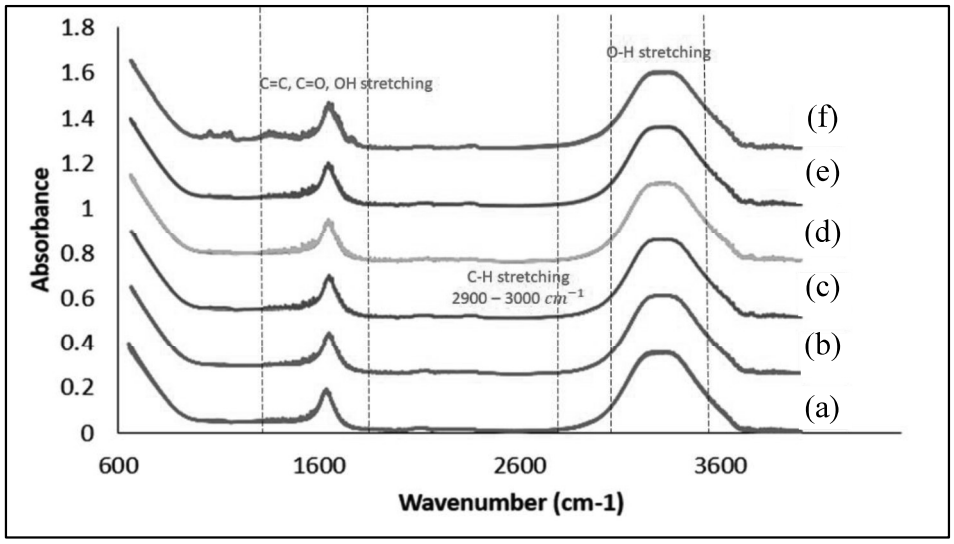


Figure 4.8: PVA/K-Car/AA Detection Using FT-IR for Different Concentrations (a) 1 w/v% AA, (b) 3 w/v% AA, (c) 5 w/v% AA, (d) 7 w/v% AA, (e) 9 w/v% AA, and (f) 11 w/v% AA

Table 4.4:
Peak of the FTIR Spectra for ODFs With AA Loaded

Observed values (cm-1)	Functional groups	References
1673 and 1754	C=O groups	(Bratu et al., 2009)
3297 - 3600	O-H stretching	(Munir et al., 2024)
1635	-C=O vibration	
1454 - 1327	C-C	
1787 - 1742	C=C	
3500	O-H	
1659	C=O	(Guler et al., 2024)
2360	O-H	
1674 and 1322	C=C	(Umer et al., 2014)
3311.88	O-H	
1762	C=O	(Ahmed et al., 2018)
1675	C=C	
1200 - 1500	C-H_2 scissoring	

1277 - 1077	C-O-C	
3526 - 3411, 3216 - 3529	O-H	
1600 - 1700	C=C & C=O	(Okur et al., 2021)
1651- 1750	C=C & C=O	(Calzado-Delgado et al., 2023)
3200 - 3600	O-H	
2941	C-H stretching	
1754	C=O	(Cheng et al., 2024)
1673	C-C	
3305	O-H stretching	(Adel Rashiq et al., 2025)
2933 - 3084	C-H bending	
1703 - 1632	C=O stretching	
3650 - 3050	O-H stretching	(Cortés-Estrada et al., 2020)
2960 - 2855	C-H stretching	
1750 - 1580	C=O	
	C=C	

4.6 Mechanical Performances of Electrospun ODFs

To ensure the mechanical integrity of oral dispersible films across the full process of production, packaging, storage, and patient handling, mechanical testing must be carried out: insufficient tensile strength easily leads to film rupture, while excessive stiffness will delay drug release, so core performance must be balanced using the indicators of tensile strength, Young's modulus, and elongation at break.

4.6.1 For PVA/κ-Car/Honey Oral Dispersible Film

In general, PVA films are recognised for their ability to form films, mechanical strength and flexibility. It is often used in combination with other polymers to improve these characteristics (Chopra et al., 2022; Makram et al., 2024). Honey is often used in films because of its antibacterial properties and also acts as a plasticiser, which may

have an adverse effect on the mechanical properties of the films (Koosha et al., 2021; Zhang et al., 2020). The honey volume increases from 1mL to 2mL leads to differences in PVA/κ-car/honey ODFs stiffness and deformation characteristics, and the stress-strain curves in Figure 4.9 and the bar graph in Figure 4.10. . The Young's modulus value are 0.0015 MPa to 0.0009 MPa to 0.0014 MPa for honey formulations, respectively. Although the values veried among the formulations, all films exhibits relatively low Young's modulus, indicating that the electrospun ODFs remained flexible rather than highly rigid. The elongation at break , remains relatively consistent and differs from 34% (1 mL), 36% (1.5 mL) and 33% (2 mL) indicating that all films maintained comparable flexibility despite differences in Young's modulus.

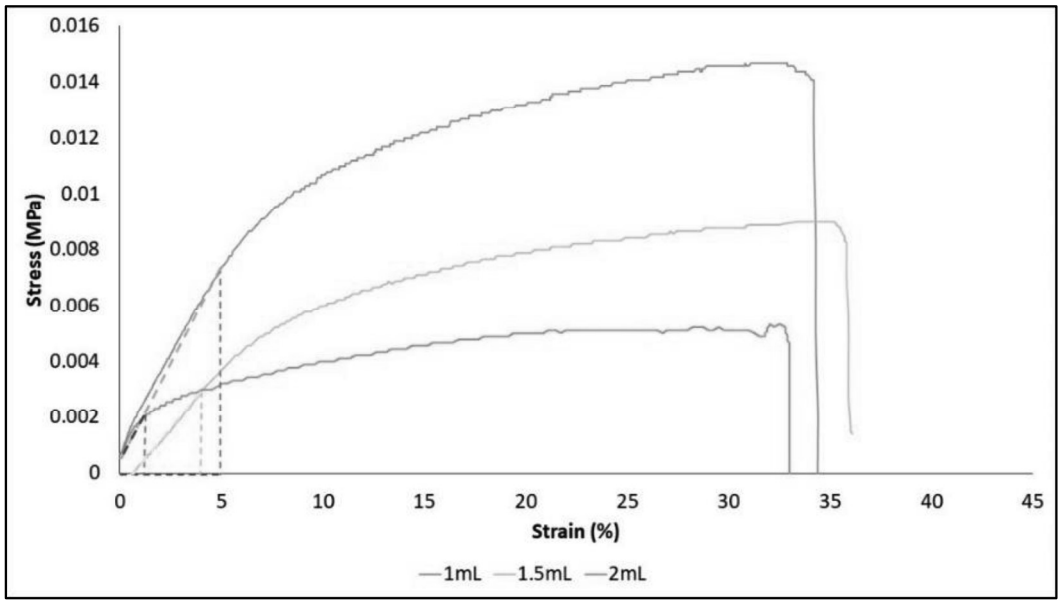


Figure 4.9: Stress-Strain Curves of Honey-Loaded ODFs

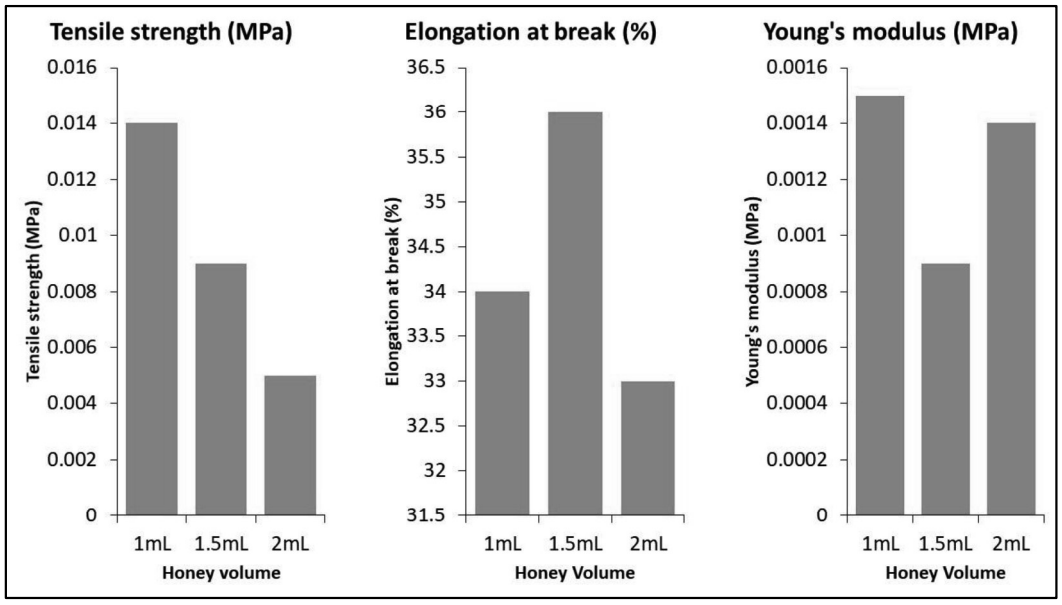


Figure 4.10: Mechanical Properties of the Electrospun ODFs

In this study, it was used as a natural or indigenous ingredient. It can form hydrogen bonds with PVA and κ-carrageenan to improve the mobility of polymer chains. Studies commonly uses honey as a film plasticizer. Measurements from this study show that the Young's modulus of films with different honey addition levels only fluctuates slightly, and their stiffness is not strictly affected by concentration. Nevertheless, higher honey loading may still weaken intermolecular interactions and reduce the mechanical integrity of the films, as reported in previous studies (Koosha et al., 2021; Mohd Azam & Amin, 2017). Studies about chitosan/PVA/honey films explain that higher levels of honey may reduce tensile strength due to honey's plasticising effects, which may weaken the film's structure (Koosha et al., 2021). A similar study has been observed with gellan gum films infused with honey. In that case, increasing the amount of honey also resulted in lower tensile strength and Young's modulus (Mohd Azam & Amin, 2017). Several factors may explain why the elongation at break for the ODF sample 1.5mL is higher compared to 1mL and 2mL. The possible reason and potential errors are that it could be due to the uneven thickness of the film. The natural variability of the ODF samples could also contribute to unequal results, leading to a difference in material batch or a slight difference in the sample preparation technique. This study confirms that the optimal volume combination for the honey film series was 1.5 mL. The performance of this sample falls between that of the other two groups: it has a tensile strength of 0.009 MPa, a Young's modulus of 0.0009 MPa, and

an elongation at break of 36%, which is the highest among the three groups, achieving a sound balance between strength and flexibility. Takeuchi et al. (2020) proposed ideal mechanical benchmarks for oral fast-dissolving films: a tensile strength of <20 MPa and an elongation at break ranging from 3% to over 100%. The formulations tested in the present study recorded measured tensile strength values of 0.0009–0.0015 MPa and elongation at break values of 13%–51%, all of which meet the specified requirements. The properties of the loaded drugs, the additives incorporated, and the molecular weight of the film- forming polymer were shown to influence the tensile strength (Zaki et al., 2023). Study conducted by Pacheco et al. (2021) used various kinds of plasticisers, additives, and polymers to exhibit higher tensile strength, such as xanthan gum and glycerol (plasticisers), polyvinyl acetate (PVAc) (fillers), glycerine, propylene glycol and HPMC, was used to increase the tensile strength. However, when the film is compared against the control value (PVA/κ-car) reported in a previous study (Yeşilyurt et al., 2025), the control PVA/κ-car exhibits a higher Young's modulus, indicating greater stiffness. The incorporation of honey reduces the Young's modulus relative to this control, indicating that honey functions as a plasticiser.

4.6.2 For PVA/κ-Car/AA Oral Dispersible Film

Ascorbic acid (AA) exhibits a significant concentration-dependent decrease in tensile strength within the PVA/κ-car/AA ODF, as shown in the stress-strain curves in Figure 4.11, as the AA concentration increases from 1 to 11 w/v%. An increase in AA concentration leads to a clear decrease in the tensile strength of films. This means that the films are losing more of their ability to resist components that decrease the film's ability to withstand tensile force. Even though the films have more strength because of their ability to withstand tensile stress, the concentration of AA leads to a quicker failure of the films. A non-linear trend can be seen in the elongation at break parameter, which starts by maintaining the same value for some time, then increases at an intermediate value of AA concentration (7 w/v%) and decreases as the concentration increases. This trend shows that for moderate AA concentration values, the films have more capacity for deformation and can have an increase in strain before rupturing (more elongation). Conversely, increasing the concentration of AA causes the elongation to decrease because the films rupture at a lower level of strain. The results obtained confirm that higher concentrations of AA mean lower values of tensile strength, while at moderate

values of concentration, the level of elongation at break is greater because of greater deformation capacity. The increase in concentration, however, leads to a decrease in elongation at break because of the weakening of the films.

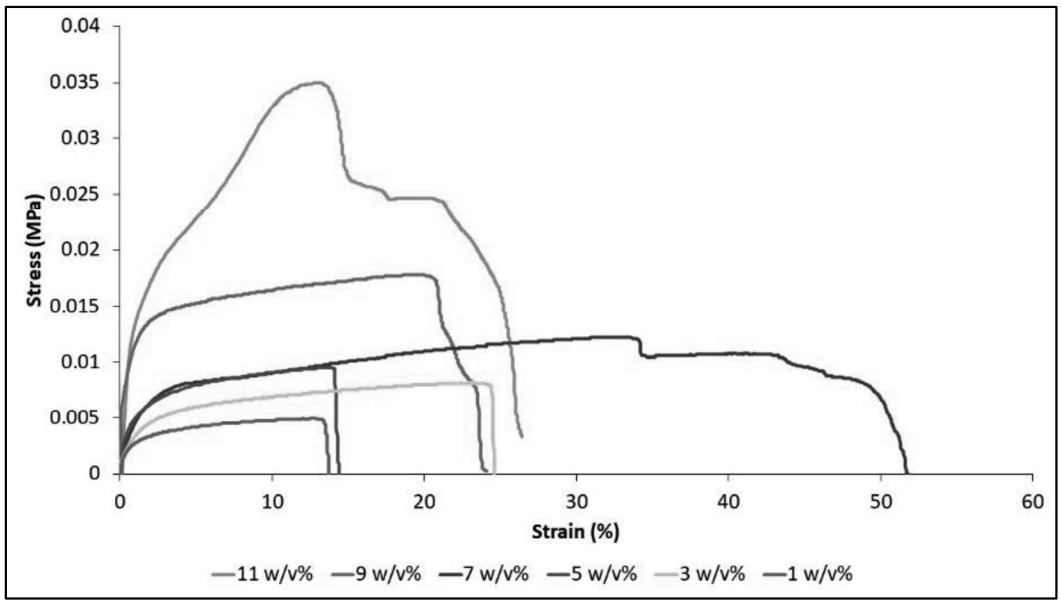


Figure 4.11: Stress-Strain Curves Of AA-Loaded ODFs

Adding more AA to PVA/κ-car films might at least increase the elongation at break due to improved flexibility. However, at some point, too much AA could cause phase and other structural issues that might reduce elongation at break. A decrease in tensile strength and an elongation at break excessive elongation at break value suggest a further loss of mechanical integrity for the film. The changes in tensile strength and elongation at break of the PVA/κ-carrageenan composite polymer network originate from alterations in molecular interactions within the network (Yoon, 2014). Ascorbic acid (AA) contains multiple hydroxyl groups and can bind via hydrogen bonding to the hydroxyl groups of PVA and the sulfate groups of κ-carrageenan, respectively. As the AA concentration gradient rises, these changes in interactions gradually emerge: at medium AA concentrations, the original intermolecular interactions between PVA molecules are disrupted, which improves the mobility of polymer chains and drives up the elongation at break (Iskalieva et al., 2023; Yang et al., 2024), at higher AA concentrations, excessive damage to the network structure leads to reduced molecular cohesion, failed interchain stress transfer, and a drop in tensile strength, at the highest AA concentration, excessive molecular mobility causes insufficient deformation

recovery capacity, so the elongation at break also decreases (Yang et al., 2024). The addition of AA weakened the flexibility of the nanofiber film, resulting in a decrease in its tensile elongation at break (Cheng et al., 2024). The properties of the loaded drugs, the additives incorporated, and the molecular weight of the film- forming polymer were shown to influence the tensile strength (Zaki et al., 2023). Mechanical properties of PVA/κ-car/AA films can be affected by the different concentrations of AA. There has to be an adjustment of the electrospinning conditions and AA concentration for an optimal equilibrium between tensile strength and elongation at break. All identified issues may require more adjustments to the formulation and processing parameters. Under a proper adjustment, the desired mechanical properties can be attained. In the AA series, 7 w/v% was the optimal concentration: it reaches an elongation at break of 51% and a tensile strength of 0.0088 MPa, values that are close to the measurements of the 9 w/v% sample. Only this concentration can greatly improve flexibility without losing mechanical strength, while samples at all other higher or lower concentrations fail to achieve this type of performance improvement. Figure 4.12 shows the mechanical properties of the electrospun ODF for all different AA concentrations.

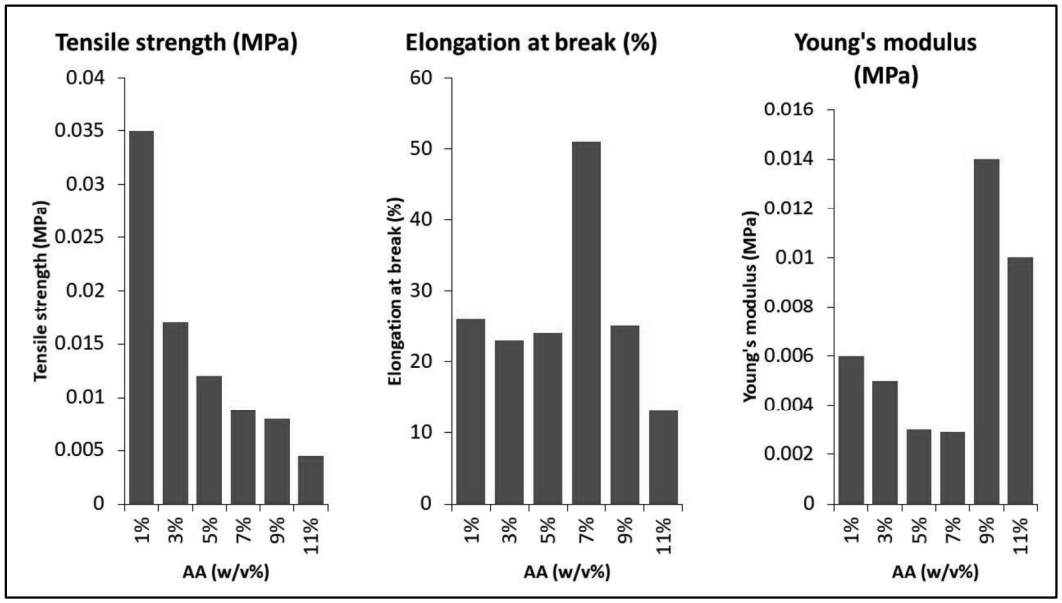


Figure 4.12: Mechanical Properties of the Electrospun ODFs

In conclusion, PVA/κ-car/honey ODF with a volume of 1.5 mL has a tensile strength of 0.009 MPa and an elongation at break of 36%. PVA/κ-car/AA ODF with a concentration of 7 w/v% has a tensile strength of 0.0088 MPa and an elongation at break

of 51%. The two formulations have similar tensile strength, while the latter has a significantly higher elongation at break, meaning it can improve the film's flexibility without compromising mechanical strength. Both formulations meet the ideal parameter range proposed by Takeuchi et al. (2020), and this AA-loaded formulation shows better overall performance. There is a deeply interconnected relationship between the mechanical properties, the dissolution, and the release behaviour of polymer films.c Films with moderate tensile strength and sufficient flexibility can accelerate water penetration into the matrix, driving rapid swelling and disintegration. Excessively high tensile strength will slow down water diffusion, while insufficient strength makes the films prone to damage before drug administration. Therefore, these two categories of properties must be balanced to meet both the requirements for handling performance and the demand for rapid drug release.

4.7 Dissolution of Electrospun PVA/κ-Car/Honey and PVA/κ-Car/AA ODFs

This study analyses the dissolution and the kelulut honey release mechanism of electrospun PVA/κ-carrageenan/kelulut honey oral fast-dissolving films (ODFs). When the films come into contact with artificial saliva, the concentration gradient between the medium and the film matrix drives water molecules to permeate into the dry polymer matrix. This osmotic process conforms to Fick's first law of diffusion. The infiltrated water acts as a plasticiser, converting the originally glassy polymer into a hydrated rubbery gel. Sustained hydration triggers swelling of the polymer network and gradual erosion of the matrix, after which the kelulut honey contained in the films diffuses into the surrounding medium. The entire release process is ultimately controlled by a dual mechanism of diffusion and erosion.

4.7.1 Batch Dissolution of Electrospun ODFs Using UV-Vis Spectroscopy

i) Batch dissolution of electrospun PVA/κ-Car/honey ODF

Uv-vis analysis was conducted to measure the content of honey in the electrospun ODF. This analysis assessed the absorbance of the samples that have honey content of 1mL, 1.5 mL, and 2mL, respectively at a wavelength of 200 nm, as the ODFs were dissolved in the artificial saliva. The maximum detectable wavelength is in the region of 280 – 285 nm (Geană et al., 2024; Mitra et al., 2023). The UV-vis spectra of

dissolution media that contain the dissolved desired ingredient (honey) can be measured at intervals over time to determine the kinetics of the honey release from the ODF. This also reveals the dissolution profile. The concentrations of honey released were determined using a linear equation obtained from a calibration curve established using UV-vis spectroscopy (refer to Appendix 1).

The four processes of dissolution can be seen in Figure 4.13. During the initial lag period (0 - 20 sec), water infiltrated the electrospun PVA/κ-carrageenan/*kelulut* honey matrix, starting the film hydration and swelling before any significant amount of *kelulut* honey was released. This period was not included in the experiment as the first sample interval was 20 seconds. Following hydration (II), a rapid release of *kelulut* honey was observed as honey molecules adjacent to the polymer fibres quickly diffused into the dissolving media. This was followed by a sustained release (II), where *kelulut* honey release was controlled by the diffusion through the swollen polymer matrix and progressive matrix degradation. This was followed by a plateau phase (IV) once most of the released *keulut* honey had diffused and the concentration was nearing equilibrium. The *kelulut* honey volumes of 1mL, 1.5 mL, and 2mL all showed a noticeable increase in release, meaning that the release of the samples began immediately and continued growing. The difference among the formulations reveals that increasing the volume of honey greatly impacts the release rate of the dissolving film. An increase in honey loading from 1−2 mL caused an increase in cumulative honey release. This is likely because more honey is available to diffuse into the artificial saliva that is dissolving the film. Furthermore, honey is a natural plasticiser. Because of water absorption, the film is more easily broken down. Regardless of the difference in volume, the overall shape of the curves is more or less the same, which indicates that a similar mechanism of release was the same. In general, the trend shows that there is a direct correlation between the volume of honey and the release of honey. All samples exhibited a rapid, early increase in release followed by a gradual release to a stable state. A study has shown that the amount of honey significantly influenced the honey release (Taher et al., 2020). The release profile of honey in the ODF system shows a controlled release profile with the concentration (mg/mL) of honey increasing steadily within seconds. Similarly, previous studies (Taher et al., 2020) on formulations containing honey and their application to wound healing showed that honey concentration increases throughout several hours (Taher et al., 2020). Though time scales vary

(seconds and hours) based on the application, all show progressive release behaviour, indicating that honey release increased over time.

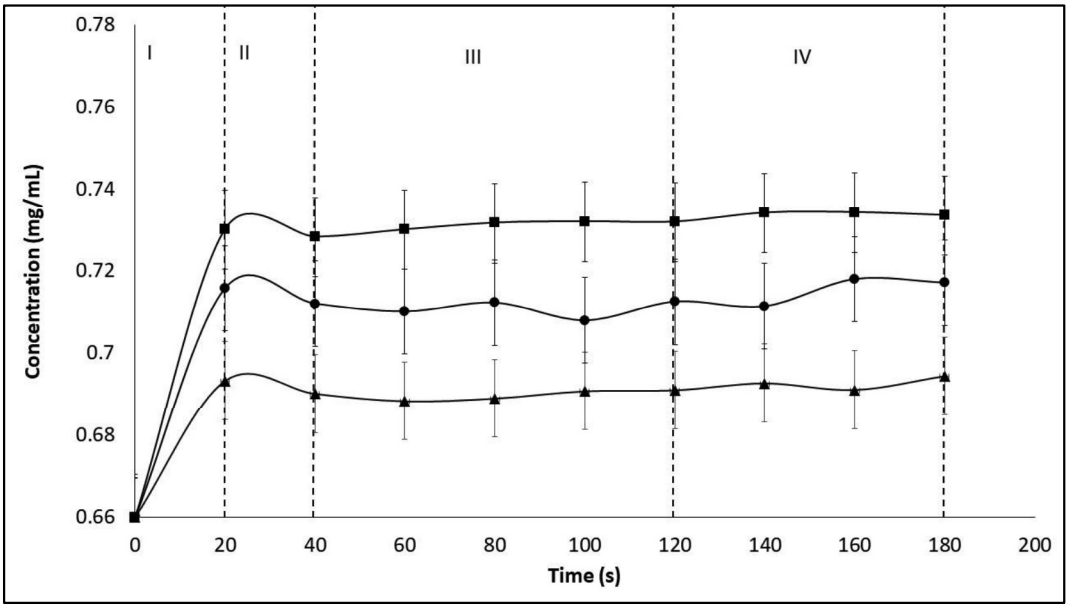


Figure 4.13: Profile Release of Honey for Batch Dissolution Using Uv-vis, I) Lag Phase II) Burst Release III) Sustained Matrix Erosion and Diffusion IV) Plateau

ii) Batch dissolution of electrospun PVA/κ-Car/AA ODF

Ascorbic acid content in the ODF was quantified using UV-Vis spectroscopy at various concentrations. This analysis assessed the absorbance of the samples that have ascorbic acid content of 0.2, 0.6, 1.0, 1.4, 1.8, and 2.2, which corresponds to 1 w/v%, 3 w/v%, 5 w/v%, 7 w/v%, 9 w/v% and 11 w/v%, respectively and the wavelength of 200 nm, as the ODFs were dissolved in the artificial saliva. The maximum detectable wavelength is in the region of 260 – 265 nm. The UV-vis spectra of dissolution media that contain the dissolved active pharmaceutical ingredient (AA) can be measured at intervals over time to determine the kinetics of the AA release from the ODF. This also reveals the dissolution profile. The concentrations of AA released were determined using a linear equation obtained from a calibration curve established using UV-vis spectroscopy (refer to Appendix 2).

The standard calibration curve, the graph shown in Figure 4.14, shows the time-dependent release profile of the AA solution at varying concentrations. The in vitro dissolution process of the ascorbic acid (AA)-loaded electrospun oral dissolving film

(ODF) prepared in this study aligns with previously reported similar honey-loaded formulations of the same type and is divided into four consecutive phases (I, II, III, IV). During the initial lag period of 0–20 seconds, the film matrix was infiltrated by artificial saliva. Since ultraviolet-visible (UV-Vis) spectrophotometric detection only started at the 20-second (the earliest sampling interval selected), this full phase was not recorded. Even so, it can still be inferred that rapid hydration of the matrix and immediate release of AA had already occurred before sampling began. With that, as the concentrations increased, the steepness of the profile increased, showing that the initial release rate was faster, and after the initial steep slope, a plateau was seen in the release. The higher concentrations released AA quickly, as seen by the higher baseline of the plateau in the AA. The release profile for ascorbic acid in the ODF formulation showed a significant initial jump in concentration (mg/mL) within a few seconds, which is a positive indicator for the fast release needed for oral dissolving films. On the other hand, previous studies on release drug delivery systems showed that ascorbic acid concentration increases gradually over a period of hours (Bańkosz, 2024). There is a release time relationship, and they all exhibit a cumulative release behaviour, which shows that ascorbic acid content increases over time. This study experimentally observed that an increase in ascorbic acid concentration widens the concentration gradient between the polymer matrix and the dissolution medium. In line with Fick's diffusion theory, this change enhances the mass transfer driving force, accelerates AA diffusion, and improves the cumulative release of active substances.

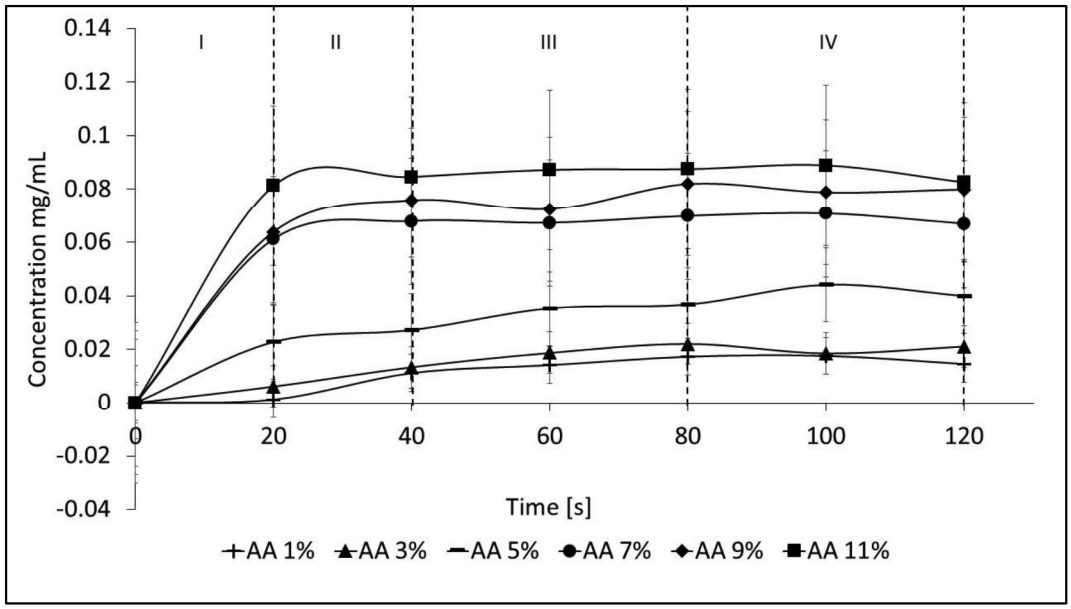


Figure 4.14: Profile Release of AA for Batch Dissolution Using Uv-vis I) Lag Phase II) Burst Release III) Sustained Matrix Erosion and Diffusion IV) Plateau

In conclusion, the initial rapid increase in the release profile can be attributed to the hydrophilic characteristics of both polymers used, which readily absorb artificial saliva upon contact. Water uptake initiates hydration and swelling of the polymer matrix, while the electrospun nanofibrous film provides a large surface area and short diffusion pathways, facilitating the rapid diffusion of *kelulu* honey and AA into the surrounding medium (artificial saliva). As dissolution progresses, the concentration gradient between the polymer matrix and the dissolution medium (artificial saliva) gradually decreases while the swollen polymer undergoes progressive erosion. Consequently, the release rate decreases and enters a sustained diffusion phase before eventually reaching equilibrium.

4.8 Instantaneous Dissolution of Electrospun PVA/κ-Car/AA ODFs Using FT-IR Spectroscopy

FT-IR spectroscopy was employed to quantify the ascorbic acid content in the ODFs at various concentrations using an instantaneous dissolution approach. By analysing the absorbance of the samples that have ascorbic acid content of 0.2, 0.6, 1.0, 1.4, 1.8, and 2.2, which correspond to 1 w/v%, 3 w/v%, 5 w/v%, 7 w/v%, 9 w/v% and 11 w/v%, respectively and the wavenumber of the 1634-1637 cm^{-1}, as the ODFs are dissolved in the artificial saliva. The maximum detectable wavelength is in the region

of 4000 – 400 cm^{-1}. The FT-IR spectra of dissolution media that contain the dissolved ODFs solution can be measured at intervals over time to determine the kinetics of the AA release from the ODF. This also reveals the dissolution profile. The concentrations of AA released were determined using a linear equation obtained from a calibration curve established using FT-IR spectroscopy (refer to Appendix 3). The electrospun PVA/κ-carrageenan/AA composite matrix prepared in this study demonstrates a clear two-stage release process for its loaded ascorbic acid in artificial saliva.

Figure 4.15 displays the in vitro release profiles of AA from the electrospun films, represented as a percentage of cumulative release over time. In the first 10 seconds, the matrix's hydrophilic property and high specific surface area nanofiber structure allow rapid water penetration that causes the film to swell, and surface molecules diffuse quickly to produce an initial burst release. As hydration continues to advance in the subsequent stage, the release of AA is dominated by diffusion through the swollen matrix and slow matrix degradation until release equilibrium is achieved. Increasing the AA content in the film resulted in an increased dissolution rate and extent of release, roughly in direct proportion. ODFs with higher initial AA loading showed a faster and more complete release of AA. A significant contributing aspect to this behaviour is fibre diameter. A greater surface-area-to-volume ratio is offered by smaller fibre diameters, which often promotes rapid fibre dissolution and more effective embedded AA release. The ODF with 11% w/v AA, which had the finest fibres with an average diameter of roughly 495 nm, released its AA content the fastest of all the tested formulations; almost the whole AA dose was dissolved in about 120 seconds. In contrast, the 5% w/v AA film, which has the biggest fibre diameter (about 643 nm), demonstrated a slower rate of release, which is in line with its thicker fibres and smaller surface area. In comparison to the 5% sample, the 7% AA film (fibre diameter ~609 nm) showed better release performance, while the 9% AA film (fibre diameter slightly larger than that of the 11% sample) had a slightly reduced release rate. These findings demonstrate that the nanoscale morphology of the fibres, which is impacted by formulation and electrospinning parameters, plays a crucial role in regulating the AA dissolution kinetics from the ODFs, in addition to the overall AA content. Sapiee et al. (2023) demonstrated that the composition of the oral dispersible films containing ascorbic acid and κ-carrageenan/polyvinyl alcohol is highly hydrophilic, which is why the films disintegrated and released the drug quickly. These results also support the

additional findings of this study that the greater the ascorbic acid concentration, the greater the cumulative release of the drug. Palezi et al. (2025) reported that ODFs containing biopolymer matrices in which AA was added exhibited a release of the drug that significantly increased with a higher concentration of AA. The results indicate that all the PVA/κ-car/AA films were instantaneously dissolved, which is a significant attribute for the oral delivery of the films. An increase in AA concentrations (1 w/v% to 11 w/v%) brought about a gradual increase in the release of concentration and an increase in the time it took to reach a plateau.

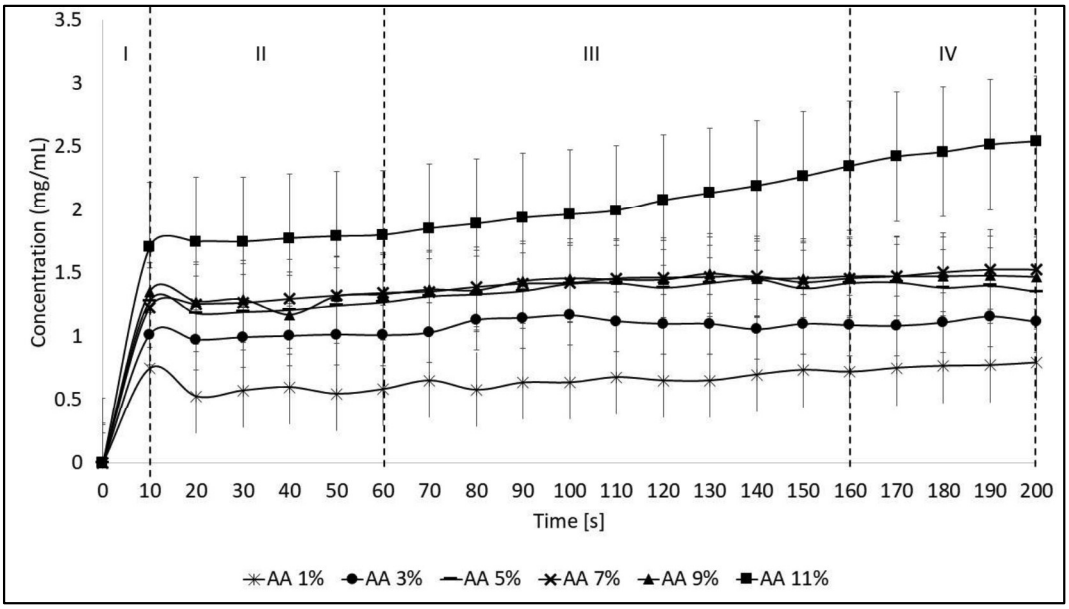


Figure 4.15: Profile Release of AA for Instantaneous Dissolution Using FT-IR spectroscopy I) Lab Phase II) Burst Release III) Sustained Matrix Erosion and Diffusion IV) Plateau

The FT-IR analysis graphs (Figure 4.15) are consistent except for the 9 w/v% AA, which differed from the other curves. Since the graph deviated from the FT-IR profile release, it exhibited some discrepancies. The release profile for the 9 w/v% AA concentration stabilises like the 7 w/v% AA concentration. The stagnation of the release medium (artificial saliva) filled with higher amounts of AA may inhibit further dissolution and release. During solution preparations, AA may have been excessively heated in the water bath, which may have compromised the sample's solution and resulted in the discrepancies in the graph. This film's structural properties may have affected the desired ingredient release kinetics, and if the solution was compromised due to excessive heat, it could have altered the release profile (Kristó et al., 2022).

In summary, this study adopted two dissolution testing methods that exhibit unique and complementary release behaviours to verify the release performance of the PVA/κ-car/AA oral fast-dissolving film (ODF). The first method is batch dissolution testing. Relying on UV-Vis spectroscopy, this test uses 30 mL of artificial saliva and collects ODF samples at 20 second-level intervals, generating a slow, diffusion-controlled release result that can reveal the intrinsic release kinetics dominated by the polymer matrix. The second method is instantaneous dissolution testing. Relying on FT-IR spectroscopy, this test uses 22 μL of artificial saliva and collects ODF samples at 10 second-level intervals to simulate the physiological environment of the oral cavity, generating a fast-release result in which ascorbic acid is nearly completely released within several minutes. This test can verify the dissolution performance of the ODF in actual oral administration scenarios, and the study ultimately confirms that this ODF meets the rapid-release requirements for an effective oral fast-dissolving film.

4.9 ANN Modelling and Prediction of Dissolution

4.9.1 Batch Dissolution Prediction of Honey from Electrospun PVA/κ-Car/Honey ODFs Using ANN

Artificial neural networks (ANNs) are predictive models derived from the biological architecture of the human brain. Artificial neural networks are used to simulate and analyse the dissolution behaviour of pharmaceutical preparations. Therefore, this modelling method can efficiently support the precise optimisation of pharmaceutical formulations and holds prominent practical value. The artificial neural network (ANN) introduced in this study mimics the pattern of human learning from repeated observations and fits the correlation between experimental variables and measured dissolution concentrations. During its training process, the model repeatedly receives dissolution data and adjusts its internal connection weights to reduce prediction errors. Once training is completed, it can estimate the dissolution concentration of active ingredients under similar conditions without requiring any additional experiments. They comprise three fundamental levels: an input layer, one or more hidden layers, and an output layer (Ebube et al., 1997). Throughout the model training, the algorithm executes multiple epochs to minimise the error, indicating the proximity of the predicted values from the ANN model to those of the ideal model or best-fit line. Table 4.5 shows the

parameters used to construct the ANN model. Table 4.6 reveals a low mean square error (MSE) and an R^2 value approaching 1.

Table 4.5:
List of Parameters

Training Algorithm	Levenberg-Marquardt
Hidden neurons	10
Input	Time (s) Wavelength (nm) Absorbance
Output	Concentration of honey (w/v%)

This study built an Artificial Neural Network (ANN) model for the honey dissolution scenario. All 30 sets of experimental values used for model training were taken from batch dissolution studies. The model's input variables are dissolution time, wavelength, and absorbance, all with their respective units; the output is *kelulut* honey volume in mg/mL. The model's core task is to fit the correlation between these variables and the concentration. The ANN model was developed using the Levenberg-Marquardt algorithm (trainlm) with a total of 30 datasets, which were split into training (80%), validation (10%) and testing (10%), to provide sufficient generalisation of the model. Multiple training sessions were conducted to achieve minimal prediction error and optimal fit. The model performance was evaluated using Mean Squared Error (MSE) and the coefficient of determination (R^2). As can be seen in Table 4.6, the trained ANN exhibited high predictive accuracy, as evidenced by low mean squared error values and an R^2 value approaching 1 (Nurrul Amilin Zainal Abidin et al., 2022).

Figure 4.16 demonstrates a nearly perfect linear correlation between predicted and experimental dissolution data over the training, validation and testing datasets. This strong correlation confirms the ANN's ability to comprehend complex nonlinear relationships and provide accurate predictions. The strong correlation between predicted and experimental values indicates that the ANN effectively identified the primary functional relationships among input variables. Nonetheless, independent validation was required to establish the model's adaptability and to exclude the

possibility of overfitting. Table 4.6 shows the MSE and R^2 values for the training, validation and testing datasets, which all exhibit little error and strong predictive correlation between ANN and experimental results. It shows that the slope has a close agreement and the output is the same as the target. The artificial neural network (ANN) model constructed in this study delivers excellent predictive performance. However, the experimental dataset used for this model has a limited scale, which only covers 30 groups of honey batch dissolution data. This model is only a predictive tool that applies within the scope of the predefined experiments, rather than a general-purpose model. In future research, larger and more diverse datasets need to be incorporated to improve the model's robustness, generalizability, and predictive capacity.

Table 4.6:
Result of Neural Network Using *Trainlm*

	MSE	**R^2**
Training	3.07733×10^{-9}	0.99999
Validation	7.65614×10^{-10}	0.999849
Testing	4.71705×10^{-9}	0.99998

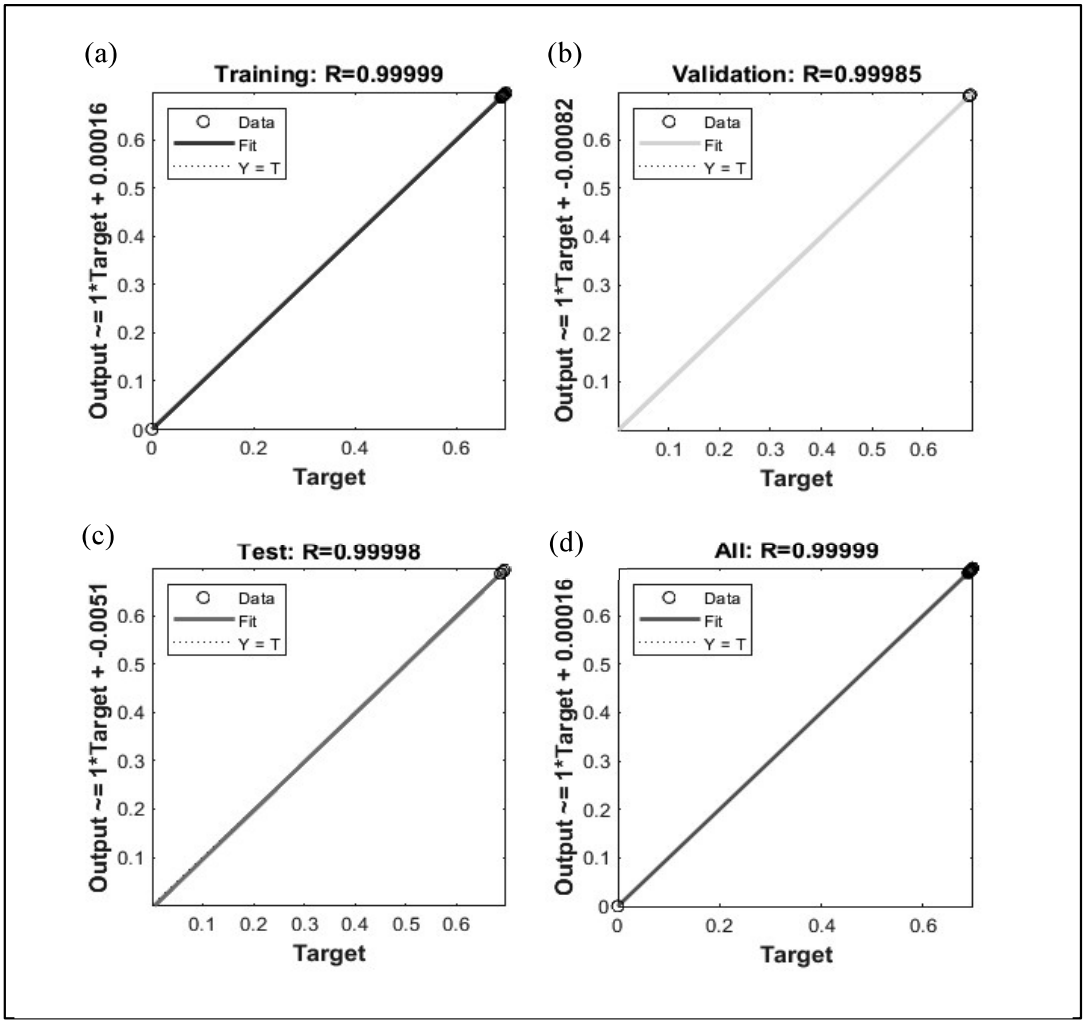


Figure 4.16: Regression Plot of ANN; (a) ANN Training Model; (b) ANN Validation Model; (c) ANN Testing Model; (d) ANN All Data Model

Figure 4.17 illustrates the error histogram, depicting the distribution of prediction errors across training, validation and testing datasets. Most errors, particularly for the training set, were clustered near the zero line, indicating minimal error and consistent predicted performance across all datasets. A narrow error distribution indicates effective model generalisation, validating findings from previous studies (Afendi et al., 2024; Taredi et al., 2024), hence affirming the potential of the ANN for dissolution prediction. In general, the error decreases as the number of epochs increases. Figure 4.18 demonstrates that the validation performance curve exhibits a consistent decline in MSE throughout training, achieving an optimal value of 7.6561×10^{-10} at epoch 10. Mohammadi et al. (2020) showed that the error reduces progressively throughout training, and the algorithm ends when the authentication error increases for

six consecutive iterations or when the maximum error level per epoch is achieved. The validation and testing errors suggest that the model performs effectively and shows no signs of overfitting. The MSE values explain that when the MSE values are near zero, the network is well-trained (Hidzer et al., 2025).

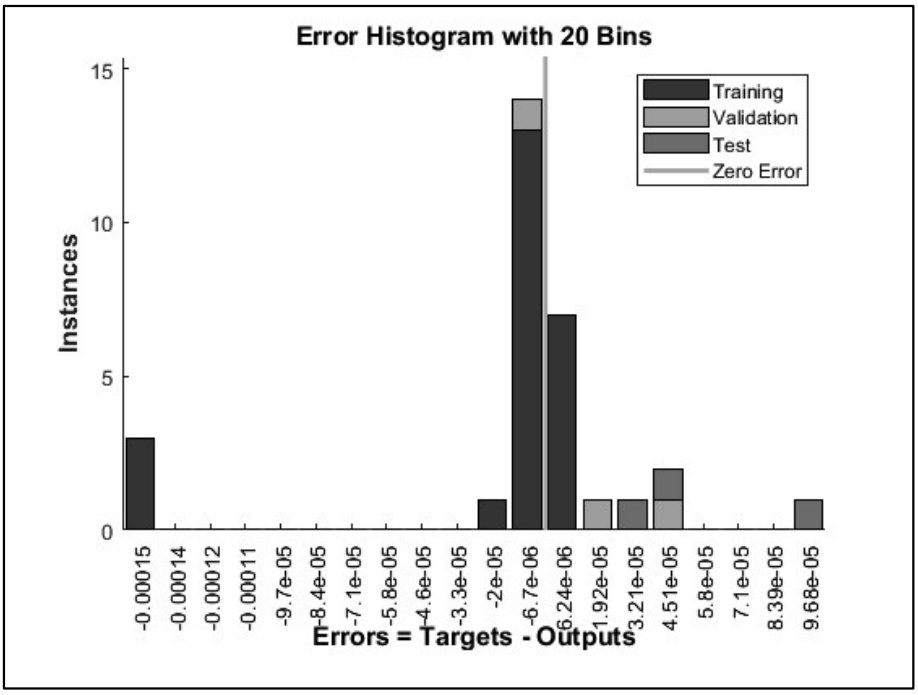


Figure 4.17: Error Histogram Plot

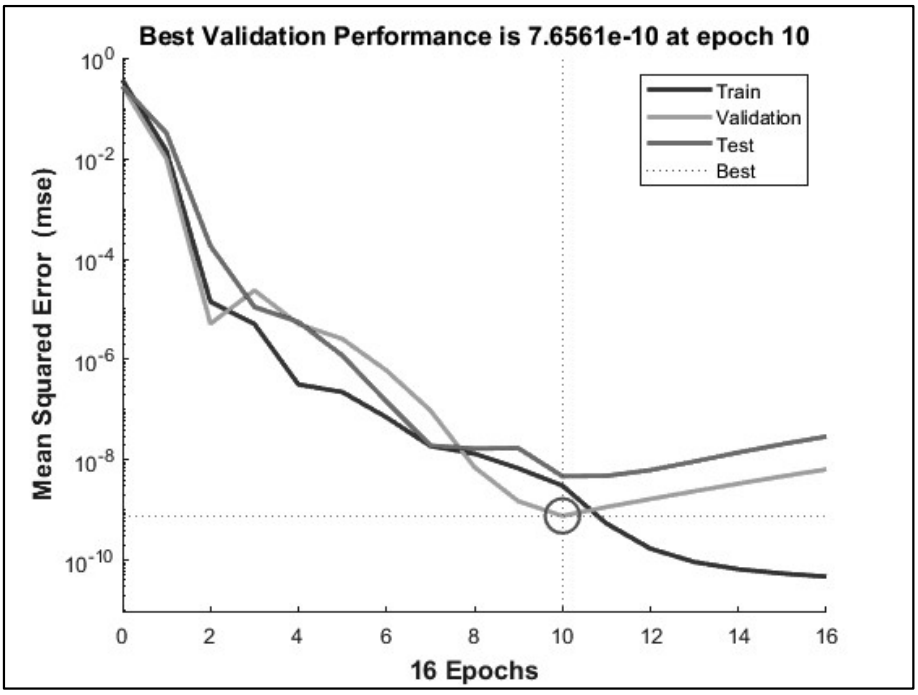


Figure 4.18: Performance Plot: Mean Squared Error vs Epoch.

Figure 4.19 illustrates the dissolution data and the trends compared to the ANN predicted values on the release of honey from PVA/κ-car/honey oral dispersible film at different honey volumes and times taken from 20 to 180 seconds. Almost all formulations show a continuous advancement of honey release over time in both data sets, reinforcing the rapid dissolving attributes of hydrophilic ODF systems. The ANN bars are approximately similar to the experimental bars, showing a strong predictive ability in a uniform release pattern. For both of the data sets, the same pattern of release was observed for both the ANN and the experimental data. In summary, the ANN prediction closely agrees with experimental release trends, demonstrating only modest inaccuracies during the early or peak release stages. These differences likely arise from experimental error. The strong correlation confirms the capabilities of ANNs to predict the honey release behaviour. Previous studies have demonstrated that ANN-based modelling is an effective tool for predicting the dissolution behaviour in pharmaceuticals industry or process analytical technology (Galata et al., 2019, 2021; Nagy et al., 2019; Péterfi et al., 2023). The artificial neural network (ANN) model validated in this study successfully predicted experimentally observed dissolution stages of honey-loaded oral dissolving films (ODFs. The model effectively predicted that increasing honey loading would increase the films cumulative release amount. Within the range of formulations examined in this study, the model captured the *kelulut* honey release. It can serve as a predictive tool to reduce the number of formulation experiments conducted during the product development stage.

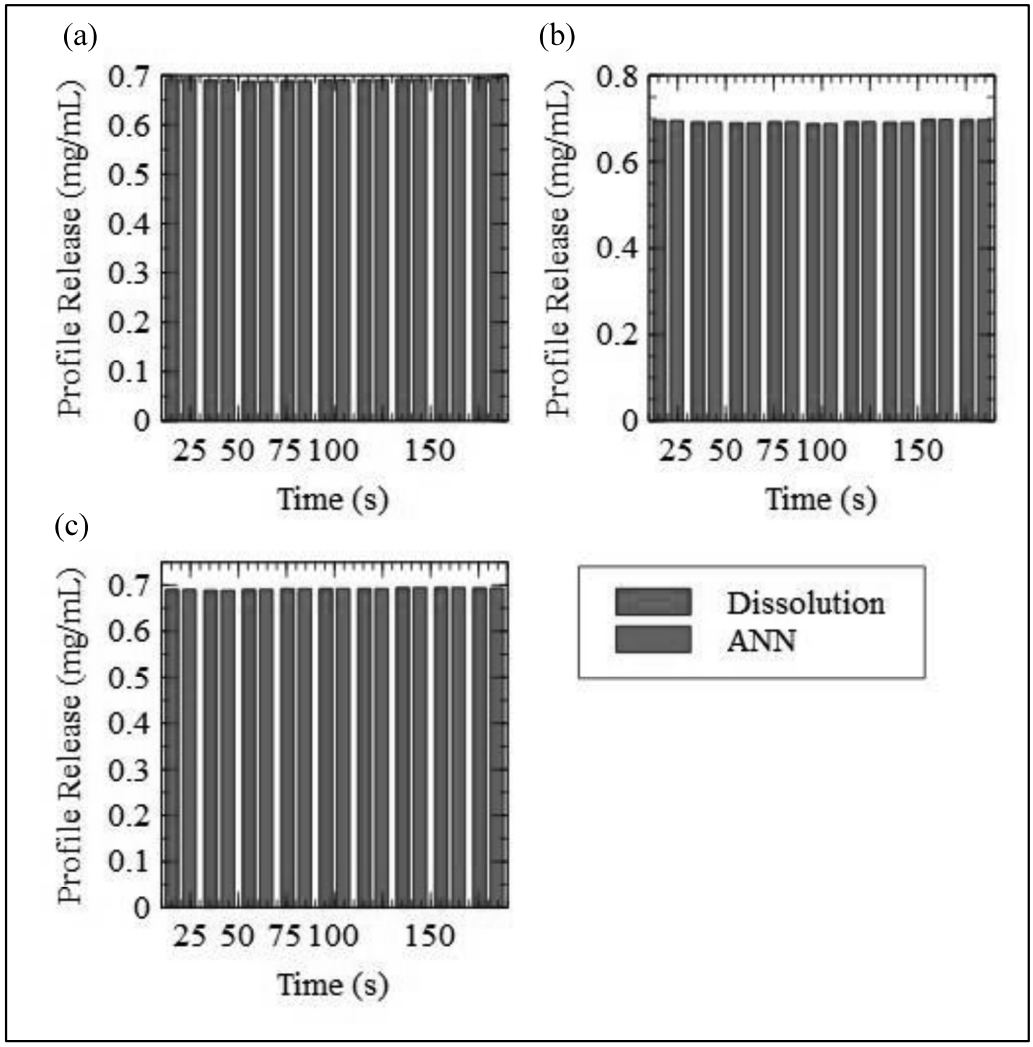


Figure 4.19: Comparison of the Volume of Honey, (a) ODFs with 1 mL; (b) ODFs with 1.5 mL; (c) ODFs with 2 mL

4.9.2 Batch Dissolution Prediction of Ascorbic Acid (AA) from Electrospun PVA/κ-Car/AA ODFs Using ANN

Artificial neural networks (ANN) are predictive models derived from the biological architecture of the human brain. They comprise three fundamental levels: an input layer, one or more hidden layers, and an output layer (Ebube et al., 1997). Throughout the model training, the algorithm executes multiple epochs to minimise the error, indicating the proximity of the predicted values from the ANN model to those of the ideal model or best-fit line. Table 4.7 shows the parameters used to construct the ANN model. Table 4.8 reveals a low mean square error (MSE) and an R^2 value approaching 1.

Table 4.7:
List of Parameters

Training Algorithm	Levenberg-Marquardt
Hidden neurons	10
Input	Time (s) Wavelength (nm) Absorbance
Output	Concentration of AA (w/v%)

This study built an Artificial Neural Network (ANN) model for the honey dissolution scenario. All 42 sets of experimental values used for model training were taken from batch dissolution studies. The model's input variables are dissolution time, wavelength, and absorbance, all with their respective units; the output is AA concentration in w/v%. The model's core task is to fit the correlation between these variables and the concentration. The ANN model was developed using the Levenberg-Marquardt algorithm (trainlm) with a total of 42 datasets, which were split into training (90%), validation (5%) and testing (5%), to provide sufficient generalisation of the model. Multiple training sessions were conducted to achieve minimal prediction error and optimal fit. The model performance was evaluated using Mean Squared Error (MSE) and the coefficient of determination (R^2). As can be seen in Table 4.8, the trained ANN exhibited high predictive accuracy, as evidenced by low mean squared error values and an R^2 value approaching 1.

Figure 4.20 demonstrates a nearly perfect linear correlation between predicted and experimental dissolution data over the training, validation and testing datasets. This strong correlation confirms the ANN's ability to comprehend complex nonlinear relationships and provide accurate predictions. The strong correlation between predicted and experimental values indicates that the ANN effectively identified the primary functional relationships among input variables. Nonetheless, independent validation was required to establish the model's adaptability and to exclude the possibility of overfitting. Table 4.8 shows the MSE and R^2 values for the training, validation and testing datasets, which all exhibit little error and strong predictive correlation between ANN and experimental results. The artificial neural network (ANN) model constructed in this study delivers excellent predictive performance. However, the experimental dataset used

for this model has a limited scale, which only covers 42 groups of AA batch dissolution data. This model is only a predictive tool that applies within the scope of the predefined experiments, rather than a general-purpose model. In future research, larger and more diverse datasets need to be incorporated to improve the model's robustness, generalizability, and predictive capacity.

Table 4.8:
Result of Neural Network Using *Trainlm*

	MSE	**R^2**
Training	1.53758×10^{-9}	0.99999
Validation	1.81902×10^{-9}	0.99999
Testing	3.38679×10^{-8}	1.00000

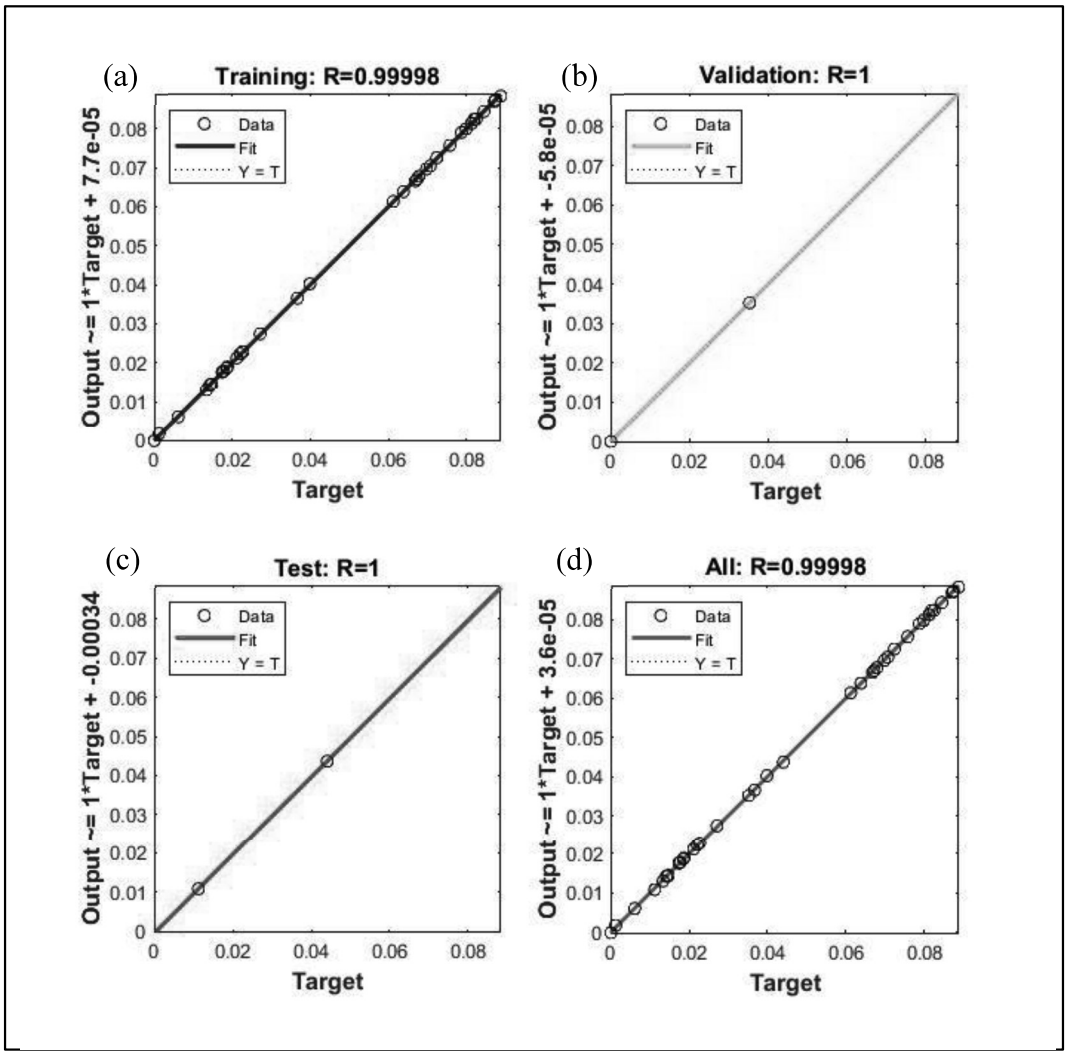


Figure 4.20: Regression Plot of ANN; (a) ANN Training Model; (b) ANN Validation Model; (c) ANN Testing Model; (d) ANN All Data Model

Figure 4.21 illustrates the error histogram, depicting the distribution of prediction errors across training, validation and testing datasets. Errors mostly cluster around zero, indicating minimal error and consistent predicted performance across all datasets. A narrow error distribution indicates effective model generalisation, validating findings from previous studies (Afendi et al., 2024; Taredi et al., 2024), hence affirming the potential of the ANN for dissolution prediction. Figure 4.22 demonstrates that the validation performance curve exhibits a consistent decline in MSE throughout training, achieving an optimal value of 1.819 × 10-9 at epoch 37. A similar trend was seen in Hidzer et al. (2025): as the error decreased, the epoch increased. The validation and testing errors suggest that the model performs effectively and shows no signs of overfitting.

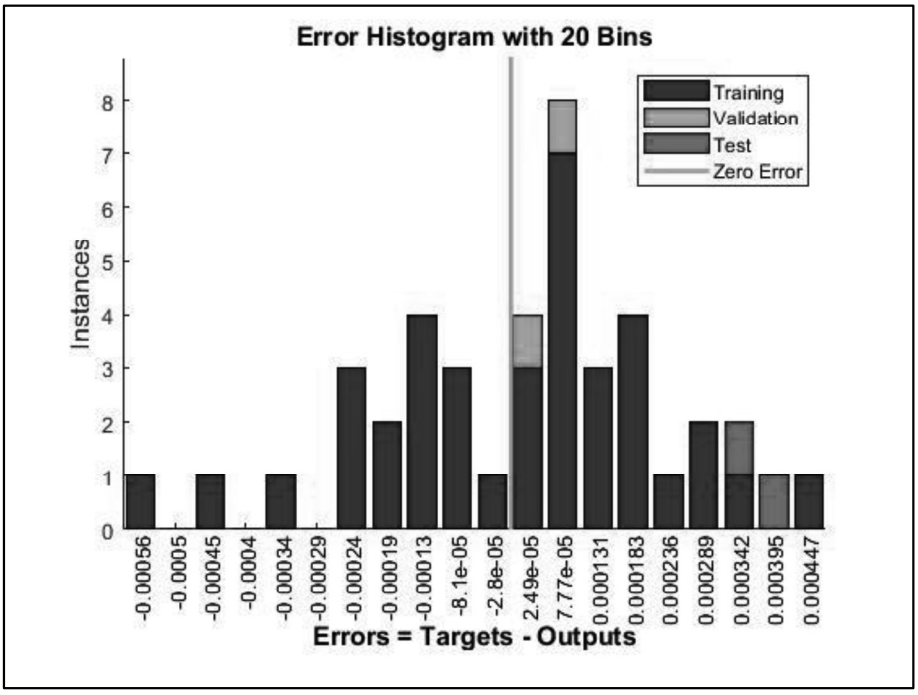


Figure 4.21: Error Histogram Plot

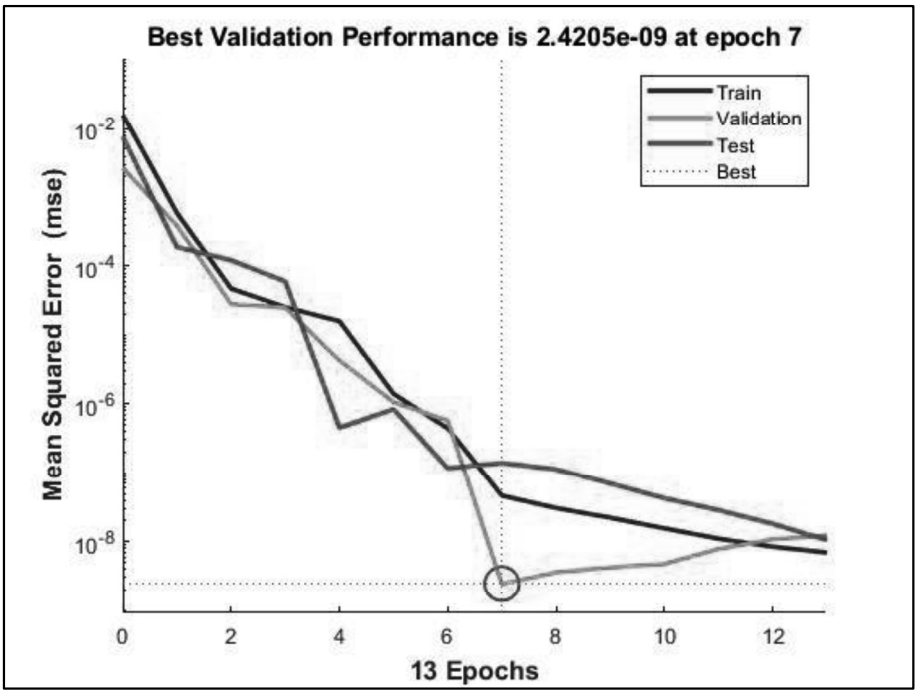


Figure 4.22: Performance Plot: Mean Squared Error vs Epoch.

Figure 4.23 illustrate the dissolution data and the trends compared to the ANN predicted values on the release of AA from PVA/κ-car/AA oral dispersible film at different AA concentrations (1-11 w/v%) and time taken from 20 to 120 seconds. Almost all formulations show a continuous advancement of AA release over time in both data sets, reinforcing the rapid dissolving attributes of hydrophilic ODF systems. The ANN bars are approximately similar to the experimental bars, reinforcing a strong predictive and observed value and moderate concentrations of AA (1-5 w/v%), attributed to the steady and uniform release pattern. This close dependence supports that the ANN predicted the major dissolution and time-dependent release pattern of AA. The histograms at AA concentrations of 7 – 11 w/v% show an increased release, which indicates the AA was more accessible within the film. For both of the data sets, the same pattern of increase was evident for both the ANN and the experimental data. In summary, the ANN predictions closely align with experimental release trends, exhibiting only minor errors during the initial or peak release phases. These differences likely arise from experimental error. The strong correlation confirms the capabilities of ANNs to mimic the dissolving kinetics and effectively predict desired ingredient release behaviour. Previous studies have demonstrated that ANN-based modelling is an effective tool for predicting the dissolution behaviour in pharmaceuticals industry

(Galata et al., 2019, 2021; Nagy et al., 2019; Péterfi et al., 2023). These results demonstrate the potential of ANN-based modelling as an efficient predictive instrument for dissolution analysis. The artificial neural network (ANN) model developed in this study successfully predicted the experimentally observed dissolution of ascorbic acid (AA)-loaded orodispersible films (ODFs. This model effectively predicted the dissolution behaviour of the films, verified that increased AA concentrations raise cumulative release amounts, and confirmed the key influence of formulation composition. This approach may significantly minimise the need for several experimental trials, hence reducing research time and costs while maintaining precision and reliability in pharmaceutical development.

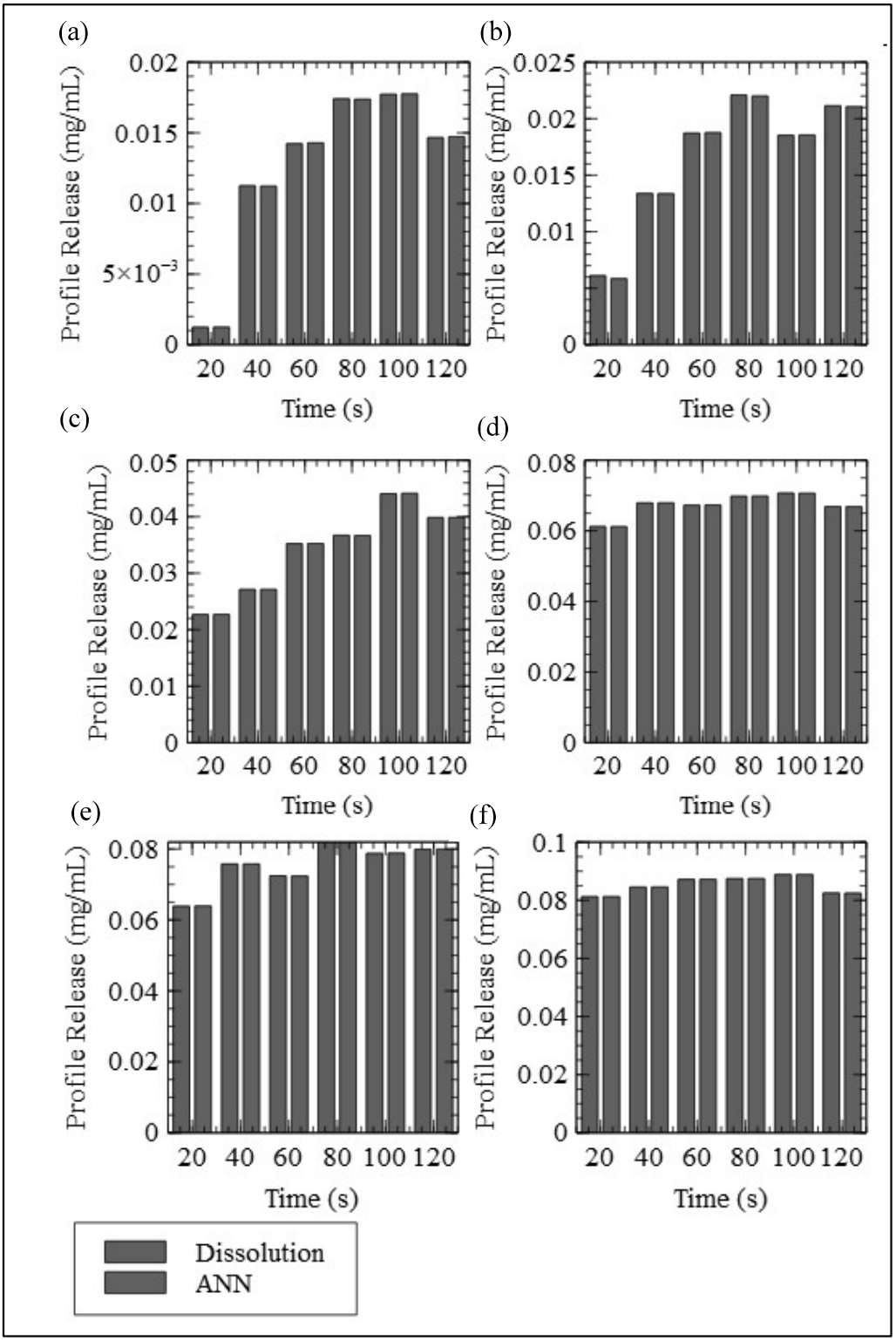


Figure 4.23: Comparison of Concentration of AA, (a) ODFs with 1w/v% of AA; (b) ODFs with 3w/v% of AA; (c) ODFs with 5w/v% of AA; (d) ODFs with 7w/v% of AA; (e) ODFs with 9w/v% of AA; (f) ODFs with 11w/v% of AA

4.9.3 Instantaneous Dissolution Prediction of Ascorbic Acid (AA) from Electrospun PVA/κ-Car/AA ODFs Using ANN

Artificial neural networks (ANN) are predictive models inspired by the biological structure of the human nervous system. They consist of three basic layers: an input layer, one or more hidden layers and an output layer (Ebube et al., 1997). During the model training, the algorithm runs for several epochs to reduce the error, which signifies how closely the predicted values from the ANN model are to the values of the optimal model or the best-fit line. Table 4.9 shows the parameters used to construct the ANN model. From Table 4.10, an MSE (mean squared error) of a low value and an R^2 value nearing 1 can be observed.

Table 4.9:
List of Parameters

Training Algorithm	Levenberg-Marquardt
Hidden neurons	10
Input	Time Wavenumber Absorbance
Output	Concentration of AA

All 48 sets of experimental values used for model training were taken from instantaneous dissolution studies. The model's input variables are dissolution time, wavenumber, and absorbance, all with their respective units; the output is AA concentration in mg/mL. The model's core task is to fit the correlation between these variables and the concentration. The dataset was split into segments where 90% was used for training the neural network, another 5% for validation and the last for testing, using the Levenberg-Marquardt algorithm. Typically, 60% is used for training, 20% for testing and 20% for validation. Usually, 90% is training, 5% is validation, and 5% is testing when handling small datasets, as training data is very important. When using small datasets, a prevalent approach is to use a greater training percentage to ensure the model learns correctly. Adequate testing and validation must follow to analyse it. The input and output variables are provided. The regression analysis, error histogram and

the performance plot are shown in Figure 4.24, Figure 4.25 and Figure 4.26, respectively. Regression analysis is shown in Figure 4.24 for the training, validation, testing and all datasets. The majority of available datasets were utilised, and the evaluation was made using a small remaining dataset. The indicators exhibit a very close relationship, indicating a very high accuracy between the expected and target values. An adjusted R^2 of 0.9999 is an excellent R^2 (Table 4.10). The regression R^2 values compare the net outputs to the net targets. A coefficient of 1 indicates a strong correlation, while 0 indicates no correlation at all. Because the test dataset produced the highest R^2 value and lowest MSE with 10 hidden neurons, the standard Levenberg-Marquardt method was used for training. The artificial neural network (ANN) model constructed in this study delivers excellent predictive performance. However, the experimental dataset used for this model has a limited scale, which only covers 48 groups of AA instantaneous dissolution data. This model is only a predictive tool that applies within the scope of the predefined experiments, rather than a general-purpose model. In future research, larger and more diverse datasets need to be incorporated to improve the model's robustness, generalizability, and predictive capacity.

Table 4.10:
Results of the Train Network

	MSE	**R^2**
Training	2.10170×10^{-5}	0.99999
Validation	3.40659×10^{-5}	0.99999
Testing	2.16882×10^{-6}	0.99999

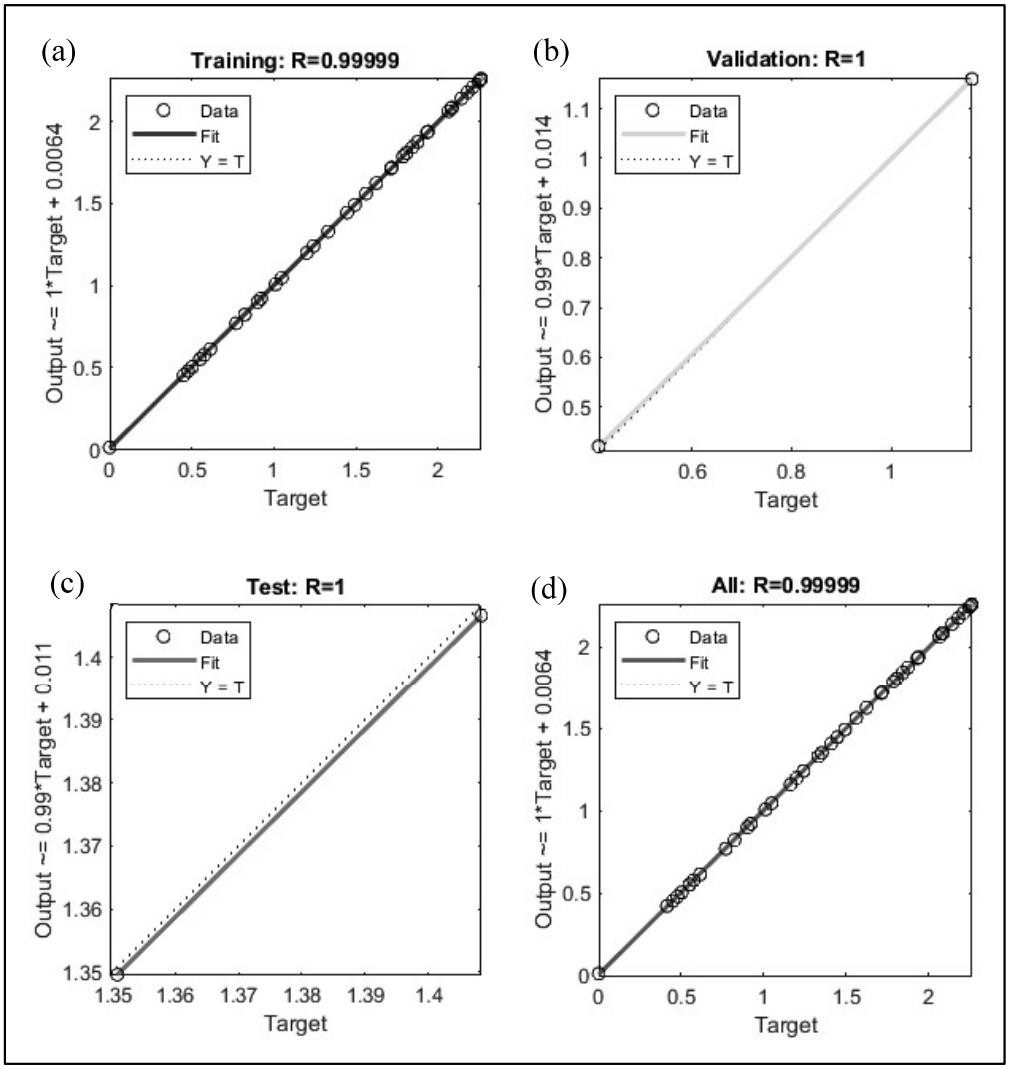


Figure 4.24: Regression Plot of ANN; (a) ANN Training Model; (b) ANN Validation Model; (c) ANN Testing Model; (d) ANN All Data Model

The error histogram (Figure 4.25) shows the distribution of 48 samples, with the y-axis showing the number of samples and the x-axis split into 20 sections. The error distribution depicts little deviation with a robust model and is unlikely to diverge significantly from the actual numbers. In general, the error contains very few deviant points, demonstrating that the model accurately represents most of the data. Figure 4.26 shows the decrease in the training, validation and test sets epochs of the ANN with the corresponding mean squared error (MSE) for each set. The mean squared error (MSE) is shown on a logarithmic scale on the y-axis, and the number of epochs is shown on the x-axis. The error for all three sets rises and then rapidly goes down during the first stage. This shows the model was trained really well and can generalise to new data. Figure 4.26 shows that the best validation scores were obtained at epoch 7, with a mean

squared error of 3.4066×10^{-5}, which tells us the ANN model is not overfit. The MSE values explain that when the MSE values are near zero, the network is well-trained (Hidzer et al., 2025). This supports the best practices in the training of ANN, suggesting that model preservation in terms of accuracy and generalisation is best served through the use of MSE with early stopping.

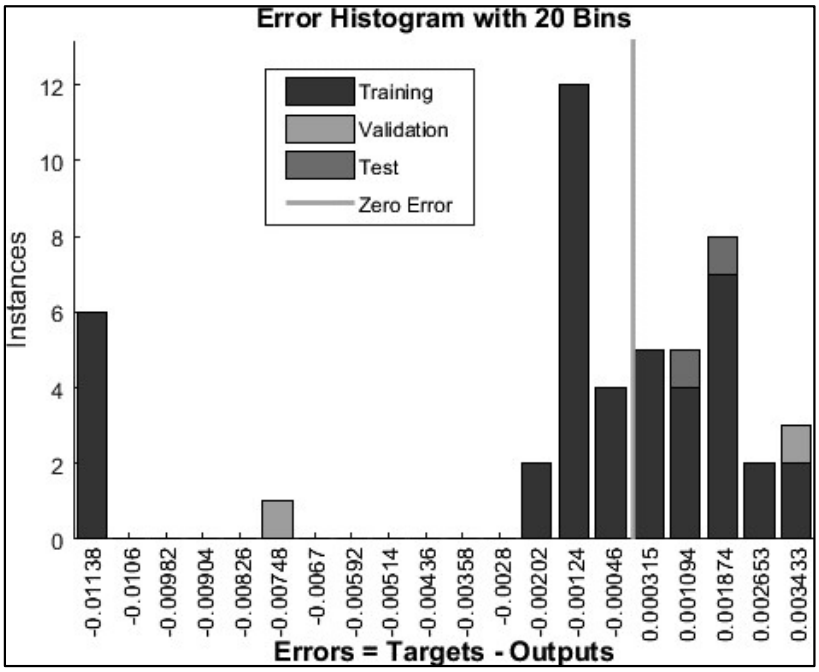


Figure 4.25: Error Histogram Plot

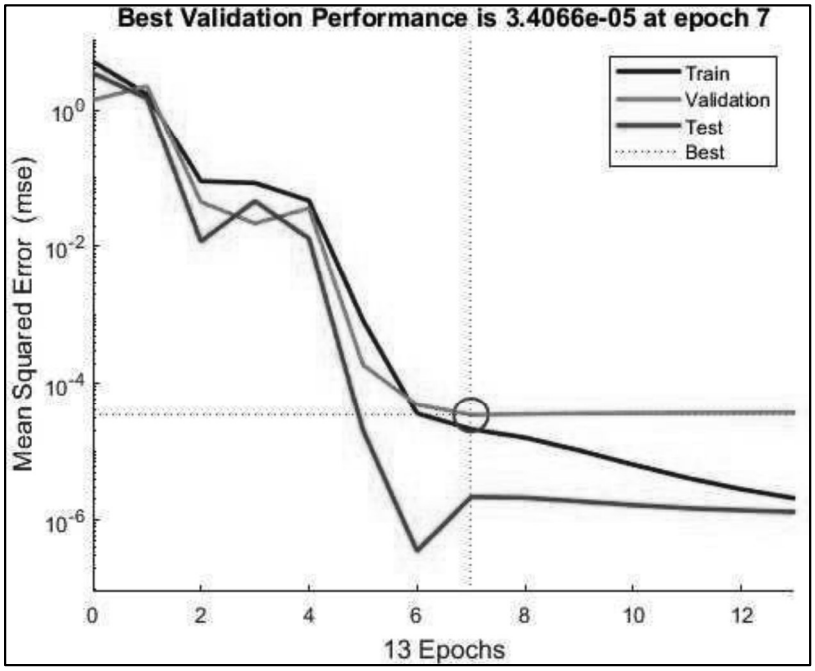


Figure 4.26: Performance Plot: Mean Squared Error vs Epoch.

The results presented in Figure 4.27 shows that the predicted versus experimental results for in vitro dissolutions of ODFs containing different amounts of ascorbic acid (AA) (1%, 3%, 5%, 7%, 9% and 11% w/v) have small errors, making it likely that the predictions made by the artificial neural network (ANN) model for the kinetics of AA release match the experimental results. ANN models have been shown to match the kinetics of AA release in extended-release tablets (Lourenço et al., 2025). The pattern across all graphs has not exhibited any substantial differences, indicating that the error is negligible. A significant correlation between the two sets of bars indicates that the ANN effectively predicts the dissolution profile. These features suggest the possible application of ANN models in predicting drug release concentrations, hence saving time and resources in pharmaceutical research. Previous studies have demonstrated that ANN-based modelling is an effective tool for predicting the dissolution behaviour in pharmaceuticals industry or process analytical technology (Galata et al., 2019, 2021; Nagy et al., 2019; Péterfi et al., 2023). These graphs demonstrate that ANN models exhibit reliability in reproducing experimental results. The artificial neural network (ANN) model developed in this study effectively predicted the instantaneous dissolution behaviour of electrospun oral dissolving films (electrospun ODFs), replicated their unique rapid burst-release characteristics, and captured the effects of AA concentration and fibre morphology on early-stage dissolution. Under the defined experimental conditions, the model produces reliable predictions, can greatly reduce trial and error in large-scale experiments, and serves as a practical method for predicting the rapid release of this type of pharmaceutical preparation.

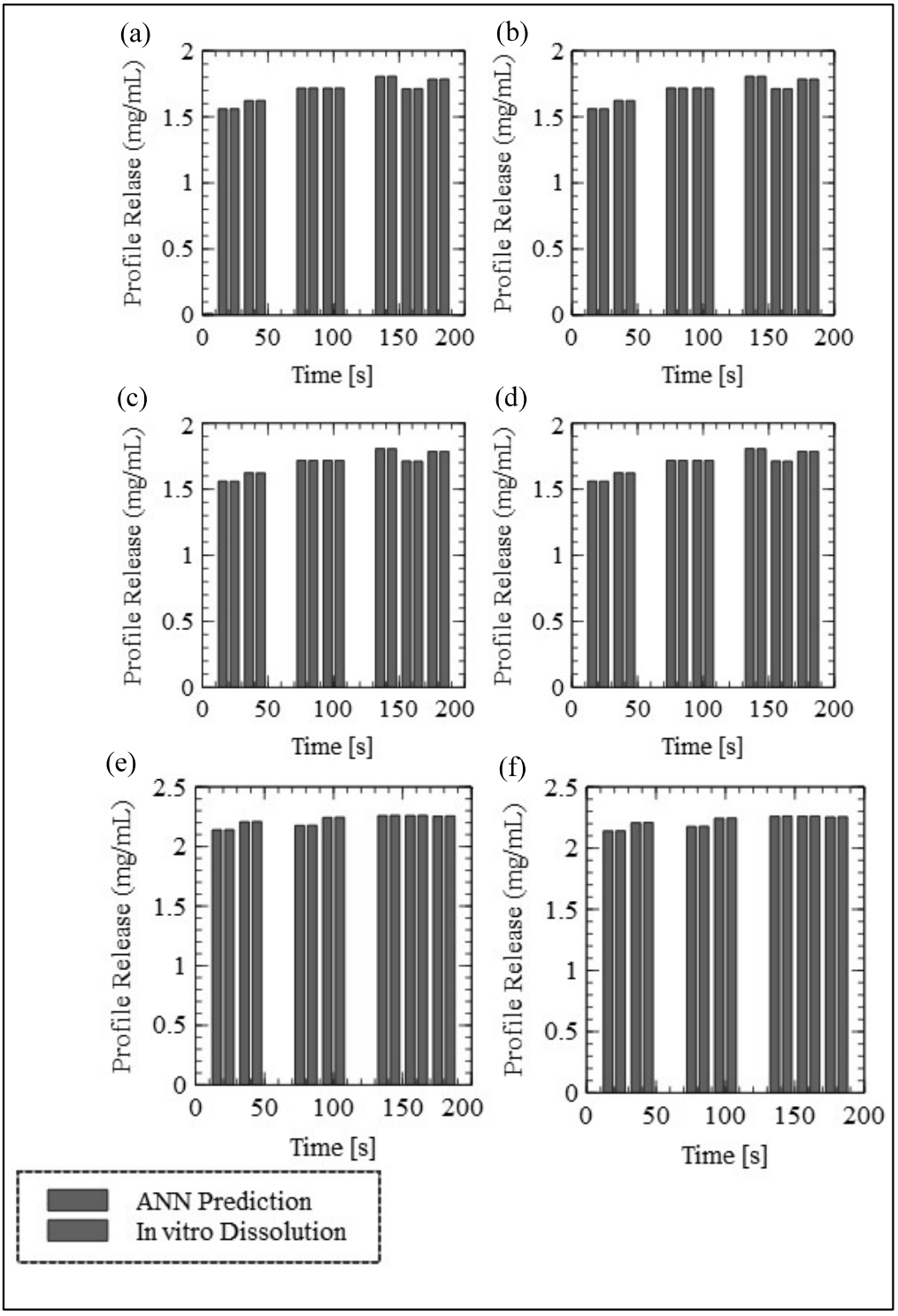


Figure 4.27: Comparison of Concentration of AA, (a) ODFs with 1w/v% of AA; (b) ODFs with 3w/v% of AA; (c) ODFs with 5w/v% of AA; (d) ODFs with 7w/v% of AA; (e) ODFs with 9w/v% of AA; (f) ODFs with 11w/v% of AA

CHAPTER 5
CONCLUSION

5.1 Conclusion

The first objective of this study was to synthesise, mechanically evaluate, and characterise two independent formulations of electrospun polyvinyl alcohol (PVA)/κ-carrageenan (κ-car) oral dissolving films (ODFs), which are incorporated with kelulut honey and ascorbic acid (AA), respectively. This objective was successfully achieved by fabricating uniform nanofiber membranes using optimised electrospinning parameters. This study established clear variable volume the kelulut honey loading in the honey-based formulations was set at three volumes: 1.0 mL, 1.5 mL, and 2.0 mL, while the ascorbic acid concentration in the AA-based formulations was set at six concentrations, 1, 3, 5, 7, 9, and 11 w/v%. The study results show that bead-free nanofibers were obtained from both formulation types, and their physicochemical, mechanical, and dissolution properties all met the requirements for oral drug delivery. The formulation loaded with 2.0 mL of kelulut honey was the optimal formulation in the honey group; it showed improved hydrophilicity and dissolution performance, with only a minor increase in fibre diameter. The 11 w/v% AA formulation was the top-performing one in the AA group, featuring the smallest average fibre diameter, fast dissolution rate, and qualified electrospinning performance. The study found that increasing concentrations of honey and AA altered the viscosity and electrical conductivity of the spinning solution, which in turn affected the formation and morphology of the resulting fibres.

The second objective of this study was to verify the dissolution performance of the prepared oral dissolving films (ODFs), and the objective was successfully achieved through testing. Both types of tested ODFs have an electrospun nanofiber structure with a high surface area, thus exhibiting consistent fast dissolution characteristics. The honey-loaded ODFs show a dissolution profile of rapid release followed by a plateau phase. For AA-loaded ODFs, the AA addition amount ranges from 1–11 w/v%, their dissolution behaviour is concentration-dependent, and they can achieve rapid release under simulated saliva conditions. This type of electrospun ODF is suitable for use as

an instant oral delivery system for natural functional ingredients and hydrophilic active pharmaceutical ingredients.

The third research objective of this study was to utilise artificial neural networks (ANNs) to predict the dissolution behaviour of two types of loaded oral dissolving films (ODFs), and this objective has now been successfully achieved. The ANNs model attained high prediction accuracy for both UV-Vis and FT-IR spectral datasets, captured the complex non-linear relationships between dissolution-related variables with a low mean squared error (MSE) and a coefficient of determination (R^2) approaching 1, can reduce experimental workload, development duration and material consumption, is suitable for the subsequent optimization of electrospun oral dispersion films, and serves as a formulation optimization tool capable of lowering experimental costs..

5.2 Recommendations

Future studies should further optimise the *kelulut* honey-loaded electrospun oral dispersible films (ODFs) by improving the formulation to achieve smoother and more uniform fibre morphology. Since honey influences both the viscosity and conductivity of the spinning solution, these properties should be carefully balanced to ensure stable electrospinning. A slight increase in the polyvinyl alcohol (PVA) content may improve fibre stability and reduce bead formation. In addition, controlled dilution of *kelulut* honey may be considered to moderately reduce solution viscosity while preserving its natural sweetness, bioactive properties, and functionality.

Improving the tensile strength to allow for commercial usage and achieving the value of suitable ODFs (< 20 mPa), adding other biopolymers such as chitosan, pullulan, HPMC and others to improve mechanical strength. This modification can balance tensile strength and flexibility while retaining the films' fast disintegration property to meet commercialisation requirements. Limited by time and resource constraints in this study, only one test was conducted to assess the mechanical properties of each formulation of electrospun oral dissolving films (n=1). The tensile strength values obtained are only preliminary observational results, and no statistical analyses such as calculation of mean ± standard deviation were performed. Future research needs to carry out at least 3 independent tests for each formulation, to calculate relevant statistical metrics and the significance of inter-group differences.

The batch dissolution experiments conducted in this study only used single measurements. The resulting dissolution curves are only preliminary observational results and cannot support statistical analysis of drug release behaviour. Follow-up studies need to improve the reliability and reproducibility of the research outcomes.

Future research can consider incorporating complementary analytical techniques to refine the instantaneous dissolution characterisation of electrospun oral dissolving films. Raman spectroscopy is less susceptible to water interference than FT-IR and can accurately identify molecular fingerprints and quantify active ingredients. XPS can analyse surface elements and chemical states before and after dissolution, revealing their surface dissolution mechanism. Further study should use artificial neural networks for predicting the fibre diameter and the electrospinning parameters of voltage, flow rate, viscosity and conductivity and increase the dataset to improve the stability of predictions.

REFERENCES

Abdelhameed, A. H., Abdelhafez, W. A., Saleh, Kh I., Hamad, A. A., & Mohamed, M. S. (2023). Formulation and optimization of oral fast dissolving films loaded with nanosuspension to enhance the oral bioavailability of Fexofenadine HCL. *Journal of Drug Delivery Science and Technology*, *85*. https://doi.org/10.1016/j.jddst.2023.104578

Abdul Rahman, N., Gizdavic-Nikolaidis, M., Ray, S., Easteal, A. J., & Travas-Sejdic, J. (2010). Functional electrospun nanofibres of poly(lactic acid) blends with polyaniline or poly(aniline-co-benzoic acid). *Synthetic Metals*, *160*(17–18), 2015–2022. https://doi.org/10.1016/j.synthmet.2010.07.031

Abou-taleb, H. A., Mustafa, W. W., Makram, T. S., Abdelaty, L. N., Salem, H., & Abdelkader, H. (2022). Vardenafil Oral Dispersible Films (ODFs) with Advanced Dissolution, Palatability, and Bioavailability. *Pharmaceutics*, *14*(3). https://doi.org/10.3390/pharmaceutics14030517

Adel Rashiq, S., Abd El-Sattar, N. E. A., abd Elhamid, H. A. E., El-Sayyad, G. S., Bassioni, G., & Ghobashy, M. M. (2025). Enhanced Bioadhesive and Antimicrobial Properties of PVA/Ascorbic Acid Composite with Tannic Acid Synthesized by Gamma Irradiation for Biomedical Applications. *ACS Omega*. https://doi.org/10.1021/acsomega.4c07119

Afendi, A. A. A., Patar, M. N. A. A., Mahmud, J., Nazri, N. A. A., & Samsudin, A. H. (2024). Failure Analysis and Prediction of Hybrid Composite Laminate under Biaxial Tension using Artificial Neural Network. *2024 IEEE 22nd Student Conference on Research and Development, SCOReD 2024*, 197–202. https://doi.org/10.1109/SCOReD64708.2024.10872670

Agasi, D., Kamal, M., Ibrahim, S. F., Kamal, H., Izhar, M., Mohd, A., & Mokhtar, M. H. (2021). *and Kelulut Honeys : A Comprehensive Review*.

Ahmed, I., Haque, A., Bhattacharyya, S., Patra, P., Plaisier, J. R., Perissinotto, F., & Bal, J. K. (2018). Vitamin C/Stearic Acid Hybrid Monolayer Adsorption at Air-Water and Air-Solid Interfaces. *ACS Omega*, *3*(11), 15789–15798. https://doi.org/10.1021/acsomega.8b02235

Ali, F., Tahir, R., & Samiullah, T. R. (2023). Evaluation of Wound Healing and Anti-Oxidative Activity of Acacia Honey and N-Acetylcysteine in Sprague Dawley

Rats. *Pakistan Journal of Zoology*, *55*(6), 2557–2564. https://doi.org/10.17582/journal.pjz/20210809080821

Arianto, D., Edikresnha, D., & Suciati, T. (2021). Materials Today : Proceedings The initial study of polyvinyl alcohol / honey / glycerin composite fibers. *Materials Today: Proceedings*, *44*, 3408–3411. https://doi.org/10.1016/j.matpr.2020.11.1025

Bakar, N. F. A., Salihfudin, M. A., Othman, N. H., Adam, F., Naim, M. N., Alias, N. H., & Rahman, N. A. (2023). Optimization of Electrospinning Parameters for Producing Carrageenan-PVA Based Nanofibers Film. *Journal of Fiber Science and Technology*, *79*(3), 57–71. https://doi.org/10.2115/fiberst.2023-0006

Balasubramaniam, M. P., Murugan, P., Chenthamara, D., Ramakrishnan, S. G., Salim, A., Lin, F. H., Robert, B., & Subramaniam, S. (2020). Synthesis of chitosan-ferulic acid conjugated poly(vinyl alcohol) polymer film for an improved wound healing. *Materials Today Communications*, *25*(August), 101510. https://doi.org/10.1016/j.mtcomm.2020.101510

Bańkosz, M. (2024). Physicochemical Characterization and Kinetics Study of Polymer Carriers with Vitamin C for Controlled Release Applications. *Materials*, *17*(22). https://doi.org/10.3390/ma17225502

Baptista, S., Baptista, F., & Freitas, F. (2023). Development of Emulsions Containing L-Ascorbic Acid and α-Tocopherol Based on the Polysaccharide FucoPol: Stability Evaluation and Rheological and Texture Assessment. *Cosmetics*, *10*(2). https://doi.org/10.3390/cosmetics10020056

Blaga, A. C., & Malutan, T. (2012). Selective separation of vitamin C by reactive extraction. *Journal of Chemical and Engineering Data*, *57*(2), 431–435. https://doi.org/10.1021/JE2010193

Bobde, S. S., & Tank, H. M. (2019). Design, characterization and statistical optimization of ramosetron hydrochloride mouth dissolving film using design of experiment. *International Journal of Applied Pharmaceutics*, *11*(2), 224–230. https://doi.org/10.22159/ijap.2019v11i2.30952

Bratu, I., Muresan-Pop, M., Kacso, I., & Frcaş, S. I. (2009). Spectroscopic investigation of the interaction between β-cyclodextrin and ascorbic acid. *Journal of Physics: Conference Series*, *182*(1). https://doi.org/10.1088/1742-6596/182/1/012004

Bureau, S., Cozzolino, D., & Clark, C. J. (2019). Contributions of Fourier-transform mid infrared (FT-MIR) spectroscopy to the study of fruit and vegetables: A

review. *Postharvest Biology and Technology*, *148*(October 2018), 1–14. https://doi.org/10.1016/j.postharvbio.2018.10.003

Calzado-Delgado, M., Guerrero-Pérez, M. O., & Yeung, K. L. (2023). Dissolvable Topical Formulations for Burst and Constant Delivery of Vitamin C. *ACS Omega*, *8*(14), 12636–12643. https://doi.org/10.1021/acsomega.2c06738

Celebioglu, A., Tekant, D., Kilic, M. E., Durgun, E., & Uyar, T. (2022). Orally Fast-Disintegrating Resveratrol/Cyclodextrin Nanofibrous Films as a Potential Antioxidant Dietary Supplement. *ACS Food Science and Technology*, *2*(3), 568–580. https://doi.org/10.1021/acsfoodscitech.1c00456

Celebioglu, A., & Uyar, T. (2019). Fast Dissolving Oral Drug Delivery System Based on Electrospun Nanofibrous Webs of Cyclodextrin/Ibuprofen Inclusion Complex Nanofibers. *Molecular Pharmaceutics*, *16*(10), 4387–4398. https://doi.org/10.1021/acs.molpharmaceut.9b00798

Celebioglu, A., & Uyar, T. (2021). Electrospun formulation of acyclovir/cyclodextrin nanofibers for fast-dissolving antiviral drug delivery. *Materials Science and Engineering C*, *118*. https://doi.org/10.1016/j.msec.2020.111514

Chaudhry, H., & Rangra, N. K. (2023). Development and validation of a stability indicating green analytical method for the simultaneous estimation of l-glutathione, n-acetyl l-cysteine and Vitamin C in marketed formulation using UV–visible spectroscopy. *Future Journal of Pharmaceutical Sciences*, *9*(1). https://doi.org/10.1186/s43094-023-00523-y

Cheng, E., Geng, Z., Xiang, L., Zhao, X., Xiang, A., & Tian, H. (2024). Development of Vitamin C-Loaded Electrospun Nanofibers of Mixture of Polysaccharides of Pullulan/Xanthan Gum for Fast Dissolving Oral Film Applications. *Materials*, *17*(4), 861. https://doi.org/10.3390/ma17040861

Chin, S. W., Azman, A. S., & Tan, J. W. (2024). Incorporation of natural and synthetic polymers into honey hydrogel for wound healing: A review. In *Health Science Reports* (Vol. 7, Issue 7). John Wiley and Sons Inc. https://doi.org/10.1002/hsr2.2251

Cho, H. W., Baek, S. H., Lee, B. J., & Jin, H. E. (2020). Orodispersible Polymer Films With The Poorly Water-Soluble Drug, Olanzapine: Hot-melt pneumatic extrusion for single-process 3D printing. *Pharmaceutics*, *12*(8), 1–16. https://doi.org/10.3390/pharmaceutics12080692

Chopra, H., Bibi, S., Kumar, S., Khan, M. S., Kumar, P., & Singh, I. (2022). Preparation and Evaluation of Chitosan/PVA Based Hydrogel Films Loaded with Honey for Wound Healing Application. *Gels*, *8*(2). https://doi.org/10.3390/gels8020111

Cleeton, C., Keirouz, A., Chen, X., & Radacsi, N. (2019). Electrospun Nanofibers for Drug Delivery and Biosensing. *ACS Biomaterials Science and Engineering*, *5*(9), 4183–4205. https://doi.org/10.1021/acsbiomaterials.9b00853

Cortés-Estrada, C. E., Gallardo-Velázquez, T., Osorio-Revilla, G., Castañeda-Pérez, E., Meza-Márquez, O. G., López-Cortez, M. del S., & Hernández-Martínez, D. M. (2020). Prediction of total phenolics, ascorbic acid, antioxidant capacities, and total soluble solids of Capsicum annuum L. (bell pepper) juice by FT-MIR and multivariate analysis. *LWT*, *126*. https://doi.org/10.1016/j.lwt.2020.109285

Cuahuizo-Huitzil, G., Olivares-Xometl, O., Eugenia Castro, M., Arellanes-Lozada, P., Meléndez-Bustamante, F. J., Pineda Torres, I. H., Santacruz-Vázquez, C., & Santacruz-Vázquez, V. (2023). Artificial Neural Networks for Predicting the Diameter of Electrospun Nanofibers Synthesized from Solutions/Emulsions of Biopolymers and Oils. *Materials*, *16*(16). https://doi.org/10.3390/ma16165720

Das, A., Datta, P., Chowdhury, A. R., & Barui, A. (2020). Honey-incorporated nanofibre reduces replicative senescence of umbilical cordderived mesenchymal stem cells. *IET Nanobiotechnology*, *14*(9), 870–880. https://doi.org/10.1049/iet-nbt.2019.0288

De Vrieze, S., Van Camp, T., Nelvig, A., Hagström, B., Westbroek, P., & De Clerck, K. (2009). The effect of temperature and humidity on electrospinning. *Journal of Materials Science*, *44*(5), 1357–1362. https://doi.org/10.1007/s10853-008-3010-6

Deshawar, D., Gupta, K., & Chokshi, P. (2020). Electrospinning of polymer solutions: An analysis of instability in a thinning jet with solvent evaporation. *Polymer*, *202*(February), 122656. https://doi.org/10.1016/j.polymer.2020.122656

Devianti, Sufardi, Hafsah, S., Sariadi, Ahmad, F., Arianti, N. D., Saputra, E., & Hartuti, S. (2023). Rapid and non-destructive determination of vitamin C and antioxidant activity of intact red chilies using visible near-infrared spectroscopy and machine learning tools. *Case Studies in Chemical and Environmental Engineering*, *8*. https://doi.org/10.1016/j.cscee.2023.100435

Doshi, J., & Reneker, D. H. (1995). Electrospinning Process and Applications of Electrospun Fibers. *Electrostatic*, *35*, 151–160.

Ebube, N. K., McCall, T., Chen, Y., & Meyer, M. C. (1997). Relating Formulation Variables to in Vitro Dissolution Using an Artificial Neural Network. *Pharmaceutical Development and Technology*, *2*(3), 225–232. https://doi.org/10.3109/10837459709031442

El-Kased, R. F., Amer, R. I., Attia, D., & Elmazar, M. M. (2017). Honey-based hydrogel: In vitro and comparative in vivo evaluation for burn wound healing. *Scientific Reports*, *7*(1). https://doi.org/10.1038/s41598-017-08771-8

El-attar, A. A., El-wakil, H. B., Hassanin, A. H., Bakr, B. A., Almutairi, T. M., Hagar, M., Elwakil, B. H., & Olama, Z. A. (2022). Silver/Snail Mucous PVA Nanofibers: Electrospun Synthesis and Antibacterial and Wound Healing Activities. *Membranes*, *12*(5). https://doi.org/10.3390/membranes12050536

Galata, D. L., Farkas, A., Könyves, Z., Mészáros, L. A., Szabó, E., Csontos, I., Pálos, A., Marosi, G., Nagy, Z. K., & Nagy, B. (2019). Fast, spectroscopy-based prediction of in vitro dissolution profile of extended release tablets using artificial neural networks. *Pharmaceutics*, *11*(8). https://doi.org/10.3390/pharmaceutics11080400

Galata, D. L., Könyves, Z., Nagy, B., Novák, M., Mészáros, L. A., Szabó, E., Farkas, A., Marosi, G., & Nagy, Z. K. (2021). Real-time release testing of dissolution based on surrogate models developed by machine learning algorithms using NIR spectra, compression force and particle size distribution as input data. *International Journal of Pharmaceutics*, *597*. https://doi.org/10.1016/j.ijpharm.2021.120338

Gao, S., Jiang, J., Li, X., Ye, F., Fu, Y., & Zhao, L. (2021). Electrospun Polymer-Free Nanofibers Incorporating Hydroxypropyl-β-cyclodextrin/Difenoconazole via Supramolecular Assembly for Antifungal Activity. *Journal of Agricultural and Food Chemistry*, *69*(21), 5871–5881. https://doi.org/10.1021/acs.jafc.1c01351

Garcia, V. A. dos S., Borges, J. G., Maciel, V. B. V., Mazalli, M. R., Lapa-Guimaraes, J. das G., Vanin, F. M., & de Carvalho, R. A. (2018). Gelatin/starch orally disintegrating films as a promising system for vitamin C delivery. *Food Hydrocolloids*, *79*, 127–135. https://doi.org/10.1016/j.foodhyd.2017.12.027

Geană, E. I., Isopescu, R., Ciucure, C. T., Gîjiu, C. L., & Joșceanu, A. M. (2024). Honey Adulteration Detection via Ultraviolet–Visible Spectral Investigation Coupled with Chemometric Analysis. *Foods*, *13*(22). https://doi.org/10.3390/foods13223630

Ghahremani-nasab, M., Akbari-Gharalari, N., Rahmani Del Bakhshayesh, A., Ghotaslou, A., Ebrahimi-kalan, A., Mahdipour, M., & Mehdipour, A. (2023). Synergistic effect of chitosan-alginate composite hydrogel enriched with ascorbic acid and alpha-tocopherol under hypoxic conditions on the behavior of mesenchymal stem cells for wound healing. *Stem Cell Research & Therapy*, *14*(1), 326. https://doi.org/10.1186/s13287-023-03567-2

Guler, E., Yekeler, H. B., Tekinalp, S. G., Parviz, G., Dogan, M., Ekentok, C., & Cam, M. E. (2024). Sublingual β-Glucan/Vitamin C-loaded nanoparticle-embedded polyethylene oxide nanofibrous mats. *Journal of Drug Delivery Science and Technology*, *102*. https://doi.org/10.1016/j.jddst.2024.106309

Gupta, R. K., Manisha, Ali, E. A. E., Areekal, N. N., Patel, J., Pipliya, S., Srivastav, P. P., Wang, C. K., & Castro-Muñoz, R. (2025). Vitamin C-infused biopolymer films: a multifunctional approach for active food packaging and preservation. *Sustainable Food Technology*, *4*(1), 25–50. https://doi.org/10.1039/d5fb00282f

Haider, A., Haider, S., & Kang, I. (2018). REVIEW A comprehensive review summarizing the effect of electrospinning parameters and potential applications of nanofibers in biomedical and biotechnology. *Arabian Journal of Chemistry*, *11*(8), 1165–1188. https://doi.org/10.1016/j.arabjc.2015.11.015

Handley, E. L., & Callanan, A. (2023). Effects of electrospun fibers containing ascorbic acid on oxidative stress reduction for cardiac tissue engineering. *Journal of Applied Polymer Science*, *140*(32), 1–14. https://doi.org/10.1002/app.54242

Hidzer, M. H., Sapiee, N. H., Rahman, W. M. N. W. A., Le, C. H., Nguyen, H. Q., & Mahmud, J. (2025). Leucaena-Silicone Biocomposite: Experimentation, Quantification and Prediction of Mechanical Properties for Potential Applications in Medicine and Healthcare. *International Journal of Automotive and Mechanical Engineering*, *22*(2), 12332–12343. https://doi.org/10.15282/ijame.22.2.2025.7.0944

Iskalieva, A., Yesmurat, M., Al Azzam, K. M., Ainakulova, D., Yerbolat, Y., Negim, E. S., Ibrahim, M. N. M., & Gulzhakhan, Y. (2023). Effect of Polyethylene Glycol Methyl Ether Methacrylate on the Biodegradability of Polyvinyl Alcohol/Starch Blend Films. *Polymers*, *15*(15). https://doi.org/10.3390/polym15153165

Islam, N., Khan, N. U., Razzaq, A., Menaa, F., Khan, Z. U., Hussain, A., Rehman, S. U., Iqbal, H., & Ni, J. (2023). Loratadine oral bioavailability enhancement via

solid dispersion loaded oro-dispersible films: Formulation, characterization and pharmacokinetics. *Colloids and Surfaces B: Biointerfaces*, *230*. https://doi.org/10.1016/j.colsurfb.2023.113526

Jacob, S., Boddu, S. H. S., Bhandare, R., Ahmad, S. S., & Nair, A. B. (2023). Orodispersible Films: Current Innovations and Emerging Trends. *Pharmaceutics 2023, Vol. 15, Page 2753*, *15*(12), 2753. https://doi.org/10.3390/PHARMACEUTICS15122753

Kaimal, A. M., & Singhal, R. S. (2023). Bigels for controlled gastric release of ascorbic acid: Impact on rheology, texture, thermal stability and antioxidant activity. *Food Hydrocolloids for Health*, *4*. https://doi.org/10.1016/j.fhfh.2023.100171

Kanimozhi, S., Kathiresan, G., Kathalingam, A., Kim, H. S., & Doss, M. N. R. (2020). Organic nanocomposite Band-Aid for chronic wound healing: a novel honey-based nanofibrous scaffold. *Applied Nanoscience (Switzerland)*, *10*(5), 1639–1652. https://doi.org/10.1007/s13204-019-01247-3

Karki, S., Kim, H., Na, S. J., Shin, D., Jo, K., & Lee, J. (2016). Thin films as an emerging platform for drug delivery. In *Asian Journal of Pharmaceutical Sciences* (Vol. 11, Issue 5, pp. 559–574). Shenyang Pharmaceutical University. https://doi.org/10.1016/j.ajps.2016.05.004

Kassem, L. M., El-Deen, A. G., Zaki, A. H., & El-Dek, S. I. (2023). Electrospun manuka honey@PVP nanofibers enclosing chitosan-titanate for highly effective wound healing. *Cellulose*, *30*(10), 6487–6505. https://doi.org/10.1007/s10570-023-05267-9

Khan, N., Singh, A. K., & Saneja, A. (2023). Preparation, Characterization, and Antioxidant Activity of L-Ascorbic Acid/HP-β-Cyclodextrin Inclusion Complex-Incorporated Electrospun Nanofibers. *Foods*, *12*(7). https://doi.org/10.3390/foods12071363

Kida, D., Konopka, T., Jurczyszyn, K., & Karolewicz, B. (2023). Technological Aspects and Evaluation Methods for Polymer Matrices as Dental Drug Carriers. In *Biomedicines* (Vol. 11, Issue 5). MDPI. https://doi.org/10.3390/biomedicines11051274

Konstantinidis, S., Karampiperis, P., & Sicilia, M. A. (2015). Enhancing the Levenberg-Marquardt Method in Neural Network training using the direct computation of the Error Cost Function Hessian. *ACM International Conference Proceeding Series*, *2015-Janua*. https://doi.org/10.1145/2797143.2797162

Koosha, M., Aalipour, H., Shirazi, M. J. S., Jebali, A., Chi, H., Hamedi, S., Wang, N., Li, T., & Moravvej, H. (2021). Physically crosslinked chitosan/pva hydrogels containing honey and allantoin with long-term biocompatibility for skin wound repair: An in vitro and in vivo study. *Journal of Functional Biomaterials*, *12*(4). https://doi.org/10.3390/jfb12040061

KOTA, S., ANANTHA, R., GOVADA, V. R., & DUMPALA, P. (2024). Chitosan/PVA Films and Silver Nanoparticle Impregnated Nanofibrous Dressings for Evaluation of their Wound Healing Efficacy in Wistar Albino Rat Model. *Journal of Polymer Materials*, *40*(3–4), 285–303. https://doi.org/10.32381/JPM.2023.40.3-4.10

Kozakiewicz-Latała, M., Dyba, A. J., Marciniak, D., Szymczyk-Ziółkowska, P., Cieszko, M., Nartowski, K. P., Nowak, M., & Karolewicz, B. (2024). PVA-based formulations as a design-technology platform for orally disintegrating film matrices. *International Journal of Pharmaceutics*, *665*, 124666. https://doi.org/10.1016/j.ijpharm.2024.124666

Kristó, K., Módra, S., Hornok, V., Süvegh, K., Ludasi, K., Aigner, Z., Kelemen, A., Sovány, T., Pintye-Hódi, K., & Regdon, G. (2022). Investigation of Surface Properties and Free Volumes of Chitosan-Based Buccal Mucoadhesive Drug Delivery Films Containing Ascorbic Acid. *Pharmaceutics*, *14*(2), 345. https://doi.org/10.3390/pharmaceutics14020345

Lee, Y., Thapa, P., Jeong, S. H., Woo, M. H., & Choi, D. H. (2017). Formulation optimization and in vitro characterization of orally disintegrating films using a factorial design and mathematical modeling for drug release. *Chemical and Pharmaceutical Bulletin*, *65*(2), 166–177. https://doi.org/10.1248/cpb.c16-00757

Liu, C., Wang, Y., Wang, P., Gong, Y., Yi, B., Ruan, J., & Wang, X. (2023). In situ electrospun aloe-nanofiber membrane for chronic wound healing. *Smart Materials in Medicine*, *4*, 514–521. https://doi.org/10.1016/j.smaim.2023.03.003

Lourenço, A. S., Schuster, T., Lopes, J. A., & Kirsch, A. (2025). A non-linear modelling approach to predict the dissolution profile of extended-release tablets. *European Journal of Pharmaceutical Sciences*, *204*. https://doi.org/10.1016/j.ejps.2024.106976

Ma, M., Zhou, H., Gao, S., Li, N., Guo, W., & Dai, Z. (2023). Analysis and Prediction of Electrospun Nanofiber Diameter Based on Artificial Neural Network. *Polymers*, *15*(13). https://doi.org/10.3390/polym15132813

Maggio, R. M., Castellano, P. M., & Kaufman, T. S. (2008). A new principal component analysis-based approach for testing "similarity" of drug dissolution profiles. *European Journal of Pharmaceutical Sciences*, *34*(1), 66–77. https://doi.org/10.1016/j.ejps.2008.02.009

Makram, T. S., Eid, S. M., Abu-Dahab, M., AbouGhaly, M. H. H., Elnahas, O. S., Chopra, H., Bibi, S., Kumar, S., Khan, M. S., Kumar, P., & Singh, I. (2024). Formulation of Saxagliptin Oral Films: Optimization, Physicochemical Characterization, In-Vivo Assessment, and In-Vitro Real-Time Release Monitoring via a Novel Polyaniline Nanoparticles-Based Solid-Contact Screen Printed Ion-Selective Electrode. *AAPS PharmSciTech*, *25*(5), 1–17. https://doi.org/10.1208/s12249-024-02828-4

Maleki, H., Gharehaghaji, A. A., & Dijkstra, P. J. (2013). A novel honey-based nanofibrous scaffold for wound dressing application. *Journal of Applied Polymer Science*, *127*(5), 4086–4092. https://doi.org/10.1002/app.37601

Mallick, A., Mandal, R., Mondal, N., Sarkar, S., Biswas, N., Maji, B., & Majumdar, G. (2024). Parametric optimization and minimization of corrosion rate of electroless Ni–P coating using Box-Behnken design and Artificial Neural Network. *Results in Surfaces and Interfaces*, *15*. https://doi.org/10.1016/j.rsurfi.2024.100228

Mammadli, S. (2017). Financial time series prediction using artificial neural network based on Levenberg-Marquardt algorithm. *Procedia Computer Science*, *120*, 602–607. https://doi.org/10.1016/j.procs.2017.11.285

Mandal, U., Gowda, V., Ghosh, A., Bose, A., Bhaumik, U., Chatterjee, B., & Pal, T. K. (2008). Optimization of metformin HCl 500 mg sustained release matrix tablets using Artificial Neural Network (ANN) based on Multilayer Perceptrons (MLP) model. *Chemical and Pharmaceutical Bulletin*, *56*(2), 150–155. https://doi.org/10.1248/cpb.56.150

Mann, J., Dressman, J., Rosenblatt, K., Ashworth, L., Muenster, U., Frank, K., Hutchins, P., Williams, J., Klumpp, L., Wielockx, K., Berben, P., Augustijns, P., Holm, R., Hofmann, M., Patel, S., Beato, S., Ojala, K., Tomaszewska, I., Bruel, J. L., & Butler, J. (2017). Validation of Dissolution Testing with

Biorelevant Media: An OrBiTo Study. *Molecular Pharmaceutics*, *14*(12), 4192–4201. https://doi.org/10.1021/acs.molpharmaceut.7b00198

Mavelil-sam, R., Ouseph, E. M., Morreale, M., Scaffaro, R., & Thomas, S. (2023). *Recent Developments and Formulations for Hydrophobic Modification of Carrageenan Bionanocomposites*.

Mészáros, L. A., Madarász, L., Ficzere, M., Bicsár, R., Farkas, A., & Nagy, Z. K. (2024). UV/VIS-imaging of white caffeine tablets for prediction of CQAs: API content, crushing strength, friability, disintegration time and dissolution profile. *International Journal of Pharmaceutics*, *663*, 124565. https://doi.org/10.1016/J.IJPHARM.2024.124565

Mitra, P. K., Karmakar, R., Nandi, R., & Gupta, S. (2023). Low-cost rapid workflow for honey adulteration detection by UV–Vis spectroscopy in combination with factorial design, response surface methodology and supervised machine learning classifiers. *Bioresource Technology Reports*, *21*(September 2022), 101327. https://doi.org/10.1016/j.biteb.2022.101327

Mohammadi, F., Bina, B., Karimi, H., Rahimi, S., & Yavari, Z. (2020). Modeling and sensitivity analysis of the alkylphenols removal via moving bed biofilm reactor using artificial neural networks: Comparison of levenberg marquardt and particle swarm optimization training algorithms. *Biochemical Engineering Journal*, *161*(June), 107685. https://doi.org/10.1016/j.bej.2020.107685

Mohd Azam, N. A. N., & Amin, K. A. M. (2017). The Physical and Mechanical Properties of Gellan Gum Films Incorporated Manuka Honey as Wound Dressing Materials. *IOP Conference Series: Materials Science and Engineering*, *209*(1). https://doi.org/10.1088/1757-899X/209/1/012027

Munir, M. A., Jamal, J. A., & Inayatullah, A. (2024). Environment-Friendly Approach to Isolate Ascorbic Acid from Plants and Micro-identified Using Fourier Transform Infrared Spectroscopy. *ACS Food Science & Technology*. https://doi.org/10.1021/acsfoodscitech.3c00575

Musazzi, U. M., Selmin, F., Ortenzi, M. A., Mohammed, G. K., Franzé, S., Minghetti, P., & Cilurzo, F. (2018). Personalized orodispersible films by hot melt ram extrusion 3D printing. *International Journal of Pharmaceutics*, *551*(1–2), 52–59. https://doi.org/10.1016/j.ijpharm.2018.09.013

Nagy, B., Petra, D., Galata, D. L., Démuth, B., Borbás, E., Marosi, G., Nagy, Z. K., & Farkas, A. (2019). Application of artificial neural networks for Process

Analytical Technology- based dissolution testing. *International Journal of Pharmaceutics*, *567*. https://doi.org/10.1016/j.ijpharm.2019.118464

Nasalapure, A. V., Chalannavar, R. K., Kasai, D. R., Reddy, K. R., & Raghu, A. V. (2021). Novel polymeric hydrogel composites: Synthesis, physicochemical, mechanical and biocompatible properties. *Nano Express*, *2*(3). https://doi.org/10.1088/2632-959X/ac11bf

Naskar, A., Chatterjee, K., Roy, K., Majie, A., Nair, A. B., Shinu, P., Morsy, M. A., Jain, N., Pandey, M., & Gorain, B. (2024). Mechanistic Roles of Different Varieties of Honey on Wound Healing: Recent Update. In *Journal of Pharmacology and Pharmacotherapeutics* (Vol. 15, Issue 1, pp. 5–18). Sage Publications India Pvt. Ltd. https://doi.org/10.1177/0976500X241237361

Nordin, A., Qisya, N., Sainik, V., Roy, S., & Bin, A. (2018). *Journal of Food Composition and Analysis Physicochemical properties of stingless bee honey from around the globe : A comprehensive review*. *73*(February), 91–102. https://doi.org/10.1016/j.jfca.2018.06.002

Nuraje, N., Khan, W. S., Lei, Y., Ceylan, M., & Asmatulu, R. (2013). Superhydrophobic electrospun nanofibers. *J. Mater. Chem. A*, *1*(6), 1929–1946. https://doi.org/10.1039/C2TA00189F

Nurhadi, B., Ikhsan, M., Tensiska, Sukri, N., & Mahani. (2019). Rheological Properties of Honey and its Application on Honey Flow Simulation through Vertical Tube. *IOP Conference Series: Earth and Environmental Science*, *334*(1). https://doi.org/10.1088/1755-1315/334/1/012041

Nurrul Amilin Zainal Abidin, Jamaluddin Mahmud, Nur Aini Sabrin Manssor, & Nor Nabilah Che Abd Rahim. (2022). Physical and Mechanical Properties of Bamboo-SiliconeBiocomposites (BaSiCs). In *BioResources* (Vol. 17, Issue 3, pp. 4432–4443).

Obregón, S., & Rodríguez-González, V. (2022). Photocatalytic TiO2 thin films and coatings prepared by sol–gel processing: a brief review. *Journal of Sol-Gel Science and Technology*, *102*(1), 125–141. https://doi.org/10.1007/S10971-021-05628-5

Okur, N., Saricam, C., Gocek, I., Kalav, B., & Sahin, U. K. (2021). Functionalized polyvinyl alcohol nanofiber webs containing β–cyclodextrin/Vitamin C inclusion complex. *Journal of Industrial Textiles*, *50*(10), 1559–1571. https://doi.org/10.1177/1528083719866933

Olechno, K., Maciejewski, B., Głowacz, K., Lenik, J., Ciosek-Skibińska, P., Basa, A., & Winnicka, K. (2022). Orodispersible Films with Rupatadine Fumarate Enclosed in Ethylcellulose Microparticles as Drug Delivery Platform with Taste-Masking Effect. *Materials*, *15*(6). https://doi.org/10.3390/ma15062126

Pacheco, M. S., Barbieri, D., da Silva, C. F., & de Moraes, M. A. (2021). A review on orally disintegrating films (ODFs) made from natural polymers such as pullulan, maltodextrin, starch, and others. *International Journal of Biological Macromolecules*, *178*, 504–513. https://doi.org/10.1016/j.ijbiomac.2021.02.180

Palezi, S. C., Latorres, J. M., Fernandes, S. S., & Martins, V. G. (2025). Development of Vitamin C-Enriched Oral Disintegration Films Using Chia Mucilage. *Processes*, *13*(1). https://doi.org/10.3390/pr13010250

Péterfi, O., Nagy, Z. K., Sipos, E., & Galata, D. L. (2023). Artificial Intelligence-based Prediction of In Vitro Dissolution Profile of Immediate Release Tablets with Near-infrared and Raman Spectroscopy. *Periodica Polytechnica Chemical Engineering*, *67*(1), 18–30. https://doi.org/10.3311/PPch.20755

Poojar, B., Ommurugan, B., Adiga, S., Thomas, H., Sori, R. K., Poojar, B., Hodlur, N., Tilak, A., Korde, R., Gandigawad, P., In, M., Sleep, R., Albino, D., Rats, W., Article, O., Schedule, P., Injury, C. C., Sori, R. K., Poojar, B., … Gandigawad, P. (2017). Methodology Used in the Study. *Asian Journal of Pharmaceutical and Clinical Research*, *7*(10), 1–5. https://doi.org/10.4103/jpbs.JPBS

Popescu, E. C., & Boscornea, C. (2007). *Structure and properties of carragenan*. https://www.researchgate.net/publication/268271114

Prete, S., Dattilo, M., Patitucci, F., Pezzi, G., Parisi, O. I., & Puoci, F. (2023). Natural and Synthetic Polymeric Biomaterials for Application in Wound Management. *Journal of Functional Biomaterials*, *14*(9), 455. https://doi.org/10.3390/jfb14090455

Priyanka, , Kumar, K., & Teotia, D. (2019). A Comprehensive Review on Pharmaceutical Oral Dissolving Films. *Journal of Drug Delivery and Therapeutics*, *9*(5-s), 170–174. https://doi.org/10.22270/jddt.v9i5-s.3641

Qin, Z. yu, Jia, X. W., Liu, Q., Kong, B. hua, & Wang, H. (2019). Fast dissolving oral films for drug delivery prepared from chitosan/pullulan electrospinning nanofibers. *International Journal of Biological Macromolecules*, *137*, 224–231. https://doi.org/10.1016/j.ijbiomac.2019.06.224

Reneker, D. H., & Yarin, A. L. (2008). Electrospinning jets and polymer nanofibers. *Polymers with Aligned Carbon Nanotubes: Active Composite Materials*, *49*(10), 2387–2425. https://doi.org/10.1016/j.polymer.2008.02.002

Rohani Shirvan, A., Hemmatinejad, N., Bahrami, S. H., & Bashari, A. (2022). A comparison between solvent casting and electrospinning methods for the fabrication of neem extract-containing buccal films. *Journal of Industrial Textiles*, *51*(1), 311S-335S. https://doi.org/10.1177/15280837211027785

Roopesh, M., Davis, D., Jyothi, M. S., Vandana, M., Thippeswamy, B. S., Hegde, G., Vinod, T. P., & Keri, R. S. (2023). Wound healing efficacy of curcumin-loaded sandalwood bark-derived carbon nanosphere/PVA nanofiber matrix. *RSC Advances*, *13*(35), 24320–24330. https://doi.org/10.1039/d3ra04181f

Sabbagh, F., Khatir, N. M., & Kiarostami, K. (2023). Synthesis and Characterization of k-Carrageenan/PVA Nanocomposite Hydrogels in Combination with MgZnO Nanoparticles to Evaluate the Catechin Release. *Polymers*, *15*(2). https://doi.org/10.3390/polym15020272

Şalva, E., Akdağ, A. E., Alan, S., Arısoy, S., & Akbuğa, F. J. (2023). Evaluation of the Effect of Honey-Containing Chitosan/Hyaluronic Acid Hydrogels on Wound Healing. *Gels*, *9*(11). https://doi.org/10.3390/gels9110856

Samadieh, S., & Sadri, M. (2020). Preparation and Biomedical properties of transparent chitosan/ gelatin/honey/aloe vera nanocomposite. *Nanomedicine Research Journal*, *5*(1), 1–12. https://doi.org/10.22034/NMRJ.2020.01.001

Santos, A. M. N., Moreira, A. P. D., Carvalho, C. W. P., Luchese, R., Ribeiro, E., McGuinness, G. B., Mendes, M. F., & Oliveira, R. N. (2019). Physically cross-linked gels of PVA with natural polymers as matrices for manuka honey release in wound-care applications. *Materials*, *12*(2). https://doi.org/10.3390/ma12040559

Sapiee, N. H., Mat Saufi, M. H., Abu Bakar, N. F., & Adam, F. (2023). Fabrication and characterization of electrospun κ-carrageenan based oral dispersible film with vitamin C. *Materials Today: Proceedings*. https://doi.org/10.1016/j.matpr.2023.04.030

Sarić, A., & Xiao, J. (2011). Efficient levenberg-marquardt minimization of the cross-entropy error function. *Proceedings of the International Joint Conference on Neural Networks*, 1–8. https://doi.org/10.1109/IJCNN.2011.6033191

Schuhladen, K., Raghu, S. N. V., Liverani, L., Neščáková, Z., & Boccaccini, A. R. (2021). Production of a novel poly(ε-caprolactone)-methylcellulose electrospun wound dressing by incorporating bioactive glass and Manuka honey. *Journal of Biomedical Materials Research - Part B Applied Biomaterials*, *109*(2), 180–192. https://doi.org/10.1002/jbm.b.34690

Seleka, W. M., Phasha, M. M., Kganyakgo, L. K., Makwakwa, D., & Makhado, E. (2025). *Preparation of a conductive hydrogel based on carrageenan , polyvinyl alcohol , and polypyrrole as a potential room temperature electrochemical hydrogen gas sensor*. *214*(May).

Shahbazi, M., Rajabzadeh, G., Rafe, A., Ettelaie, R., & Ahmadi, S. J. (2016). The physico-mechanical and structural characteristics of blend film of poly (vinyl alcohol) with biodegradable polymers as affected by disorder-to-order conformational transition. *Food Hydrocolloids*, *60*, 393–404. https://doi.org/10.1016/j.foodhyd.2016.03.038

Shahid, M. A., & Khan, M. S. (2022). Preparation and characterization of electrospun nanofiber membrane from polyvinyl alcohol loaded with Glycyrrhiza glabra extract. *Polymers and Polymer Composites*, *30*. https://doi.org/10.1177/09673911221109422

Sheth, T. S., & Acharya, F. (2024). Optimization and evaluation of modified release solid dosage forms using artificial neural network. *Scientific Reports*, *14*(1). https://doi.org/10.1038/s41598-024-67274-5

Shin, H. J., Chang, J. H., & Han, J. A. (2023). Physicochemical and in-vitro release characteristics of vitamin C-loaded antioxidant orally disintegrating films with different catechin levels. *Food Bioscience*, *53*. https://doi.org/10.1016/j.fbio.2023.102733

Shirzaiy, M., Heydarirad, G., & Bakhshipour, S. (2022). Effects of honey-lemon spray on recurrent aphthous stomatitis comparing to Triamcinolone ointment; a randomized controlled clinical trial. *Brazilian Journal of Oral Sciences*, *22*. https://doi.org/10.20396/BJOS.V22I00.8667560

Siddeeq, A., & Al-Douri, A. S. (2008). of Honey on the Healing of Oral Ulcers. In *Clinical Study). Al-Rafidain Dent J* (Vol. 8, Issue 2). www.rafidaindentj.net

Singh, G., Gaur, A., Bisht, P., & Mahato, R. N. (2023). Structural, Morphological, and Magnetocaloric Properties of Nanocrystalline Pr 0.7 La 0.3 MnO 3 . *ECS*

Journal of Solid State Science and Technology, *12*(8), 087002. https://doi.org/10.1149/2162-8777/ACEAAA

Singh, P., Dwivedi, P., & Kant, V. (2019). A hybrid method based on neural network and improved environmental adaptation method using Controlled Gaussian Mutation with real parameter for short-term load forecasting. In *Energy* (Vol. 174, pp. 460–477). Elsevier Ltd. https://doi.org/10.1016/j.energy.2019.02.141

Skrovankova, S., Mlcek, J., Sochor, J., Baron, M., Kynicky, J., & Jurikova, T. (2015). Determination of ascorbic acid by electrochemical techniques and other methods. *International Journal of Electrochemical Science*, *10*(3), 2421–2431. https://doi.org/10.1016/s1452-3981(23)04857-5

Sthefany, B., Pinheiro, S., Thainan, D., Lima, S., Resende, C. X., Sergipe, U. F. De, & Sergipe, U. F. De. (2025). *Influence of Plasticizers Honey and Glycerol on the Properties of Membranes Based on Babassu Coconut Mesocarp*. *28*(i), 1–9.

Stoica, A. E., Albuleț, D., Bîrcă, A. C., Iordache, F., Ficai, A., Grumezescu, A. M., Vasile, B. Ștefan, Andronescu, E., Marinescu, F., & Holban, A. M. (2023). Electrospun Nanofibrous Mesh Based on PVA, Chitosan, and Usnic Acid for Applications in Wound Healing. *International Journal of Molecular Sciences*, *24*(13). https://doi.org/10.3390/ijms241311037

Suflet, D. M., Popescu, I., Pelin, I. M., David, G., Serbezeanu, D., Rîmbu, C. M., Daraba, O. M., Enache, A. A., & Bercea, M. (2022). Phosphorylated Curdlan Gel/Polyvinyl Alcohol Electrospun Nanofibres Loaded with Clove Oil with Antibacterial Activity. *Gels*, *8*(7). https://doi.org/10.3390/gels8070439

Sukum, P., Punyodom, W., Dangtip, S., Poramapijitwat, P., Daranarong, D., Jenvoraphot, T., Nisoa, M., Kuensaen, C., & Boonyawan, D. (2023). Argon Plasma Jet-Treated Poly (Vinyl Alcohol)/Chitosan and PEG 400 Plus Mangifera indica Leaf Extract for Electrospun Nanofiber Membranes: In Vitro Study. *Polymers*, *15*(11). https://doi.org/10.3390/polym15112559

Taher, M. A., Zahan, K. A., Rajaie, M. A., Ring, L. C., Rashid, S. A., Mohd Nor Hamin, N. S., Nee, T. W., & Yenn, T. W. (2020). Nanocellulose as drug delivery system for honey as antimicrobial wound dressing. *Materials Today: Proceedings*, *31*(xxxx), 14–17. https://doi.org/10.1016/j.matpr.2020.01.076

Takeuchi, Y., Ikeda, N., Tahara, K., & Takeuchi, H. (2020). Mechanical characteristics of orally disintegrating films: Comparison of folding endurance and tensile

properties. *International Journal of Pharmaceutics*, *589*(September), 119876. https://doi.org/10.1016/j.ijpharm.2020.119876

Taredi, A. A., Patar, M. N. A. A., & Mahmud, J. (2024). Natural Frequencies Prediction of Hybrid Composite Laminate based on Finite Element Simulation and Artificial Neural Network. *2024 IEEE 22nd Student Conference on Research and Development, SCOReD 2024*, *December*, 186–191. https://doi.org/10.1109/SCOReD64708.2024.10872682

Tedesco, M. P., Monaco-Lourenço, C. A., & Carvalho, R. A. (2016). Gelatin/hydroxypropyl methylcellulose matrices — Polymer interactions approach for oral disintegrating films. *Materials Science and Engineering C*, *69*, 668–674. https://doi.org/10.1016/j.msec.2016.07.023

Teixeira, M. A., Antunes, J. C., Seabra, C. L., Fertuzinhos, A., Tohidi, S. D., Reis, S., Amorim, M. T. P., Ferreira, D. P., & Felgueiras, H. P. (2022a). Antibacterial and hemostatic capacities of cellulose nanocrystalline-reinforced poly(vinyl alcohol) electrospun mats doped with Tiger 17 and pexiganan peptides for prospective wound healing applications. *Biomaterials Advances*, *137*(April), 212830. https://doi.org/10.1016/j.bioadv.2022.212830

Teixeira, M. A., Antunes, J. C., Seabra, C. L., Fertuzinhos, A., Tohidi, S. D., Reis, S., Amorim, M. T. P., Ferreira, D. P., & Felgueiras, P. (2022b). Biomaterials Advances Antibacterial and hemostatic capacities of cellulose nanocrystalline-reinforced poly (vinyl alcohol) electrospun mats doped with Tiger 17 and pexiganan peptides for prospective wound healing applications. *Biomaterials Advances*, *137*(April), 212830. https://doi.org/10.1016/j.bioadv.2022.212830

Thabet, Y., & Breitkreutz, J. (2018). Orodispersible films: Product transfer from lab-scale to continuous manufacturing. *International Journal of Pharmaceutics*, *535*(1–2), 285–292. https://doi.org/10.1016/j.ijpharm.2017.11.021

Topuz, F., Kilic, M. E., Durgun, E., & Szekely, G. (2021). Fast-dissolving antibacterial nanofibers of cyclodextrin/antibiotic inclusion complexes for oral drug delivery. *Journal of Colloid and Interface Science*, *585*, 184–194. https://doi.org/10.1016/j.jcis.2020.11.072

Tran, T. P. A., Luong, A. H., & Lin, W. C. (2024). Characterizations of Centrifugal Electrospun Polyvinyl Alcohol/Sodium Alginate/Tamanu Oil/Silver Nanoparticles Wound Dressing. *IEEE Transactions on Nanobioscience*, *23*(2), 368–377. https://doi.org/10.1109/TNB.2024.3371224

Tuna, B. H., Gürbüz, M., Uğur, H., Çatak, J., & Yaman, M. (2023). Vitamin C bioaccessibility of commercially available dietary supplements: Quantity vs efficiency, does it matter? *Journal of Food Composition and Analysis*, *123*. https://doi.org/10.1016/j.jfca.2023.105558

Uddin, M. N., Mohebbullah, M., Islam, S. M., Uddin, M. A., & Jobaer, M. (2022). Nigella/honey/garlic/olive oil co-loaded PVA electrospun nanofibers for potential biomedical applications. *Progress in Biomaterials*, *11*(4), 431–446. https://doi.org/10.1007/s40204-022-00207-5

Umer, A., Naveed, S., Ramzan, N., Rafique, M. S., & Imran, M. (2014). A green method for the synthesis of copper nanoparticles using l-ascorbic acid. *Revista Materia*, *19*(3), 197–203. https://doi.org/10.1590/S1517-70762014000300002

Üstün, B., Aydın, H., Koç, S. N., Uluslu, A., & Kurtan. (2023). Electrospun polyethylenimine (PEI)-derived nitrogen enriched carbon nanofiber for supercapacitors with artificial neural network modeling. *Journal of Energy Storage*, *73*. https://doi.org/10.1016/j.est.2023.108970

Vuković, J. S., Perišić, S., Nikolić, A., Milošević, I., Mirilović, M., Bolka Prokić, B., & Lužajić Božinovski, T. (2025). Toward Natural Wound Healing Therapy: Honey and Calendula officinalis Loaded κ-Carrageenan Films with Promising Hemostatic Potential. *Pharmaceutics*, *17*(5). https://doi.org/10.3390/pharmaceutics17050578

Xue, J., Wu, T., Dai, Y., & Xia, Y. (2019). Electrospinning and electrospun nanofibers: Methods, materials, and applications. In *Chemical Reviews* (Vol. 119, Issue 8, pp. 5298–5415). American Chemical Society. https://doi.org/10.1021/acs.chemrev.8b00593

Yang, T., Wu, J., Yao, Y., Wang, K., Zhang, Q., & Fu, Q. (2024). Towards the toughness-strength balance of poly(vinyl alcohol) films via synergic plasticization. *Polymer*, *301*(March). https://doi.org/10.1016/j.polymer.2024.127031

Yasin, S. N. N., Said, Z., Halib, N., Rahman, Z. A., & Mokhzani, N. I. (2023). Polymer-Based Hydrogel Loaded with Honey in Drug Delivery System for Wound Healing Applications. In *Polymers* (Vol. 15, Issue 14). Multidisciplinary Digital Publishing Institute (MDPI). https://doi.org/10.3390/polym15143085

Yeşilyurt, A., Mayakrishnan, G., Parın, U., Kim, I. S., Parın, F. N., & Ullah, A. (2025). Design and Characterization of Polyvinyl Alcohol/Kappa-Carrageenan

Pickering Emulsion Biocomposite Films for Potential Wound Care Applications. *Journal of Biomedical Materials Research - Part A*, *113*(1). https://doi.org/10.1002/jbm.a.37850

Yoon, S. Do. (2014). Cross-linked potato starch-based blend films using ascorbic acid as a plasticizer. *Journal of Agricultural and Food Chemistry*, *62*(8), 1755–1764. https://doi.org/10.1021/jf4024855

Yu, J. H., Fridrikh, S. V., & Rutledge, G. C. (2006). The role of elasticity in the formation of electrospun fibers. *Polymer*, *47*(13), 4789–4797. https://doi.org/10.1016/j.polymer.2006.04.050

Yupanqui Mieles, J., Vyas, C., Aslan, E., Humphreys, G., Diver, C., & Bartolo, P. (2022). Honey: An Advanced Antimicrobial and Wound Healing Biomaterial for Tissue Engineering Applications. In *Pharmaceutics* (Vol. 14, Issue 8). MDPI. https://doi.org/10.3390/pharmaceutics14081663

Zahra, F. T., Quick, Q., & Mu, R. (2023). Electrospun PVA Fibers for Drug Delivery: A Review. In *Polymers* (Vol. 15, Issue 18, p. 3837). Multidisciplinary Digital Publishing Institute. https://doi.org/10.3390/polym15183837

Zainuddin, A. N. Z., Mustakim, N. N., Rosemanzailani, F. A., Fadilah, N. I. M., Maarof, M., & Fauzi, M. B. (2025). A Comprehensive Review of Honey-Containing Hydrogel for Wound Healing Applications. *Gels*, *11*(3), 1–37. https://doi.org/10.3390/gels11030194

Zaki, R. M., Alfadhel, M., DevanathaDesikan Seshadri, V., Albagami, F., Alrobaian, M., Tawati, S. M., Warsi, M. H., & Almurshedi, A. S. (2023). Fabrication and characterization of orodispersible films loaded with solid dispersion to enhance Rosuvastatin calcium bioavailability. *Saudi Pharmaceutical Journal*, *31*(1), 135–146. https://doi.org/10.1016/j.jsps.2022.11.012

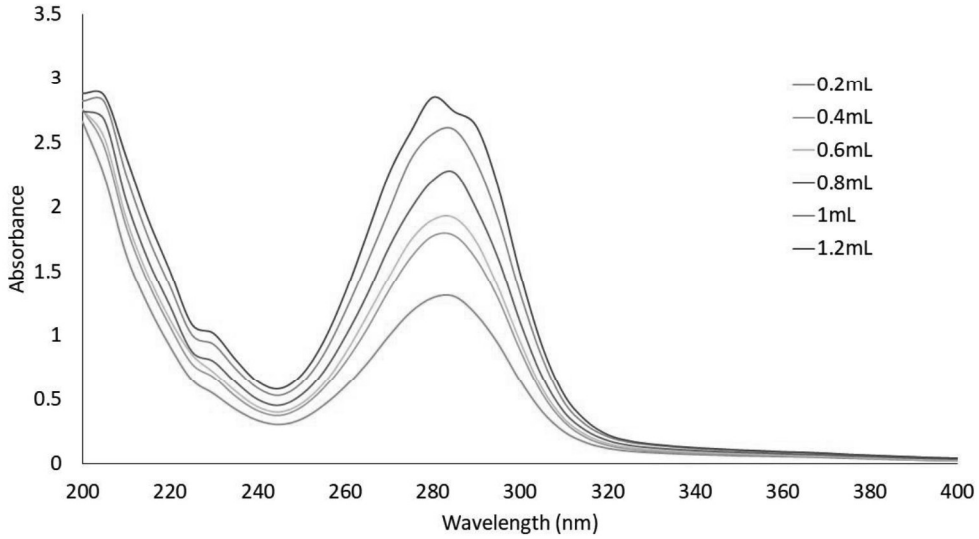
Zhang, Q., Lin, Z., Zhang, W., Huang, T., Jiang, J., Ren, Y., Zhang, R., Li, W., Zhang, X., & Tu, Q. (2020). Fabrication of green poly(vinyl alcohol) nanofibers using natural deep eutectic solvent for fast-dissolving drug delivery. *RSC Advances*, *11*(2), 1012–1021. https://doi.org/10.1039/d0ra08755f

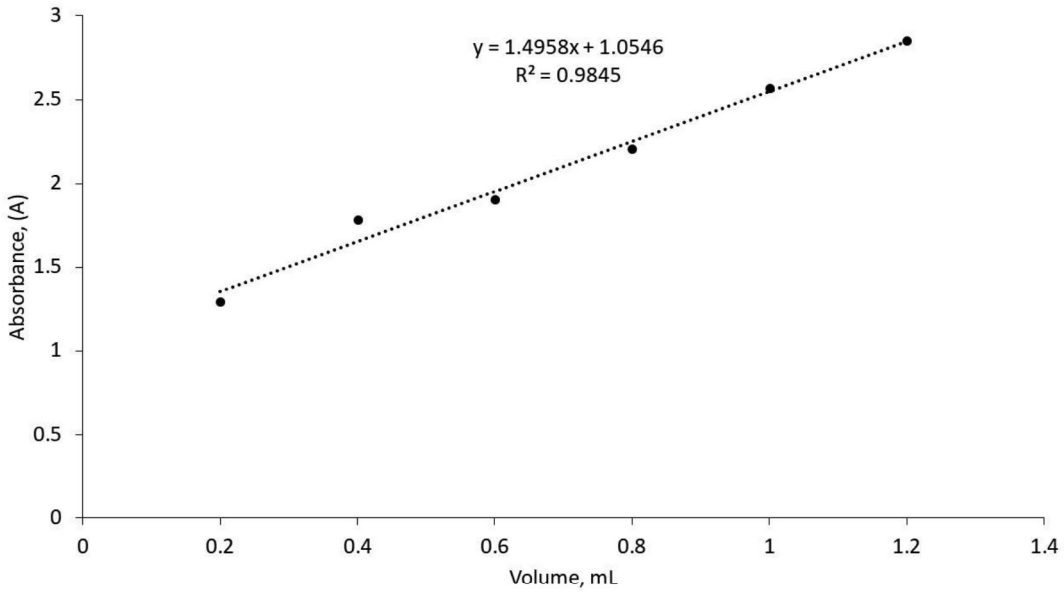
Zhou, Y., Chen, F. Q., Chen, S., Xiao, Q., Weng, H. F., Yang, Q. M., & Xiao, A. F. (2021). Preparation and characterization of κ-carrageenan modified with maleic anhydride and its application in films. *Marine Drugs*, *19*(9). https://doi.org/10.3390/md19090486

APPENDICES

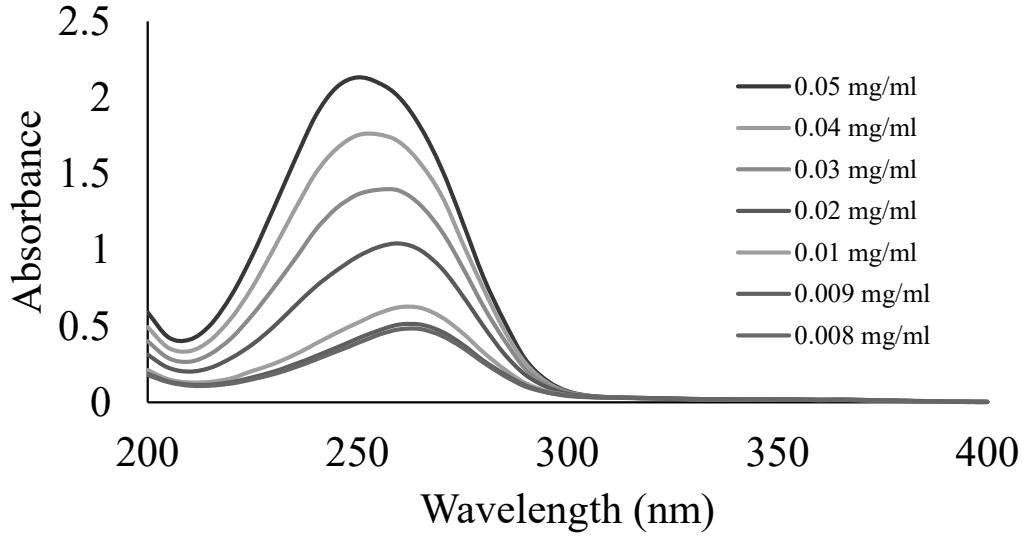
APPENDIX 1

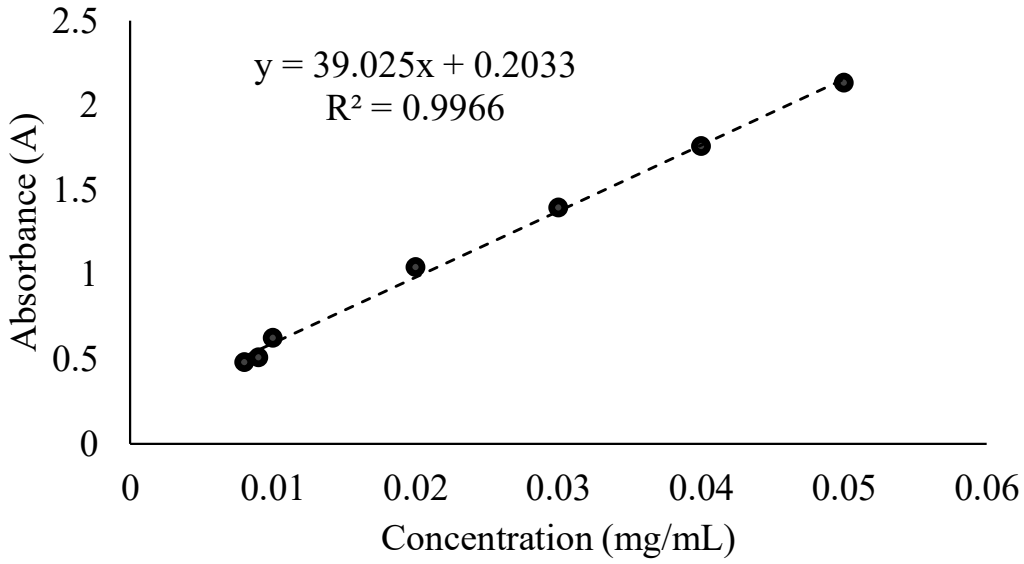
Calibration curve for PVA/κ-car/Honey using Uv-Vis Spectroscopy





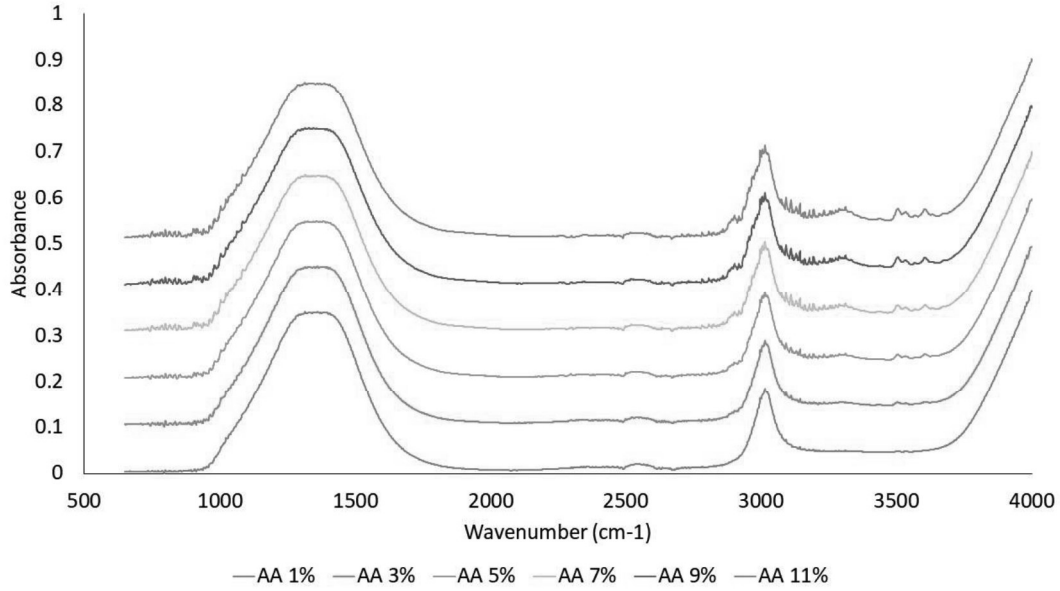
Calibration curve for PVA/κ-car/AA using Uv-Vis Spectroscopy

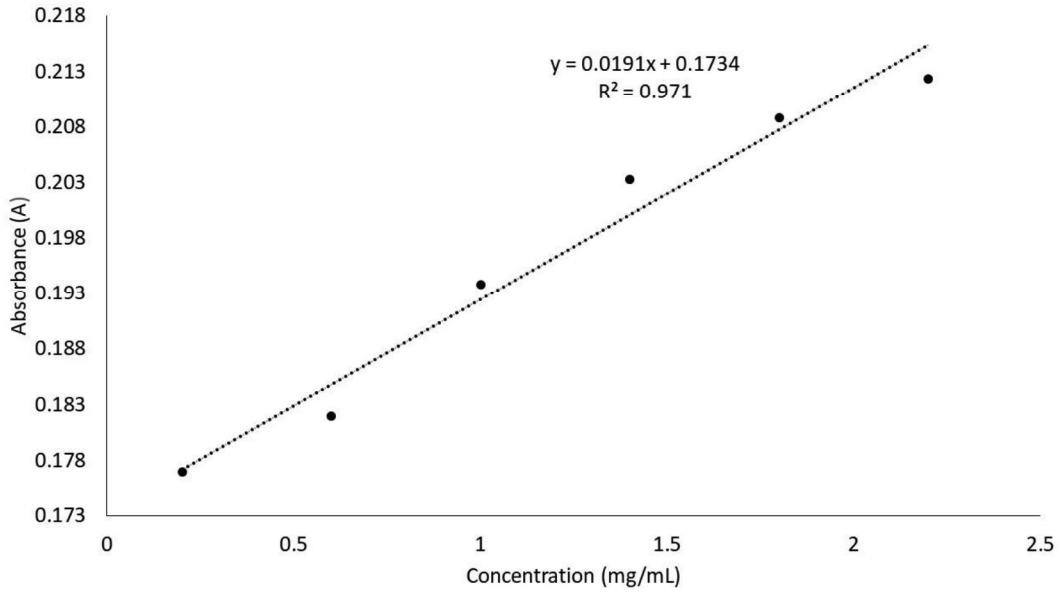




APPENDIX 2

Calibration curve for PVA/κ-car/AA using FT-IR Spectroscopy





AUTHOR'S PROFILE



Fetriya Fatihah Nasar was born in Sungai Petani, Kedah. She obtained his Bachelor of Engineering (Hons.) Chemical in 2024 from Universiti Teknologi (MARA) UiTM, Shah Alam. Currently, she is pursuing a Master of Science in Chemical Engineering at UiTM Shah Alam. Her MSc thesis entitled "Fabrication Characterisation and Dissolution Prediction of Electrospun PVA/K-Carrageenan Oral Dispersible Film Containing Kelulut Honey or Ascorbic Acid". Her MSc thesis involves characterisation of thin film and dissolution studies and predictive modelling of dissolution for batch and instantaneous dissolution using Artificial Neural Network (ANN).

LIST OF PUBLICATION:

Nasar, F. F., Bakar, N. F. A., & Mahmud, J. (2024). Prediction of In-vitro Dissolution Profile for Oral Dispersible Film (ODF) using Artificial Neural Network. *IEEE Xplore*, 192–196. https://doi.org/10.1109/scored64708.2024.10872643

Nasar, F. F., Bakar, N. F. A., Nazri, N. a. A., & Mahmud, J. (2026). Prediction of ascorbic acid dissolution by UV-VIS spectroscopy for oral dispersible film (ODF) using Artificial Neural Network (ANN). *Materials Science Forum*, *1189*, 83–90. https://doi.org/10.4028/p-5xijnv

Nasar, F. F., Mahmud, J., Bakar, N. F. A., & Nazri, N. a. A. (2026, June 18). *Predictive modelling of stress and tensile properties of oral dispersible film using artificial neural network*.

https://publisher.uthm.edu.my/ojs/index.php/ijie/article/view/23854

LIST OF COPYRIGHT:

Copyright registration for Electrospun Kelulut Honey-Enriched Oral Dispersible Film for Fast Dissolution Applications (O'Melhive), IP/CR/09912 (CRLY2026W03547) – Certificate

LIST OF AWARDS:

Best Paper Award, IEEE SCOReD 2024, IEEE International Conference on Smart Computing and Systems Engineering (SCOReD 2024)

Best Paper Award AMMEM 2025 4th International Conference on Advances in Materials, Mechanical Engineering (AMMEM 2025)

Gold Medal Award, DASAT2025 – International Conference on Innovation (DASAT 2025) (Innovation Medals)